View metadata, citation and similar papers at core.ac.uk
brought to you by CORE
provided by Wits Institutional Repository on DSPACE

NOVEL METHODOLOGY FOR THE SYNTHESIS OF XANTHONES

Jeremy Morgan Naidoo

Supervised by Prof. C. B. de Koning and Dr E. M. Mmutlane

A dissertation submitted to the Faculty of Science,
University of the Witwatersrand, Johannesburg,
in fulfilment of the requirements for the
Degree of Master of Science

March 2009

DECLARATION

I declare that the work presented in this thesis was carried out exclusively by myself under the joint supervision of Professor C.B. de Koning and Dr E.M. Mmutlane (CSIR). It is being submitted for the degree of Master of Science to the University of the Witwatersrand, Johannesburg, and has not been submitted before for any degree or examination at any other university.

March 2009

TO

my father Morgan and mother Gonum,

sisters, Cheryl and Tamra

and

my wife Casey

TABLE OF CONTENTS

ACKNOWLEDGEMENTS

I wish to thank my supervisors Professor C. B. de Koning and Dr E. M. Mmutlane for their continual guidance, encouragement, patience and advice throughout the course of this work.

I would also wish to thank the organic team for their assistance in the laboratory as well as their friendship, which made this research output an enjoyable experience.

A special thanks goes to Dr M. Fernandes and Dr C. B. Perry for performing crystallographic studies. I am also grateful to Mr R. Mampa for running the NMR spectra and Miss M. Potgieter for running the mass spectra.

Financial support from the National Research Foundation and Professor C. B. de Koning of the University of the Witwatersrand are gratefully acknowledged.

My gratitude goes out to my parents and wife for their continual support and patience throughout the course of this work. Last but most importantly, thanks goes to God Almighty, for the moments of inspiration and innovation that got me through the barren patches of this research output, for without his divine intervention this work would not have been successful.

ABSTRACT

In this MSc, novel methodology for the synthesis of xanthones and related compounds was discovered.

It was found that treatment of (1,4-dimethoxynaphthalen-2-yl)(2-hydroxyphenyl)methanone with ceric ammonium nitrate (CAN) resulted in the formation of 12a-methoxy-5*H*-benzo[*c*]xanthene-5,7(12a*H*)-dione as the product. The structure was confirmed by X-ray crystallography.

Exposure of a related compound (2,5-dimethoxyphenyl)(2-hydroxyphenyl)methanone to CAN afforded 2-methoxy-9*H*-xanthen-9-one as the major product with 4a-methoxy-2*H*-xanthene-2,9(4a*H*)-dione formed as the minor product. This reaction sequence has opened a new door for research into xanthone synthesis at the University of the Witwatersrand

LIST OF ABBREVIATIONS

AIDS	acquired immune-deficiency virus
aq.	aqueous
Bn	benzyl
Bu	butyl
BuLi	butyllithium
CAN	ceric ammonium nitrate
cat.	catalytic
CCl_4	carbon tetrachloride
CH_2Cl_2	dichloromethane
cm^{-1}	wavenumber
DCC	*N*,*N*-dicyclohexylcarbodiimide
DDQ	2,3-dichloro-5,6-dicyanobenzoquinone
DMF	*N*,*N*-dimethylformamide
DMSO	dimethyl sulfoxide
DNA	deoxyribonucleic acid
Et	ethyl
h	hour(s)
HIV	human immune-deficiency virus
Hz	hertz, s^{-1}
IBX	2-iodosobenzoic acid/iodoxybenzoic acid
IR	infrared
LDA	lithium diisopropylamide
Me	methyl
MeOH	methanol
MOM	methoxymethyl
mp.	melting point
NBS	*N*-bromosuccinimide
NMR	nuclear magnetic resonance
PCC	pyridinium chlorochromate
PPA	polyphosphoric acid
PPh_3	triphenylphosphine

ppm	parts per million
Pr	propyl
rt	room temperature
TDA-1	tris[2-(2-methoxy-ethoxy)ethyl]amine
THF	tetrahydrofuran
TLC	thin layer chromatography
TFA	trifluoroacetic acid
TFAA	trifluoroacetic anhydride
p-TSA	*p*-toluenesulfonic acid
UV	ultra violet

INTRODUCTION

Oxygenated heterocycles play an important role in the design and discovery of new physiological/pharmacologically active compounds[1]. Chemically xanthones (9*H*-xanthen-9-ones) are heterocyclic compounds with the dibenzo-γ-pyrone framework (**1**). In nature xanthones, are secondary metabolites that occur in fungi and higher plant families such as lichens[2]. Naturally occurring xanthones with nearly one thousand known members, contain different types of substituents in different positions, leading to a large variety of pharmacological activities[3].

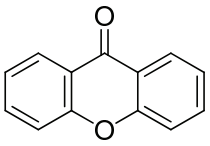

(**1**)

Figure 1: The basic skeletal structure of xanthones.

WITS INTEREST IN XANTHONES

In 1988 de Koning and Giles synthesized bikaverin (**2**), a wine red pigment isolated from several species of the fungal genera *Fusarium*, *Gibberella* and *Mycogone*[4]. It held a number of interesting biological activities which included vacuolation[5], anti-protozoal[6] and anti-tumour activities[7]. The core structural feature of bikaverin (**2**) was its xanthone nucleus. Bikaverin (**2**) was identified by Kjaër and co-workers, along with norbikaverin (**3**) in 1971[8].

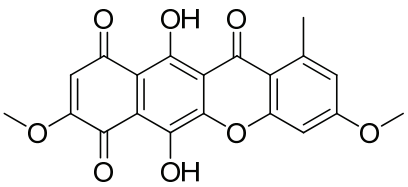

(**2**)

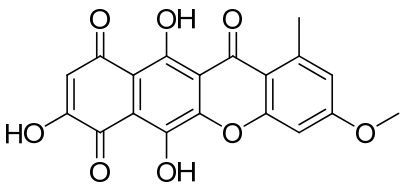

(**3**)

Figure 2: The structures of bikaverin (**2**) and norbikaverin (**3**).

To construct the xanthone nucleus (***Scheme 1***), de Koning *et al.*[4] first introduced the carbonyl bridge via a mild Friedel Crafts reaction using trifluoroacetic anhydride (TFAA) with the prepared naphthalene derivative (**4**) and the aryl acid (**5**), to give the desired product as a single regioisomer (**6**) in 51% yield. Compound (**6**) was then deprotected using palladium on carbon in the presence of hydrogen under pressure, to afford the phenol (**7**) in 80% yield. The phenol (**7**) was oxidised using DDQ, which surprisingly produced the spiro-compound (**8**) in 61% yield. The spiro compound (**8**) was hydrolyzed to the desired trione (**9**) using aqueous trifluoroacetic acid (TFA) in 94% yield. The trione (**9**) underwent pyrolytic isomerization to produce the xanthone-based compound (**2**) in 93% yield.

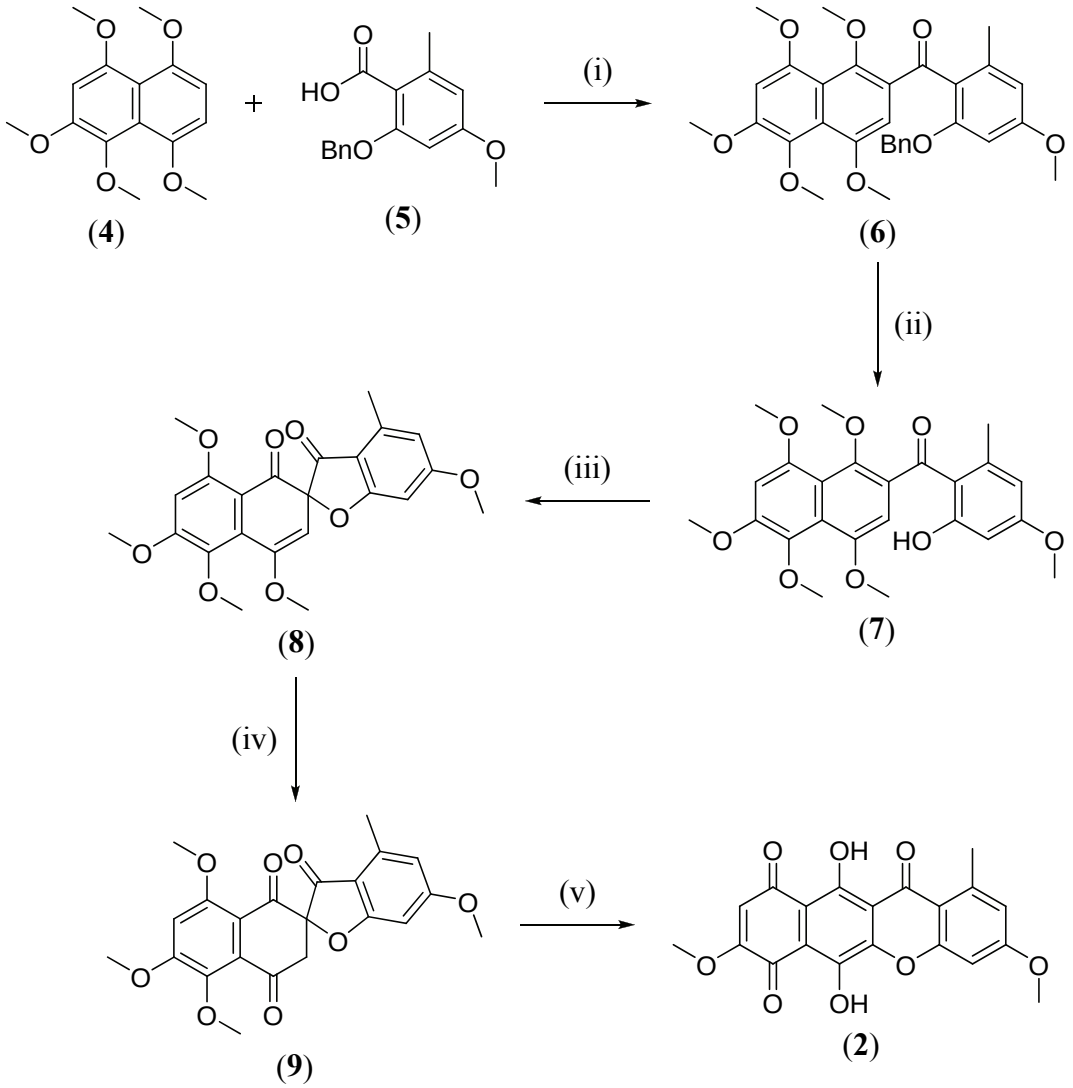

Scheme 1: (i) TFAA, dry CH_2Cl_2, rt, 90 h, 51%; (ii) 10% Pd/C, H_2, 5 bar, 1 h, 80%; (iii) DDQ, dry benzene, rt, 68 h, 61%; (iv) TFA (aq), CH_2Cl_2, rt, 5 min, 94%; (v) 200 °C, 1.1 bar, 1 h, 93%.

Since this synthesis, very little exploratory work has been done in investigating the mechanism of the DDQ facilitated reaction leading to the formation of the spiro-compound (**8**). There was also a need to explore the flexibility of this novel synthesis particularly on more electron poor precursors. Due to the diverse biological activity of xanthones, it is important to find a versatile synthetic approach that allows for the maximum amount of flexibility to afford a range of xanthone ring systems.

This MSc dissertation will be divided into the following sections: Firstly a general discussion on the biological activity of xanthones. Only a few examples will be selected in this section, as this field is vast. The second section will deal with some of the synthetic methods reported in the literature for the assembly of xanthones. These will then be followed by a discussion of the results obtained in our laboratories which will be discussed in detail.

We will highlight our novel methodology discovered during the course of this MSc that led to the formation of xanthones and related compounds.

BIOLOGICAL ACTIVITY

The xanthone nucleus comprises of an important class of the oxygenated heterocycles[9]. The growing interest in this class of compounds has been associated with its diverse pharmacological properties. Pharmacological investigations of xanthones date back to 1968, when Bhattacharya reported the diuretic and cardiotonic actions of the natural glycoside mangeferin (**10**)[10].

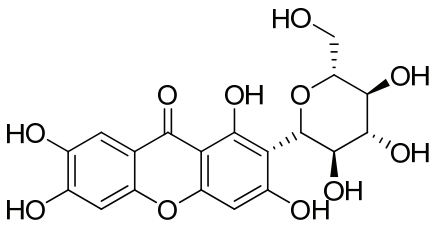

(**10**)

Figure 3: The structure of mangeferin (**10**).

Discussed below are a few xanthones that exhibit activity against cancer, HIV-AIDS and malaria.

ANTI-CANCER XANTHONES

Among the myriad of biological activities described for xanthones, the *in vitro* growth inhibitory activity on tumor cell lines appeared to be quite remarkable, since they are biologically active on a wide range of tumor cell lines[3]. Apart from the anti-tumor activity, some xanthones have been described for their anti-mutagenic effects[11] and for their cancer chemo-preventative effects, acting as inhibitors of tumor promoters *in vitro*[12] and *in vivo*[13].

PSOROSPERMIN

Psorospermin (**11**) is a naturally occurring compound, containing an angular furanoxanthone as well as a reactive epoxide moiety. Psorospermin (**11**) was first isolated by Kupchan and co-workers, from the dried roots of a woody plant ,of tropical Africa known as *Psorospermum febrifugum*[14]. They managed to elucidate the

structure but could not assign the absolute stereochemistry of the dihydrofuran ring or the epoxide moiety. The ethanolic extract of *Psorospermum febrifugum* was found to exhibit significant activity *in vivo* against P-388 lymphocytic leukemia in mice and *in vitro* against a cell culture derived from a human epidermoid carcinoma of the nasopharynx (9KB)[15]. Kupchan and co-workers demonstrated that this activity was due to psorospermin (**11**) which exhibited activity against P-388 lymphocytic leukemia in doses ranging from 0.1 $mg.kg^{-1}$ to 8 $mg.kg^{-1}$ and showed some cytotoxicity against the KB cell culture ($ED_{50} = 10^{-1}$ $\mu g.mg^{-1}$)[14].

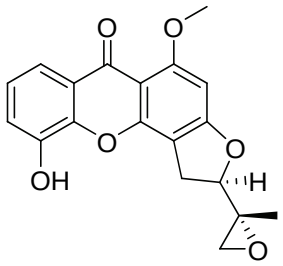

(**11**)

Figure 4: The structure of psorospermin (**11**).

Years later, Cassady *et al.*[16] were able to assign the absolute stereochemistry of psorospermin (**11**) as being 2'*R*, 3'*R*, using ^1H NMR spectroscopy and X-Ray crystallographic studies. After elucidating the absolute stereochemistry, Cassady *et al.*[16] synthesized three derivatives (**12-14**) but their activity was significantly less than psorospermin, therefore establishing the importance of the configuration and functionality of the epoxydihydrofuran moiety to activity *in vivo*.

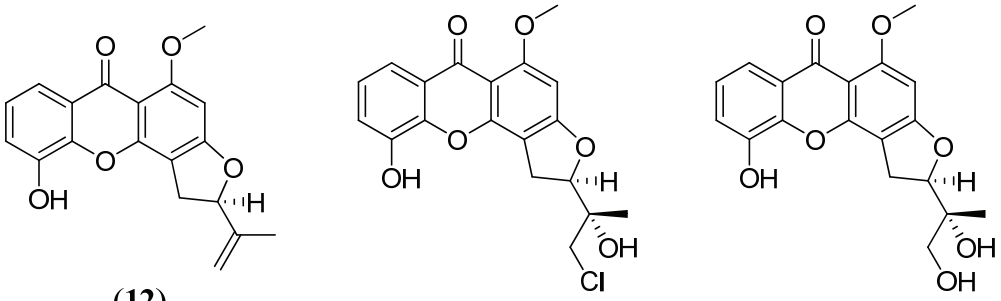

(**12**) (**13**) (**14**)

Figure 5: The structures of psorospermin derivatives (**12-14**).

Cassady and co-workers[17] also attempted a total synthesis of psorospermin (**11**) but only managed to synthesize methyl-(±)-(2'*R*,3'*S*)-psorospermin (**15**) but this synthesis did, however, lay the foundations for future work. More recently Schwaebe and co-workers[18] used the similar "zipper type" reaction to afford the first total synthesis of psorospermin (**11**) in 13 steps with an overall yield of 1.7%.

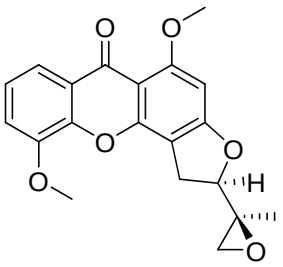

(**15**)

Figure 6: The structure of methyl-(±)-(2'*R*, 3'S)-psorospermin (**15**).

The xanthone structure plays a pivotal role in the cancer activity of psorospermin (**11**). Psorspermin (**11**) is believed to be a topoisomerase II poison. Topoisomerase II is an enzyme that plays several key roles in DNA metabolism and chromosome structure[19]. Psorospermin (**11**) intercalates into the DNA helix, and the epoxide ring undergoes nucleophilic attack by N7 of guanine (**16**) creating ion (**17**) that is cationic in nature and therefore may dipurinate inside cells[20] (***Scheme 2***). Psorospermin (**11**) intercalates parallel to the helical axis and it shows poor reactivity and poor selectivity towards duplex DNA but in the presence of topoisomerase II, alkylation reactivity of psorospermin (**11**) increases significantly[20].

Hurley *et al.*[21] proved that the carbonyl and ether linkage of the xanthone backbone play a vital role in the reactivity as they interact with 2-amino groups from the topoisomerase II-DNA complex ensuring that the epoxide is in close proximity to the N7 of guanine (**16**). Psorospermin (**11**) irreversibly binds to the topoisomerase-DNA complex thus having a clinical advantage associated with more potent cytotoxic effects towards cancer cells[22].

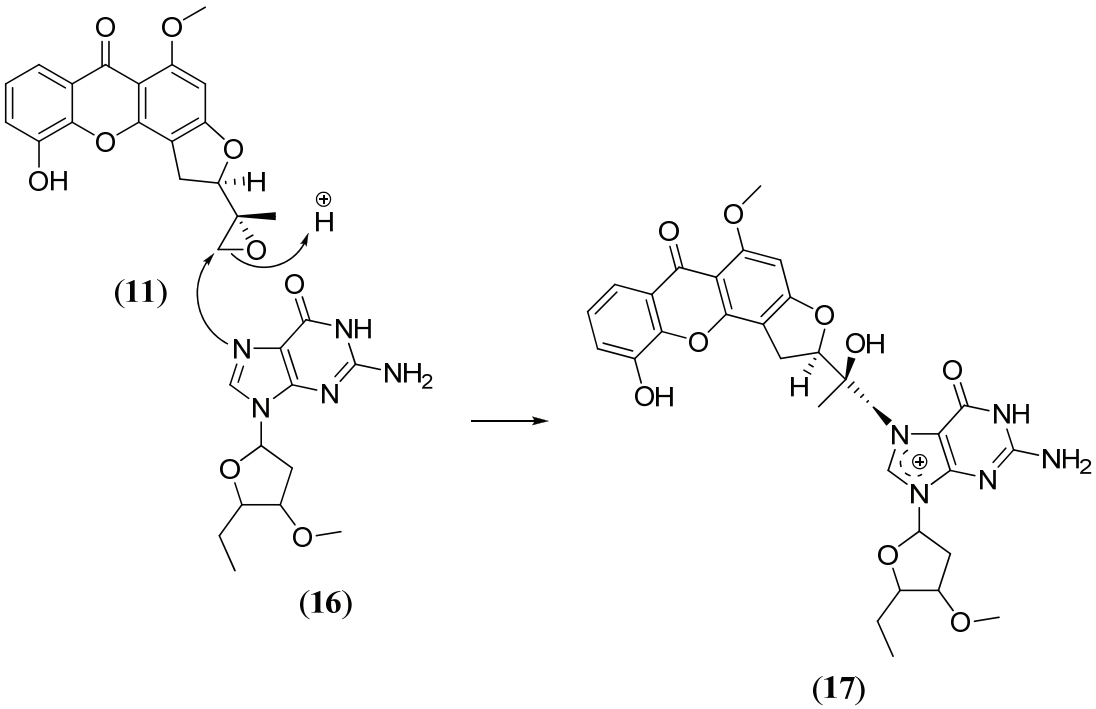

Scheme 2

GAMBOGIN AND GAMBOGIC ACID

Gambogin (**18**) and gambogic acid (**19**) have an unusual molecular architecture. They contain caged motifs attached to a xanthone scaffold. In 1996, Tada and co-workers isolated gambogin (**18**) and gambogic acid (**19**) from the gamboges resin of *Garcinia hamburyi*[23]. Gambogin and gambogic acid were tested against the cancer cell lines HeLa and HEL (Human Embryonic Lung Fibroblasts). Both gambogin (**18**) and gambogic acid (**19**) showed good cytotoxicity of 6.25 $\mu g.ml^{-1}$ and 12 $\mu g.ml^{-1}$ respectively against the respective cell lines[23].

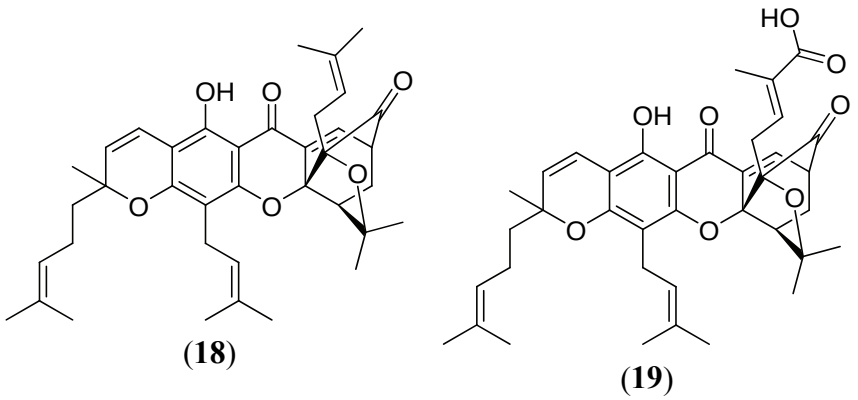

Figure 7: The structures of gambogin (**18**) and gambogic acid (**19**).

By 2005 Nicoloau *et al.*[24] had reported the biomimetic total synthesis of gambogin (**18**), via a site selective Claisen/Diels Alder/Claisen rearrangement. Gambogin (**18**), along with derivatives (**20**) and (**21**), were tested against the human epidermoid cancer cell line KB-31 with good success, exhibiting high cytotoxicity.

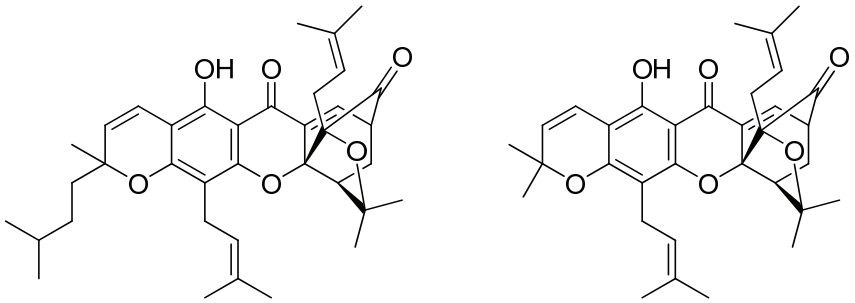

(**20**) (**21**)

Figure 8: The structures of gambogin derivatives (**20-21**).

The anti-cancer activity of gambogin (**18**) and gambogic acid (**19**) has been identified as proceeding by apoptosis induction[25]. Apoptosis, also known as programmed cell death, plays critical roles in normal cell development as well as elimination of excessive or dysfunctional cells[26]. Caspases, especially caspase 3, also known as executioner proteins, are pivotal in apoptosis because it cleaves multi-protein substrates in cells, leading to irreversible cell death[27]. Inadequate apoptosis such as, defects in the molecular machinery to activate the caspase cascade, is one of the hallmarks of cancer cells[28]. Cai and co-workers found that the 9-10 carbon-carbon double bond of the α,β-unsaturated ketone, relating to the carbonyl bridge of the xanthone backbone, in gambogin (**18**) and gambogic acid (**19**), was found to be critical in its apoptosis activity[29]. If the double bond is saturated, gambogin (**18**) and gambogic acid (**19**) are devoid of apoptosis inducing and anti-proliferative activity[29]. Thus the xanthone scaffold is vital to the activity of gambogin (**18**) and gambogic acid (**19**).

α-MANGOSTIN

Phytochemical studies have shown that the pericarps of mangosteen, *Garcinia mangostana*, contain a variety of secondary metabolites, such as oxygenated and

prenylated xanthones[30]. One of these xanthones is α-mangostin (**22**), which shows considerable activity against many cancer cell lines.

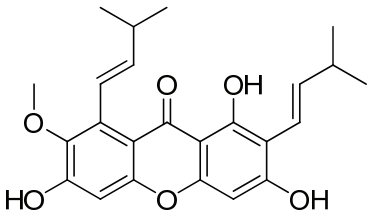

(**22**)

Figure 9: The structure of α-mangostin (**22**).

The total synthesis of α-mangostin (**22**) was reported by Iikubo *et al.*[31] (***Scheme 3***). They used PPh_3/CCl_4 and silica to cyclize the benzophenone (**23**) to α-mangostin (**22**)

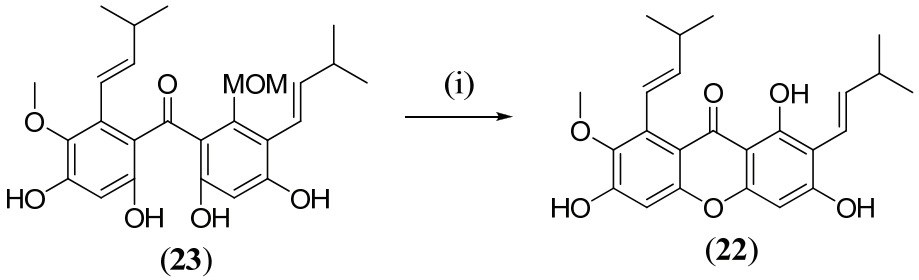

(**23**) (**22**)

Scheme 3: (i) PPh_3, CCl_4, THF, silica, rt.

Matsumoto and co-workers[32] proved that α-mangostin (**22**) in a dose as low as 10 μM induced apoptosis in the human leukemia cell line HL60. Unlike gambogin (**18**) and gambogic acid (**19**), α-mangostin (**22**) induced programmed cell death by targeting the mitochondria and causing loss in cell membrane potential rather than caspase activation[33]. α-Mangostin (**22**) was tested against human colon cancer DLD-1 cells and showed inhibition at 20 μM by inducing cell cycle arrest via the same pathway[34], which was detected in the increase in measurement of endonuclease G from the cells due to loss of cell membrane potential[35].

The anti-cancer activity of α-mangostin (**22**) can be attributed in part to the number of phenolic groups on the molecule and the replacement with a methoxy group remarkably reduced the potency to decrease cell membrane potential.[33]

α-Mangostin (**22**) has shown moderate activity against breast cancer. The risk of breast cancer increases with prolonged estrogen exposure[36]. A strategy to decrease estrogen production involves aromatase inhibition. Aromatase is responsible for catalyzing the biosynthesis of estrogens from androgens[37]. α-Mangostin (**22**) caused aromatase inhibition at a moderate concentration of 20 $\mu g.ml^{-1}$ [38].

The xanthone structure thus plays an important role in the cancer activity of α-mangostin (**22**) as it allows for many sites for the phenolic group substituents on the bridged benzene rings on either side of the carbonyl bridge, while still maintaining its aromaticity. This allows for intercalation of the xanthone to DNA in cells, as well as hydrogen bonding between the carbonyl and ether bridges with amino acid residues in enzymes.

ANTI HIV-AIDS XANTHONES

More recently natural xanthones have shown activity against the human immunodeficiency virus (HIV). Apart from their activity against the virus directly, many xanthones have secondary therapeutic properties against fungal infections in immune-compromised patients due, to acquired immunodeficiency syndrome (AIDS)[39].

SWERTIFRANCHESIDE

Swertifrancheside (**24**), a complex xanthone containing compound, was first isolated by Cordell and co-workers in 1994, from *Swertia franchetiana*[40]. Swertifrancheside (**24**) is a flavone xanthone glycoside and is a moderately potent inhibitor of HIV reverse transcriptase.

Over the past 25 years, substantial progress has been made in defining strategies for the treatment of HIV infection, the cause of AIDS[41]. Since reverse transcriptase is required early in proviral synthesis[42], inhibition of reverse transcriptase-catalyzed polymerization of DNA from viral RNA, inhibits virus replication. Reverse

transcriptases may be viral specific and are thus considered viable chemotherapeutic targets.

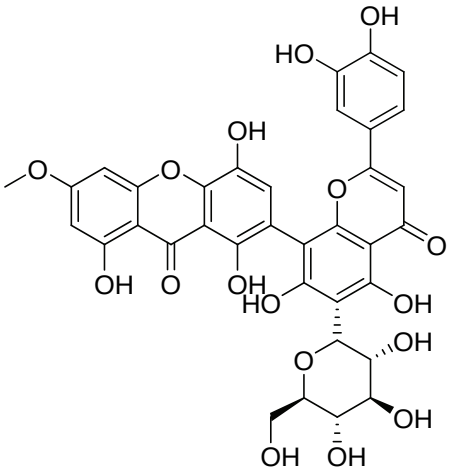

(**24**)

Figure 10: The structure of swertifrancheside (**24**).

Swertifrancheside (**24**) showed inhibitory activity of 99.8% at 200 μg.ml^{-1} (ED_{50}= 30.9 μg.ml^{-1}) in HIV 1 reverse transcriptase[40]. Cordell *et al.*[41] proved that swertifrancheside (**24**) binds to DNA to mediate inhibition, thus the xanthone scaffold plays a vital role in swertifrancheside (**24**) activity, as it provides a source of intercalation with DNA, due to the xanthone aromaticity. Although, not as potent as AZT triphosphate, it has no appreciable cytotoxicity to mammalian cells, making it a desirable candidate for clinical development.

MACLURAXANTHONE B AND MACLURAXANTHONE C

Macluraxanthone B (**25**) and macluraxanthone C (**26**) are prenylated xanthones which were first isolated by Boyd and co-workers in 2000 from the bark of *Maclura tinctoria*[43].

Macluraxanthone B (**25**) and macluraxanthone C (**26**) were subjected to a primary anti-HIV screen, and showed good potential with EC_{50} levels of 1.1-2 μg.ml^{-1}. The catechol functionality of macluraxanthone B (**25**) and macluraxanthone C (**26**) appear to offer enhanced HIV inhibitory activity but exhibit high toxicity toward CEM-SS host cells with IC_{50} levels of 2.2 - 3.7 μg.ml^{-1}.

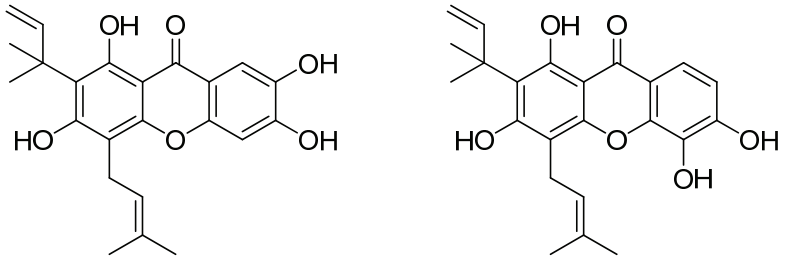

(**25**) (**26**)

Figure 11: The structures of macluraxanthone B (**25**) and macluraxanthone C (**26**).

ANTI MALARIA XANTHONES

The great panacea of malaria treatment, would be the development of a long lasting vaccine. Xanthones express potent activity against the malaria parasite *P. falciparum* and in particular chloroquine resistant strains[44], making them important leads in the discovery of the next anti-malarial.

F2C5

Malaria is caused by protozoan parasites of the genus *Plasmodium*, which specifically attack erythrocytes. *P. falciparum* is responsible for over 80% of malaria cases worldwide and it causes the most severe, often fatal form of the disease[45].

The digestive vacuole is an acidic proteolytic compartment central to the metabolism of the *plasmodium* parasite and may be considered as its Achilles heel[46]. In this vacuole haemoglobin is degraded to provide amino acids for parasite growth in a process known as hemoglobinolysis. Hemoglobinolysis also yields toxic heme (**28**), which serves as a reservoir of iron for ferroproteins. Although most of the heme is detoxified via polymerization into insoluble hemozoin[45].

Riscoe and co-workers have synthesized the xanthone 3,6-bis(ω-*N*,*N*-diethylaminoamyloxy)-4,5-difluoroxanthone (F2C5) (**27**)[47]. F2C5 (**27**) was tested against multidrug resistant malaria strains W2 and D6 of *P. falciparum* and IC_{50} values of 150 nM and 93 nM were obtained for the respective strains.

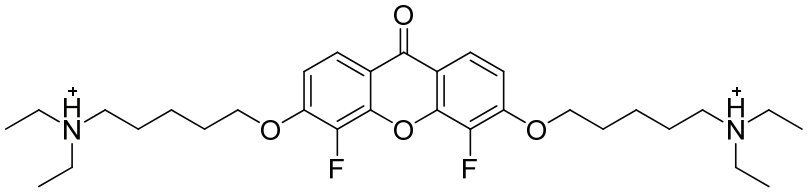

(**27**)

Figure 12: The structure of F2C5 (**27**).

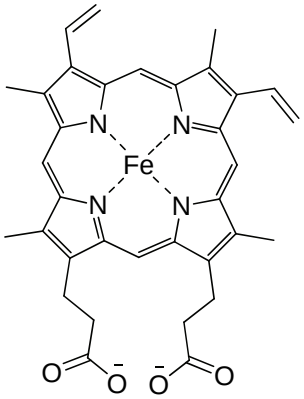

(**28**)

Figure 13: The structure of heme (**28**).

The xanthone structure of (**27**) is vital to anti-malarial activity. It is believed that the carbonyl bridge co-ordinates to the heme (**28**) iron atom. The aromatic rings on either side of the carbonyl bridge undergo π-π stacking with co-planar aromatic rings of the heme (**28**)[44]. The introduction of protonable amine chains of five carbon length adds to the reactivity of (**27**) because of the ionic interaction with heme (**28**) propionate groups and for targeting the drug to the parasites acidic vacuole[44]. The placement of halogens, in this case fluorine, improved activity because they are considered isosteres of phenolic groups in biological systems[45]. Secondly, placement of one or more halogens on the xanthone nucleus should diminish the likelihood of biological oxidations at these positions and thirdly halogens may facilitate complexing to heme (**28**) by mesomeric and/or inductive effects[48].

Thus the xanthone scaffold is pivotal in the activity of a heme poison such as F2C5 (**27**) to the malarial life cycle as it positions the molecule in a way that the structural features of the molecule can maximize its inhibitory potential.

DEMETHYLCALABAXANTHONE AND CALOTHWAITESIXANTHONE

Demethylcalabaxanthone (**29**) was first isolated from the root bark of the tree *Calophyllum caledonicum* found in New Caledonia by Ampofo *et al.*[49] in 1986 while Dharmaratne *et al*.[50] first isolated calothwaitesixanthone (**30**) from the root bark of the same plant in the same year.

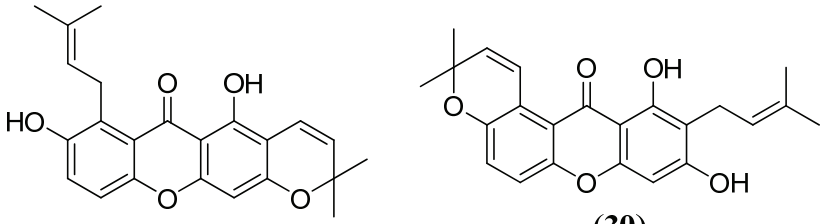

(**29**) (**30**)

Figure 14: The structures of demethylcalabaxanthone (**29**) and calothwaitesixanthone (**30**).

Demethycalabaxanthone (**29**) and calothwaitesixanthone (**30**) were tested against chloroquine resistant strain of *Plasmodium falciparum* and IC_{50} levels of 0.9 $\mu g.ml^{-1}$ and 1.0 $\mu g.ml^{-1}$ respectively, were reported by Hay and co-workers[51]. They hypothesized that the reason for the high anti-malaria activity is the position of the hydroxyl groups on the xanthone scaffold. Also effecting the activity is the presence of a 1, 1-dimethyl allyl side chain and additional pyranic ring. It's believed that these skeletal additions contribute to the electronic features rather than steric factors. These electronic features along with the xanthone nucleus contribute primarily to the inhibitory activity against hematin aggregation thus making these xanthones potential anti-malarials[52].

There are many other biological activities apart from those mentioned in this section such as anti-microbial and anti fungal activities. Due to the wide range of bio-activities, the discovery of many versatile and short synthetic routes to the xanthone structure have been developed, some of which will be discussed in the next section

SYTHETHIC APPROACHES TO XANTHONES

There is an increasing interest in new xanthone type structures due to their diverse pharmacological activities[3]. In the field of medicinal chemistry, the groups of compounds that can bind to different classes of receptors have attracted much attention[53]. Xanthones can be considered as potential structures in this field as was discussed in the previous section related to their biological activity. Xanthones obtained by synthesis represent a significant part of the derivatives described in the literature. The main object of xanthone syntheses is not only for the development of more diverse and complex bioactive compounds for biological activity and structure-activity relationship studies but also for other applications in medicinal chemistry, such as preparation of fluorescent probes, due to the photochemical properties of xanthones[54].

In this section, a number of synthetic methods for the construction of xanthones will be discussed. They will be divided in to three categories; classical methods, non conventional methods and new approaches for xanthone synthesis.

CLASSICAL METHODS

One of the first methods for the synthesis of xanthones was introduced by Michael[55]. This involved the distillation of a mixture of a phenol, salycylic acid and acetic anhydride to produce simple hydroxyxanthones. The method was poor yielding, experimental conditions were harsh and there was a possibility of decarboxylation, auto-condensation and other side reactions[56]. However in 1955, Grover, Shah and Shah developed a general method for the synthesis of xanthones that still enjoys great popularity today[57].

THE GROVER, SHAH AND SHAH REACTION

The Grover, Shah and Shah reaction offers a convenient method for preparing hydroxyxanthones due usually to the accessibility of the starting materials[54]. It

requires a salicylic acid derivative such as (**31**) and a suitable phenol for example (**32**) and these were heated together with zinc chloride in phosphoryl chloride[57]. The Grover, Shah and Shah method can afford the xanthone skeleton (**34**) directly only if the benzophenone intermediate (**33**) carries another phenol substituent in an alternate site for cyclization (*) (***Scheme 4***).

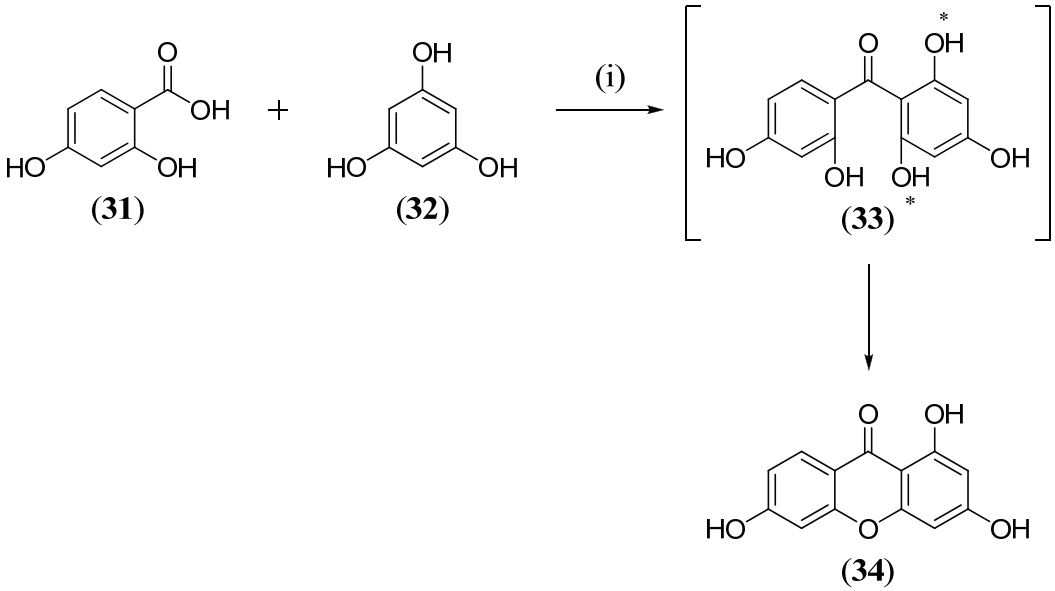

Scheme 4: (i) $ZnCl_2$, $POCl_3$, 70 °C, 2 h.

There have been recent modifications to the Grover, Shah and Shah reaction[39]. Better results have been reported using a mixture of phosphorus pentoxide-methanesulfonic acid (Eaton's reagent) instead of phosphoryl chloride-zinc chloride as a catalyst. The former acylation catalyst was found to be an excellent condensation agent between phloroglucinol (**32**) and 3-methyl-salicylic acid (**35**) providing high yields of the xanthone (**36**) with no detectable amounts of the related benzophenone[54] (***Scheme 5***).

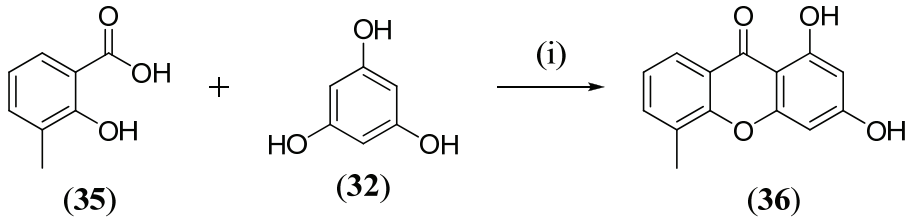

Scheme 5: (i) P_2O_5, CH_3SO_3H, 80 °C, 20 min.

There are a number of limitations on the original Grover, Shah and Shah reaction such as the necessity of a phenolic group to promote direct cyclization and not the formation of the benzophenone intermediate[58]. Although it is possible to cyclize the benzophenone intermediate on heating, the overall yields are moderate, thus other methods have grown in popularity compared to this one pot synthesis.

SYNTHESIS VIA A BENZOPHENONE INTERMEDIATE

The benzophenone derivatives are commonly accessible through condensation by Friedel-Crafts acylation of an appropriate substituted benzoyl chloride such as (**37**) with anisole (**38**). Barton *et al.*[59] presented an alternative to the Grover, Shah and Shah reaction, involving the formation of 2-hydroxy-2'-methoxy-benzophenones (**39**) followed by the quantitative elimination of methanol in the presence of alkali to give the desired xanthone (**1**) (***Scheme 6***).

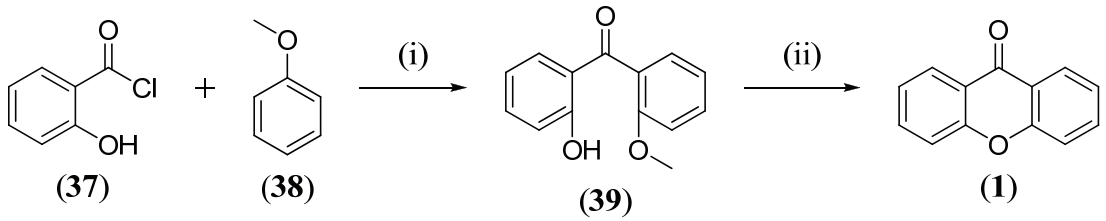

Scheme 6: (i) $AlCl_3$, dry ether, rt, 1 h; (ii) NaOH, methanol, reflux, 6 h.

Scheinmann *et al.*[60] demonstrated the usefulness of this reaction by successfully synthesizing numerous analogs which were difficult to obtain using the Grover, Shah and Shah method due to unwanted demethylations.

The synthesis of benzophenones suitable as precursors for cyclization to xanthones is conveniently achieved at room temperature by the Friedel-Crafts acylation of methoxybenzene (**41**) derivatives with the appropriately substituted benzoyl chloride (**40**) in ether (***Scheme 7***). In cases where acylation occurs adjacent to a methoxy group, selective demethylation in the presence of aluminium trichloride occurs at the site *ortho* to the carbonyl group. The fact that extended reaction time (30 h) causes *ortho*-monodemethylation has led to convenient syntheses of substituted 2-hydroxy-2'-methoxy intermediates such as benzophenone (**42**) suitable for cyclization to substituted xanthones (**43**) by the elimination of methanol.

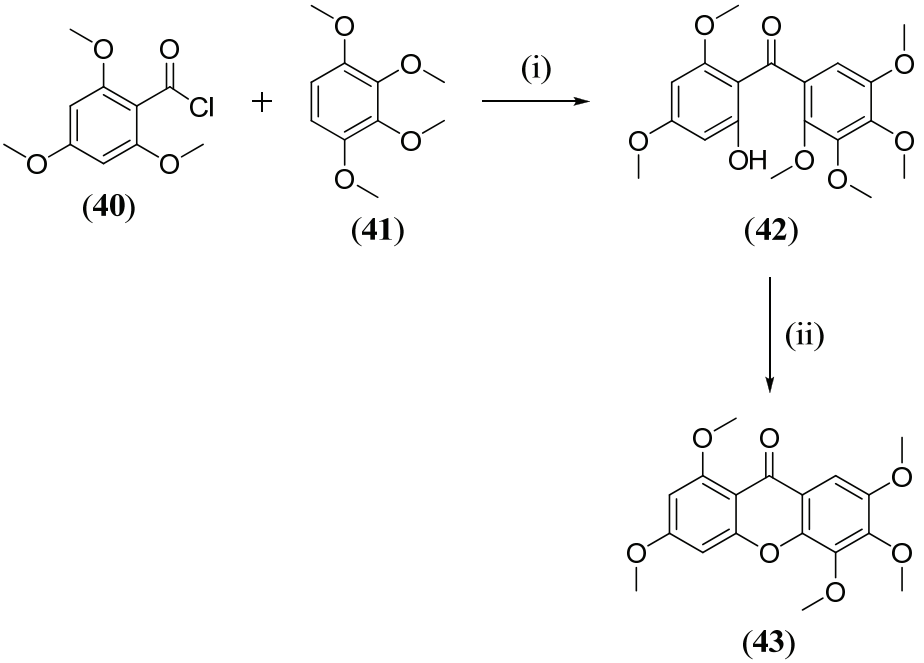

(**40**) (**41**) (**42**) (**43**)

Scheme 7: (i) $AlCl_3$, dry ether, rt, 30 h; (ii) NaOH, methanol, reflux, 6 h.

Modifications of the Friedel-Crafts reaction have included achieving the acylation reaction in the presence of TFAA, demethylations and subsequent cyclization of the benzophenone (**46**) in aqueous medium under pressure and heating[61] (***Scheme 8***).

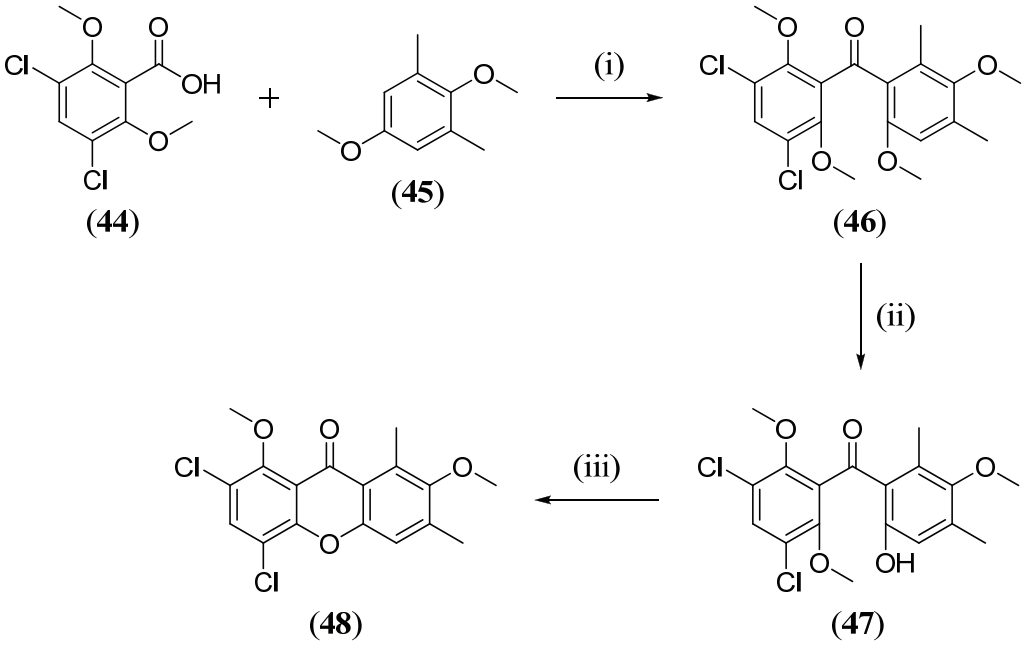

(**44**) (**45**) (**46**) (**47**) (**48**)

Scheme 8: (i) TFAA, dry CH_2Cl_2, reflux, 18 h; (ii) BBr_3, dry CH_2Cl_2, –10 °C, 2 h; (iii) water, 120 °C, 16 h.

Another modification of the reaction was the use of triphenylphosphine in carbon tetrachloride as the final bond forming reaction to build the xanthone framework. This constituted a new method for the total synthesis of α-mangostin (**22**). The benzophenone (**23**) was obtained through the parent alcohol (**51**) by aryl anion addition to the substituted benzaldehyde (**49**), to furnish α-mangostin (**22**) (***Scheme 9***). A slightly different approach involving *ortho*-lithiation as the key step for the synthesis of benzophenones followed by classical cyclization to xanthones was utilized[31].

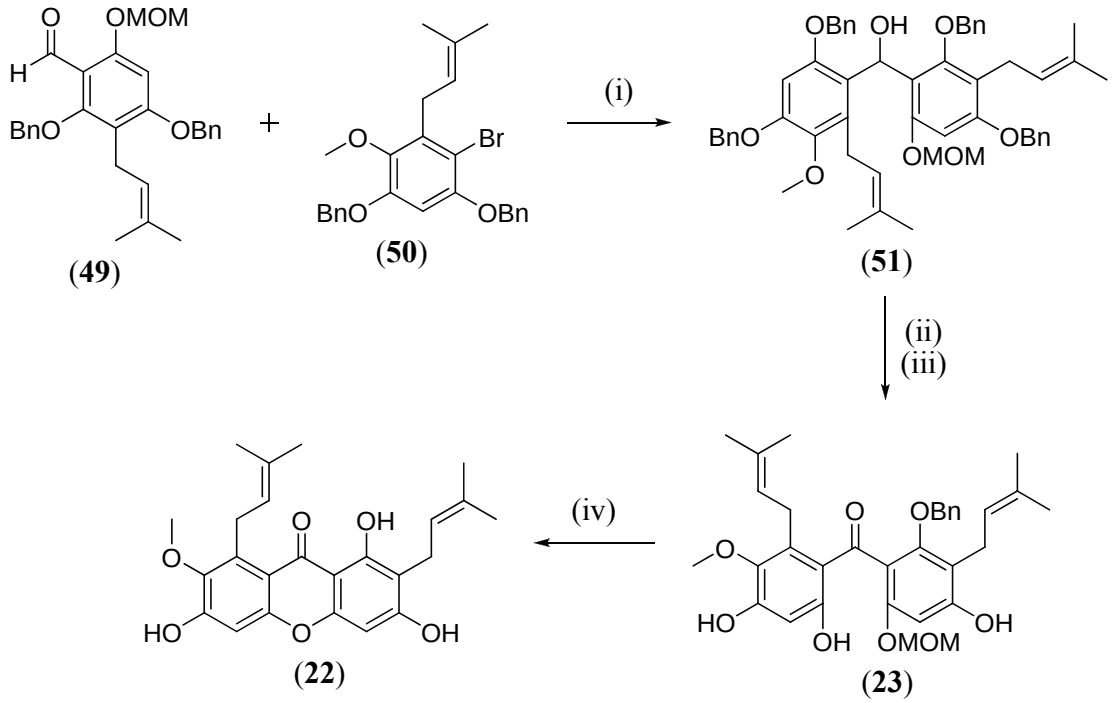

Scheme 9: (i) *s*-BuLi, THF, –78 °C; (ii) IBX, toluene: DMSO (1:1), rt; (iii) 10% Pd/C, HCO_2NH_4, acetone, rt; (iv) PPh_3, CCl_4, THF, silica, rt.

A strategy that has been used with considerable success was accessing the benzophenone via a diaryl ester by using a photo-Fries rearrangement (***Scheme 10***). Finnegan *et al.*[62] developed methodology to access 2,5-dihydroxyxanthone (**58**) via a photo-Fries reaction. The 2,3-dimethoxybenzoyl chloride (**52**) was condensed with *para*-methoxy-phenol (**53**) to afford the desired diaryl ester (**54**). The diaryl ester (**54**) underwent a photo-Fries reaction and produced the desired benzophenone (**56**) in a moderate yield of 43% as well as the solvolysis product (**55**) in 17% yield.

Demethylation of (**56**) followed to form benzophenone (**57**) which was heated in a sealed vessel to give 2,5-dihydroxyxanthone (**58**).

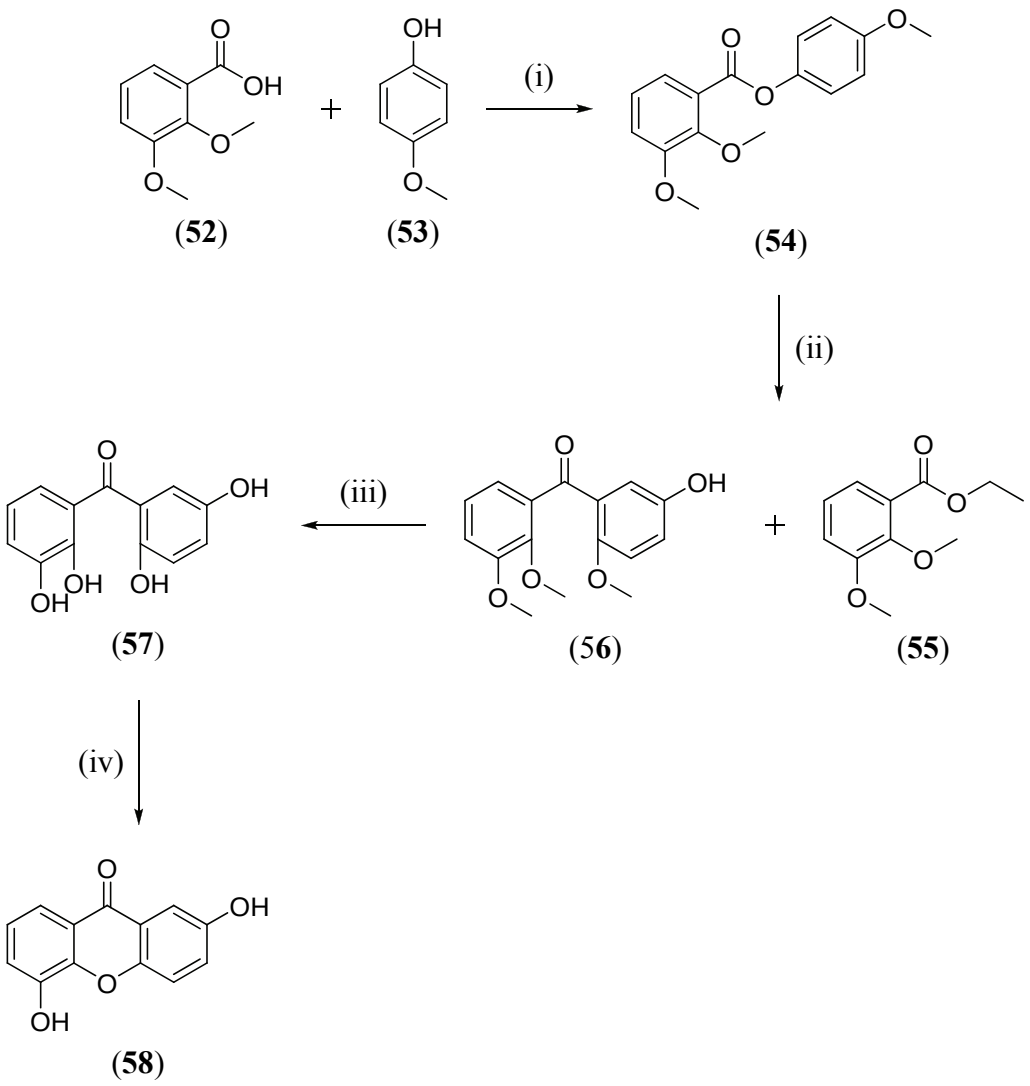

(**52**) (**53**) (**54**) (**55**) (**56**) (**57**) (**58**)

Scheme 10: (i) Pyridine, reflux, 4.5 h; (ii) hν, ethanol, 40 °C, 9 h; (iii) acetic acid, HBr, reflux, 4 h; (iv) 225 °C, 17 h.

SYNTHESIS VIA DIARYL ETHERS

The diaryl ether synthesis of xanthones uses the reaction of phenols such as (**60**) with benzoic acids bearing halogens in the *ortho*-position, for example (**59**), and the ring formation is accomplished by electrophilic cycloacylation of the initially formed 2-aryloxybenzoic acid (**61**)[54] as shown in ***Scheme 11***.

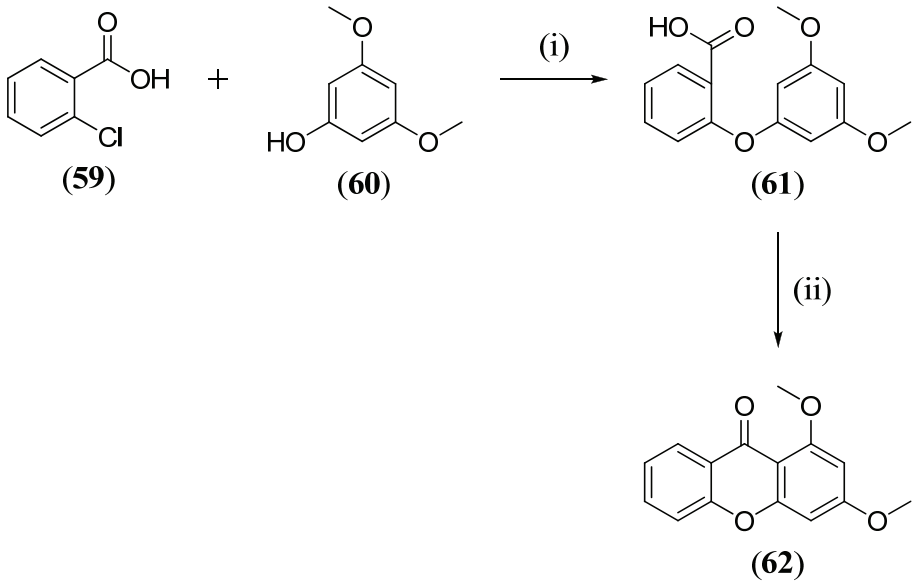

Scheme 11: (i) Cu, K_2CO_3, dry DMF, reflux, 3.5 h; (ii) H^+, 100 °C, 3 h.

A classical method to produce the ether linkage of the xanthone scaffold is via the Ullmann coupling reaction. Reisch and co-workers have prepared xanthone derivatives in their synthesis of acronycine isosteres[63]. For example, 2-chloronicotinic acid (**63**) was coupled with 3,5-dimethoxy-phenol (**60**) using Ullmann coupling procedures to yield (**64**). This was then cyclized to the xanthone (**65**) using polyphosphoric acid (PPA) (***Scheme 12***).

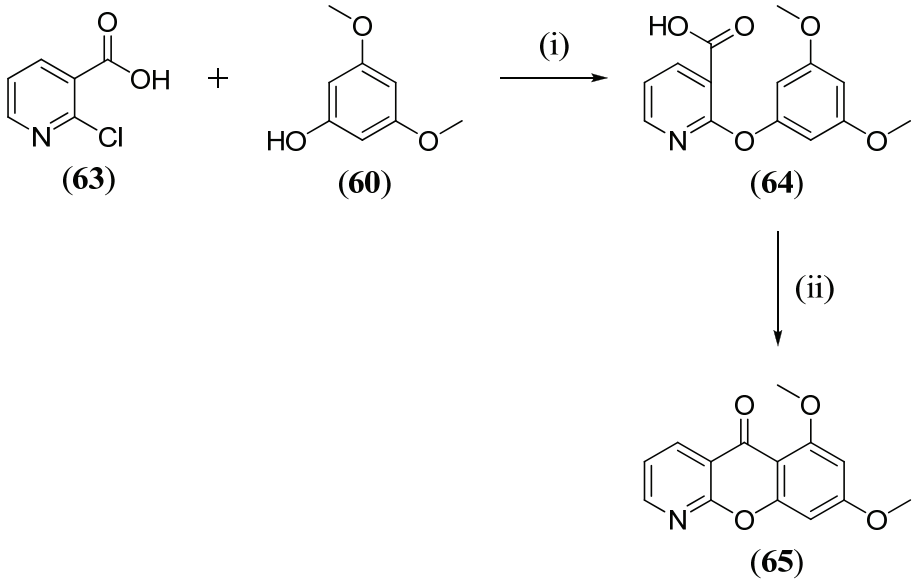

Scheme 12: (i) Cu, K_2CO_3, dry DMF, reflux, 3.5 h; (ii) PPA, 100 °C, 3 h.

Atwell *et al.*[64] synthesized a xanthone-containing compound using a phase transfer reagent in the presence of copper that improves the yield as compared to when using ordinary Ullmann conditions. The disodium salt of hydroxyphenylacetic acid (**67**) and the salt of the benzoic acid derivative (**66**) where submitted to Ullmann coupling conditions with the phase transfer catalyst tris[2-(2-methoxy-ethoxy)ethyl]amine (TDA-1) to afford (**68**). This was followed by selective acid catalyzed ring closure to yield the desired xanthone (**69**) as depicted in ***Scheme 13***.

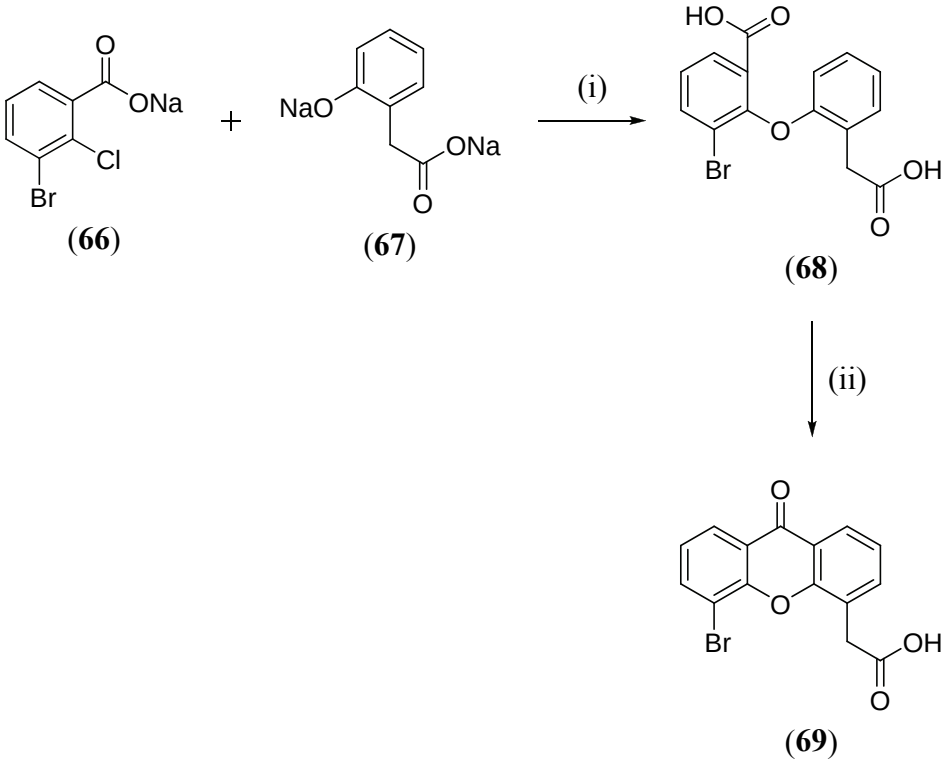

(**66**) (**67**) (**68**) (**69**)

Scheme 13: (i) CuCl, TDA-1, dry dioxane, dry DMSO, 110 °C, 12 h; (ii) H_2SO_4, water, 80 °C, 10 min.

Remarkable improvements have been achieved in the synthesis of 1,2-dioxygenated xanthones. For example xanthone (**74**) has been synthesized by the application of a direct metallation procedure on diphenyl ether intermediates using lithium di-isopropylamide (LDA)[65]. Snieckus and co-workers have accomplished the LDA-mediated synthesis of the natural product deoxyjacareubin (**74**) from the appropriate diaryl ether carboxamide (**72**)[65] (***Scheme 14***). The cyclization step is dictated by the coordination effects of direct metallation groups in contrast with the

electrophilic substitution of the corresponding carboxylic acids and is driven by Complex Induced Proximity Effect (CIPE)[66].

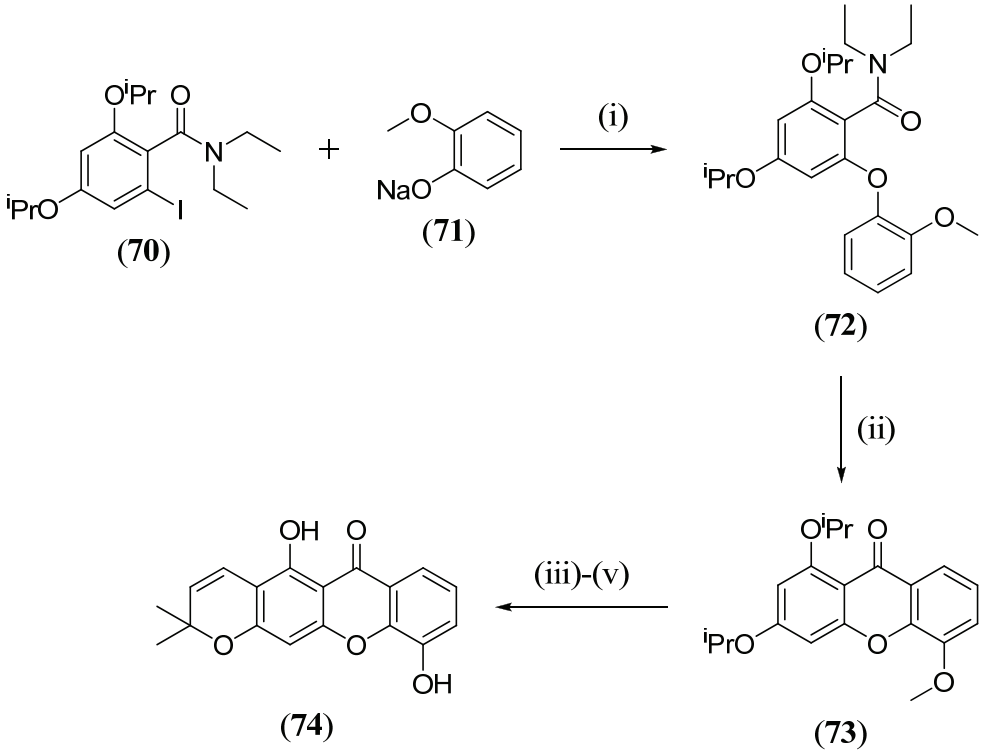

Scheme 14: (i) CuCl, TDA-1, pyridine, 150 °C, 5 h; (ii) LDA, THF, 0 °C, 1 h; (iii) BCl_3, CH_2Cl_2, 0 °C, 1 h; (iv) 3-methyl-but-2-enal, $PhB(OH)_2$, AcOH (1:5), toluene, reflux, 16 h; (v) BBr_3, CH_2Cl_2, –78 °C, 1 h.

Elix and co-workers accessed the diaryl ether intermediate (**78**) via a Smiles re-arrangement of the diaryl ester (**77**) en route to xanthone (**79**)[61] (***Scheme 15***). Ester formation was effected by the condensation of the acid (**75**) and phenol (**76**) in the presence of *N*, *N*'-dicyclohexylcarbodiimide (DCC). The diaryl ester (**77**) was treated with potassium carbonate to effect the Smiles rearrangement to the diaryl ether (**78**). Cyclization of the ether (**78**) by treatment with TFAA gave xanthone (**79**).

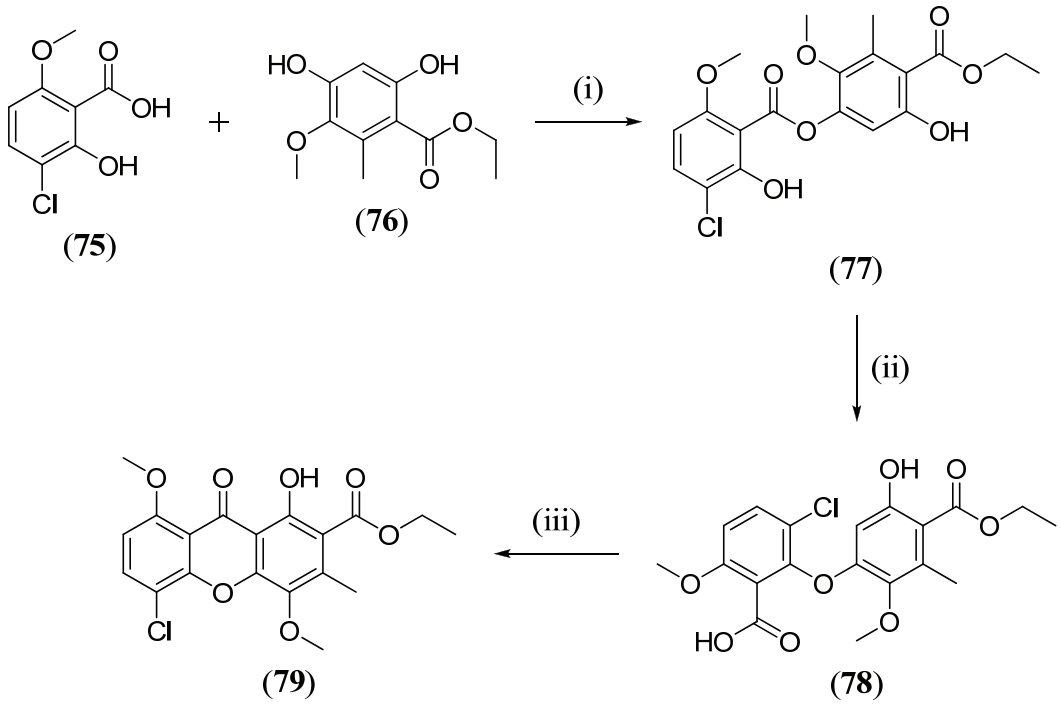

Scheme 15: (i) DCC, toluene, dry ether, rt, 24 h; (ii) K_2CO_3, dry DMSO, 80 °C, N_2, 16 h; (iii) dry toluene, TFAA, rt, 17 h.

NON CONVENTIONAL METHODS

Some so called less conventional methods for the synthesis of xanthones have been reported over the years. Although limited in their application to more complex xanthone structures, these methods laid the foundation for future and more promising work.

SYNTHESIS VIA KETIMINE AND THIOXANTHONE

As shown in ***Scheme 16***, in 1922 Nishikawa *et al.*[67] synthesized 1,3-dihydroxyxanthone via a ketimine intermediate. Phloroglucinol (**32**) was reacted with *meta*-hydroxybenzonitrile (**80**) in the presence of zinc chloride to afford the ketimine derivative (**81**) in moderate yield. The ketimine (**81**) was then subjected to aqueous basic conditions to effect the formation of the 1,3-dihydroxyxanthone (**82**). This was a new approach to synthesize simple xanthones but the yields were poor and the method limited.

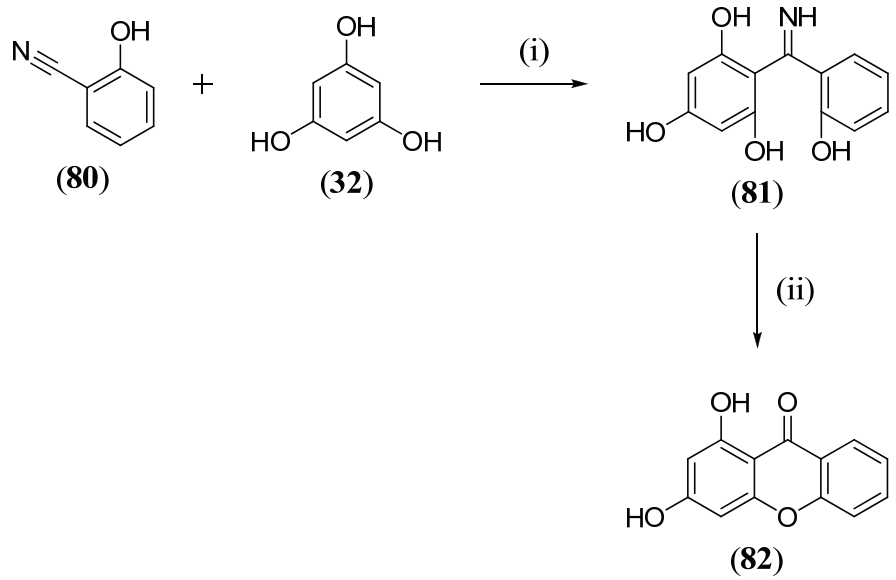

Scheme 16: (i) Dry ether, $ZnCl_2$, HCl, 2 h; (ii) $NaOH_{(aq)}$, reflux.

Bennet and co-workers synthesized xanthone (**85**) from thioxanthone (**83**) intermediates[68] (***Scheme 17***). The thioxanthone (**83**) was treated with a caustic solution in dioxane to afford the hydroxybenzophenonesulfinic acid (**84**). The sulfinic acid (**84**) was then subjected to basic conditions to afford the desired xanthone (**85**).

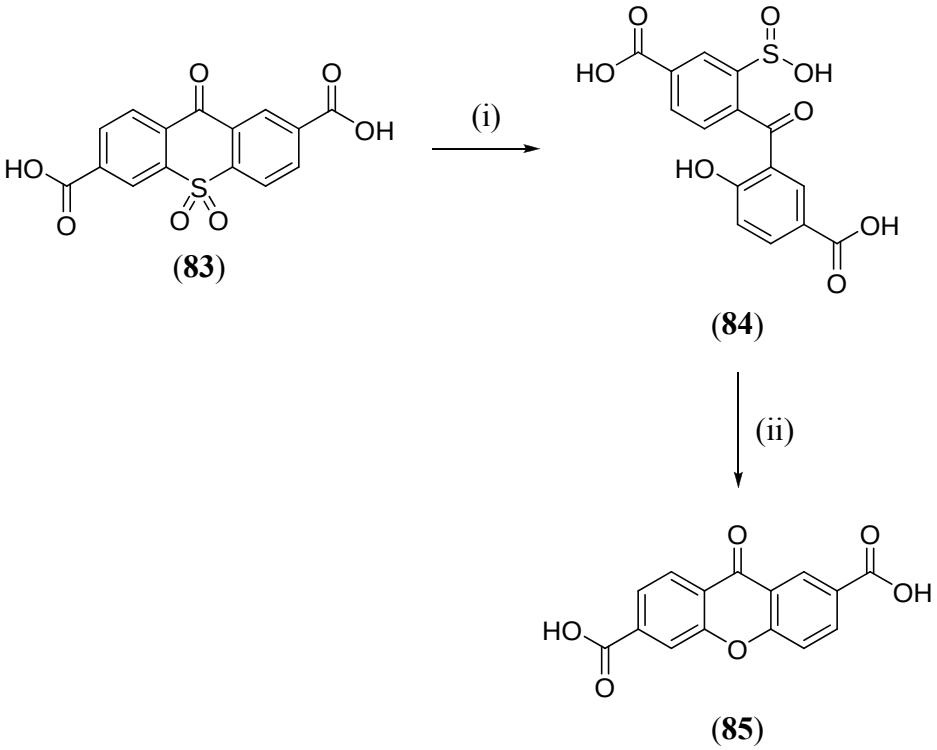

Scheme 17: (i) NaOH, dioxane-H_2O, reflux, 5 h; (ii) $NaOH_{(aq)}$, reflux, 4 h.

The thioxanthone (**83**) was synthesized via a procedure by Amstutz *et al.*[69] as shown in ***Scheme 18***. The chlorobenzoic acid (**86**) was condensed with 4-mecaptobenzoic acid (**87**) in aqueous ethanol to furnish the aldehydo-diphenyl sulphide (**88**). The aldehydo-diphenyl sulphide (**88**) was heated in concentrated sulphuric acid and produced two inseparable products, thiaxanthene (**89**) and thiaxanthone (**90**). Both thiaxanthene (**89**) and thiaxanthone (**90**) were refluxed in acetic acid and hydrogen peroxide to give the thioxanthone (**83**).

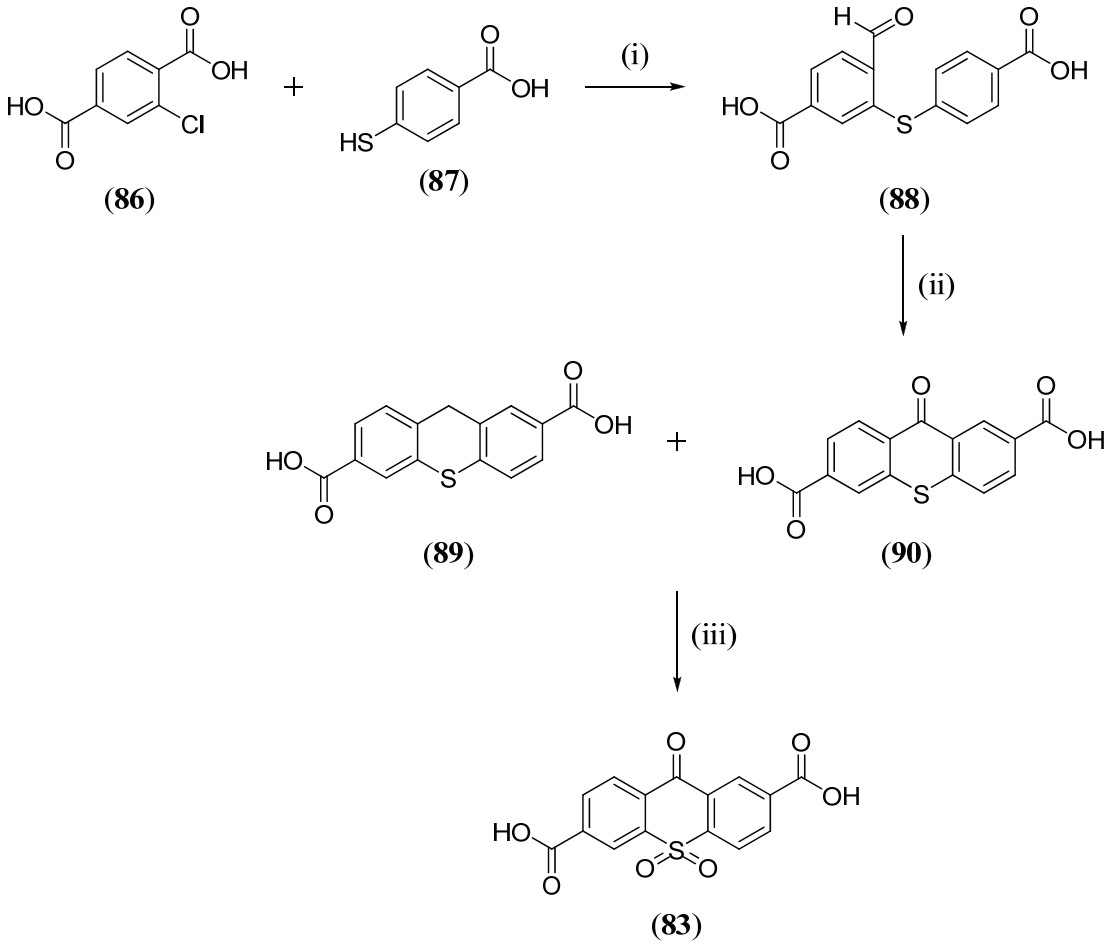

Scheme 18: (i) Ethanol$_{(aq)}$, rt, reflux, 75 min; (ii) conc. H_2SO_4, 60 °C, 30 min; (iii) acetic acid, 30% H_2O_2, reflux, 4 h.

This method was far more flexible than the ketimine method mentioned above in terms of functionalizing the xanthone skeleton but the yields were poor and synthesis of the starting material was difficult and reaction conditions harsh.

CYCLIZATION OF POLY-β-KETONES

In 1977, Harris *et al.*[70] developed an innovative biomimetic synthetic pathway to the naturally occurring secondary metabolite lichexanthone (**98**) (***Scheme 19***).

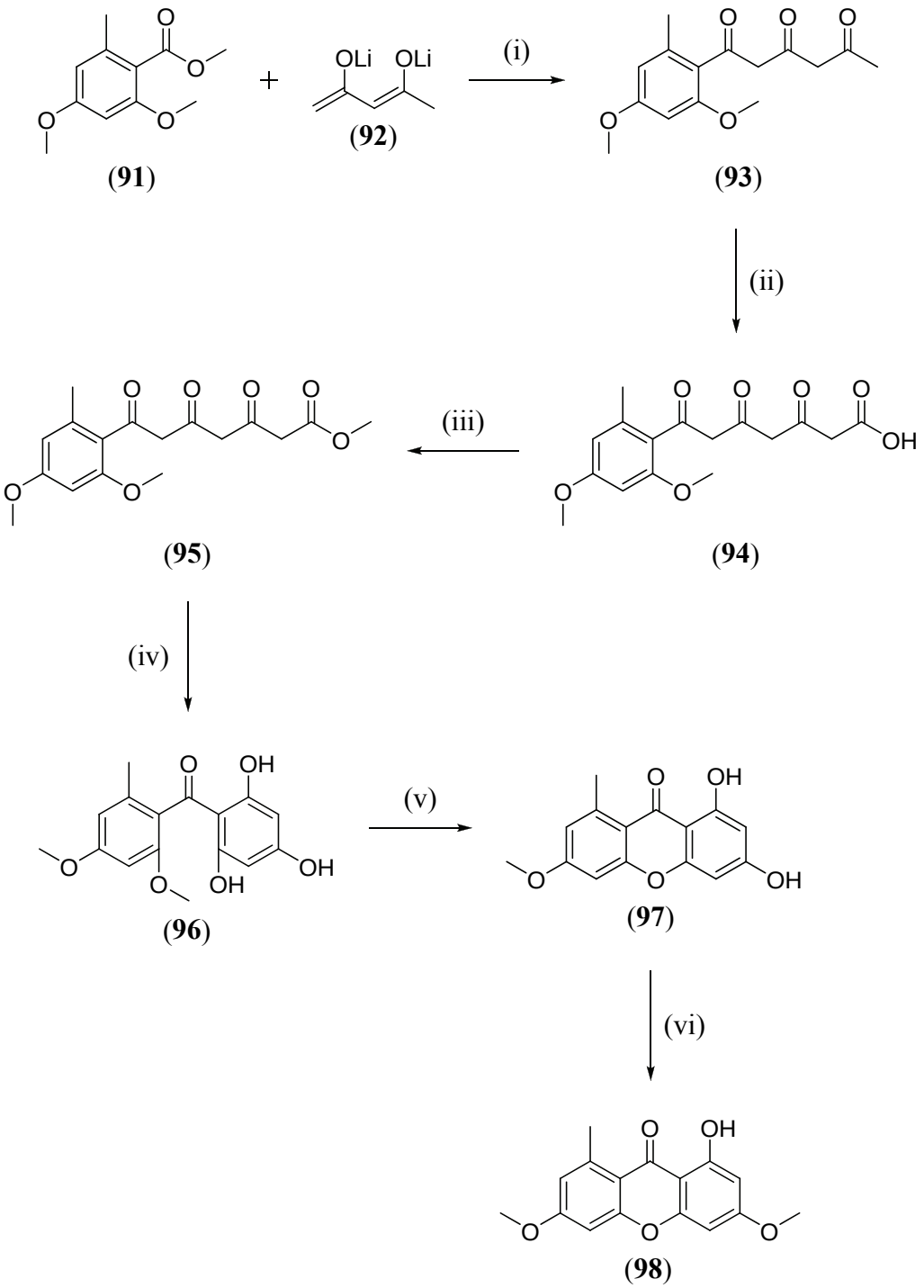

Scheme 19: (i) LDA, THF, 0 °C, N_2, rt for 16 h; (ii) LDA, THF, 0 °C, N_2, $CO_{2(g)}$, 10 min; (iii) dry ether, CH_2N_2, rt, 1 min; (iv) $KOH_{(aq)}$, rt, 70 h; (v) 10% KOH/MeOH, reflux, 7.5 h; (vi) dry ether, CH_2N_2, rt, 1 min.

They first acylated the dimethyl ether of methyl orsellinate (**91**) with dilithioacetylacetone (**92**) to give triketone (**93**). Carboxylation of the trilithium salt of triketone (**93**) gave triketo acid (**94**) which was esterified to give the ester (**95**). The ester (**95**) was treated with aqueous KOH which allowed a 1, 6 Claisen cyclization to the benzophenone (**96**) and ring closure was effected with methanolic KOH to give the xanthone (**97**), which was methylated to furnish lichexanthone (**98**).

Sandifer and co-workers realized the possibilities of cyclizing tetraketones such as (**102**) to xanthones, for example (**104**)[71] (***Scheme 20***). They successfully synthesized the fungal metabolite *ortho*-methylgriseoxanthone C (**104**).

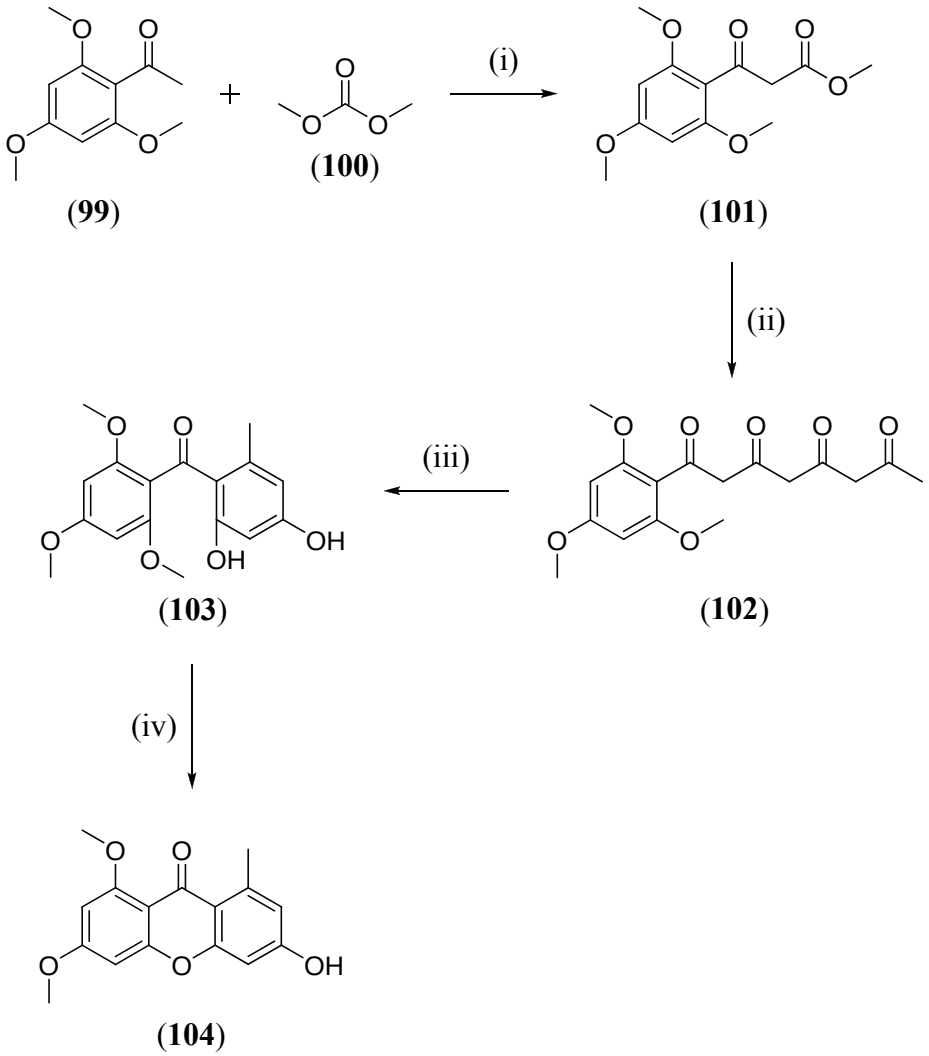

Scheme 20: (i) NaH, THF, rt, 1 h, N_2, reflux for 15 h; (ii) NaH, THF, (**92**), 0 °C, N_2, 30 min, 40 °C for 22 h; (iii) triethylamine, dry THF, reflux, N_2, 38 h; (iv) NaOMe, methanol, reflux, N_2, 63 h.

Reaction between the enolate anion of (**99**) and dimethyl carbonate (**100**) afforded the β-ketoester (**101**) which was subsequently acylated with dianion (**92**) to finally produce tetraketone (**102**). Under mildly basic conditions, tetraketone cyclized to the benzophenone (**103**). A second ring closure to *ortho*-methylgriseoxanthone C (**104**) occurred when benzophenone (**103**) was treated with sodium methoxide in methanol.

Although the cyclization of poly-β-ketones was considered a valuable addition to the many syntheses of xanthones, its approach is limited to simple xanthones due to the problems of many side reactions, poor yields and its inflexibility to more complicated xanthone structures. Thus in the last few years, many new approaches to synthesizing xanthones have been developed, some of which will be discussed in the next section.

NEW APPROACHES

Different methodologies to construct the xanthone core have emerged in the last two decades. The strategies to these methods were to provide an advantage for building highly polyoxygenated xanthones with regioselectivity. In this section a few examples will be discussed that have totally digressed from the classical approaches and have proved to be more successful[54].

HAUSER'S METHOD[72]

Hauser *et al.*[72] described the reaction between phthalide (**106**) and benzopyrone (**105**) to produce the natural product bikaverin (**2**) as portrayed in ***Scheme 21***.

Instead of synthesizing the carbonyl bridge and ether linkage which are distinctive to the xanthone nucleus, their approach involved building one of the aromatic rings onto the pre-built scaffold. Condensation of the anion of phthalide (**106**) with the chromone (**105**) furnished the xanthone (**107**) which was converted into bikaverin (**2**).

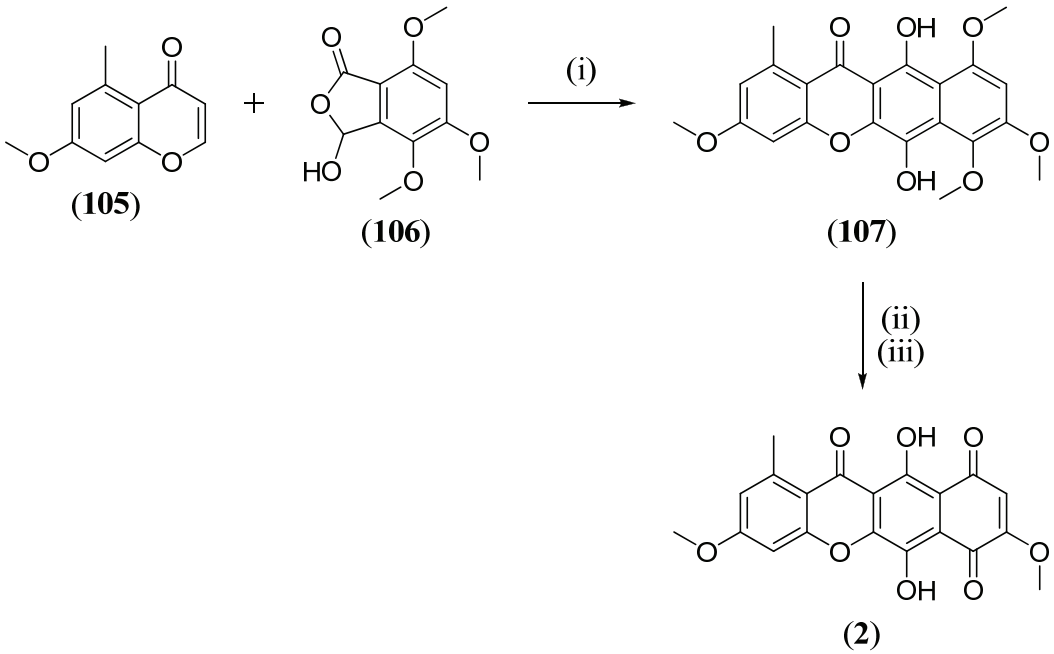

(**105**) (**106**) (**107**) (**2**)

Scheme 21: (i) LiO^{t}Bu, THF, –78 °C, reflux; (ii) Ag_2CO_3-celite; (iii) LiI, DMF.

The methodology was extended to angular polycyclic xanthones by condensation of benzopyranophthalide (**108**) with various Michael acceptors (**109**)[73] (***Scheme 22***). The synthesized benzophthalide was treated with LiO^{t}Bu and afforded the xanthone (**110**) in good yields.

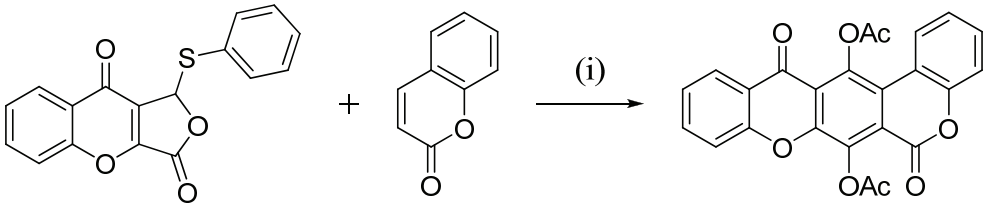

(**108**) (**109**) (**110**)

Scheme 22: (i) LiO^{t}Bu, THF, –78 °C, Ac_2O.

The annulation provides a general, high yielding route to not only xanthones but also xanthone containing polycyclic aromatic systems. The use of chromones as Michael acceptors expands the utility of the sulfone annulation for regiospecific preparation of xanthone systems[72].

LIEBESKIND-MOORE METHOD[74]

Liebeskind *et al.*[74] provided a novel approach to highly fused, highly substituted xanthones such as (**115**) using a process based on the benzannulation of alkenyl, aromatic and heteroaromatic lithiates for example (**112**) with dithiane protected benzopyrone-fused cyclobutenediones like (**111**). The lithiated alkene (**112**) attacks the less hindered carbonyl that also undergoes *ortho*-acylation to form the intermediate (**113**). The intermediate (**113**) undergoes a cascade of electrocyclization reactions initiated by the ring opening of the cyclobutanone ring to afford benzophenone (**114**) as shown in ***Scheme 23***. The dithiane group was removed and the benzophenone (**114**) underwent internal cyclization eliminating methanol to furnish the xanthone (**115**).

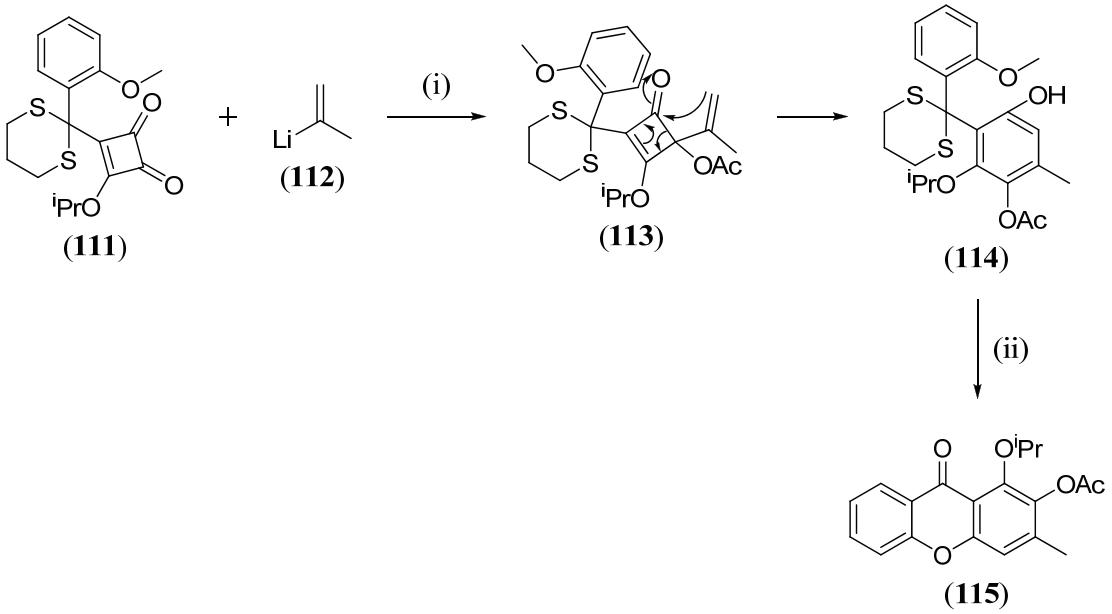

Scheme 23: (i) THF, –78 °C, Ac_2O, reflux; (ii) $HgCl_2/CaCO_3$, mesitylene/H_2O, reflux.

Another example using this methodology is the synthesis of the angular fused xanthone (**121**) (***Scheme 24***). 2-Hydroxyphenylacetaldehyde was protected with 1,3-propanedithiol to afford dithiane (**116**), which was reacted with the cyclobutenedione (**117**) to produce adduct (**118**). Treatment of the intermediate (**118**) with 2-lithiodihydrofuran (**119**) afforded compound (**120**) regiospecifically. The angular fused xanthone (**121**) was directly formed under the Hg(II)-catalyzed reaction conditions used for hydrolyzing the dithiane group.

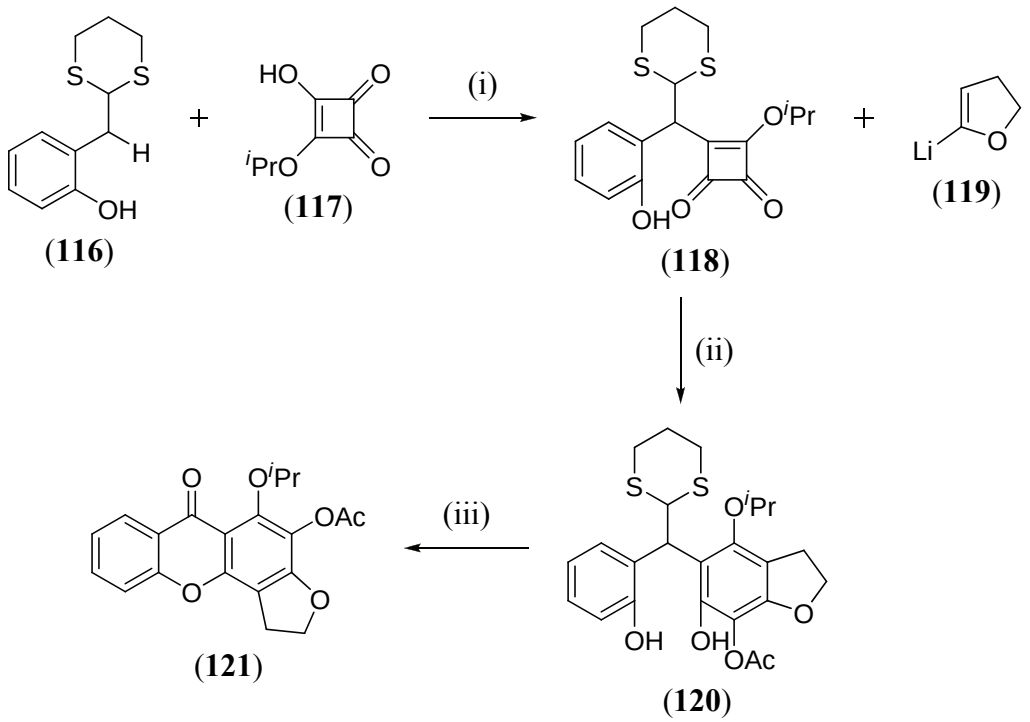

Scheme 24: (i) ^{t}BuLi, dry THF, -78 °C; (ii) Ac_2O, -78 °C, dry THF, reflux; (iii) $HgCl_2/CaCO_3$, mesitylene/H_2O, reflux.

This is a synthetically flexible approach to highly substituted xanthones which relies on cyclobutenediones as scaffolds for the construction of a diverse range of molecular structures. The control of regiochemistry combined with short reaction sequence make it an attractive approach to naturally occurring xanthones as long as cyclobutenediones are available[75]. However, the availability or synthesis of the cyclobutenediones is the limitation of this methodology

CASILLAS'S METHOD[76]

Casillas *et al.*[76] developed an alkylnitrilium modification of the Hoeben-Hoesch reaction to synthesize xanthone derivatives. Their synthesis was based on the reactivity of *N*-alkylnitrilium salts with activated aromatic rings in a Friedel Crafts reaction. This strategy hinges on the reaction of the appropriate arylnitrile (**122**) and an excess of benzoate (**123**) as shown in ***Scheme 25***. The acylation reaction of alkylnitrilium salts surpasses the Hoeben-Hoesch acylation method, shown in the prior section during Nishikawa and co-workers' ketimine synthesis[67], owing to the enhanced electrophilicity of the intermediate.

The nitrilium salt was prepared from 2-fluoro-6-methoxybenzonitrile (**122**) using the Lewis acid $SbCl_5$ in 2-chloropropane. The nitrilium salt (**123**) was reacted with the methyl ester (**124**) to form the benzophenone ketimine (**125**), which was treated with a base to hydrolyze (**125**) to the desired xanthone (**126**).

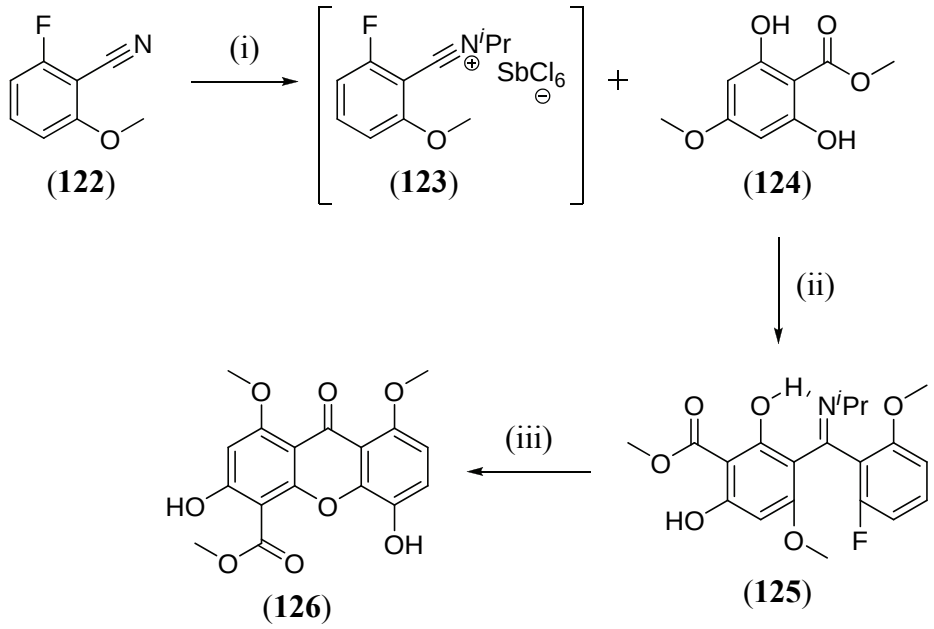

Scheme 25: (i) $SbCl_5$, 2-chloropropane,dry CH_2Cl_2, rt, 2 h; (ii) reflux, 60 h, dry CH_2Cl_2, (iii) K_2CO_3, dry acetonitrile, reflux, 23 h, $MeOH/H_2O$.

The construction and dual protection of the nitrile group provides a general strategy for the synthesis of complex xanthone based natural products[77].

GHOSH'S METHOD[78]

Ghosh *et al.*[78] synthsized xanthones using a Diels Alder [4+2] cycloaddition reaction. Their approach was similar to Hauser *et al.*[72]; whereby they built the second aromatic ring onto the pre-existing carbonyl bridge and ether linkage, contained within a chromanone.

The dienamine (**127**) was reacted with *N*-phenylmaleimide (**128**) to form the [4+2] cycloadduct which readily eliminates dimethylamine to form the xanthone (**130**) as depicted in ***Scheme 26***.

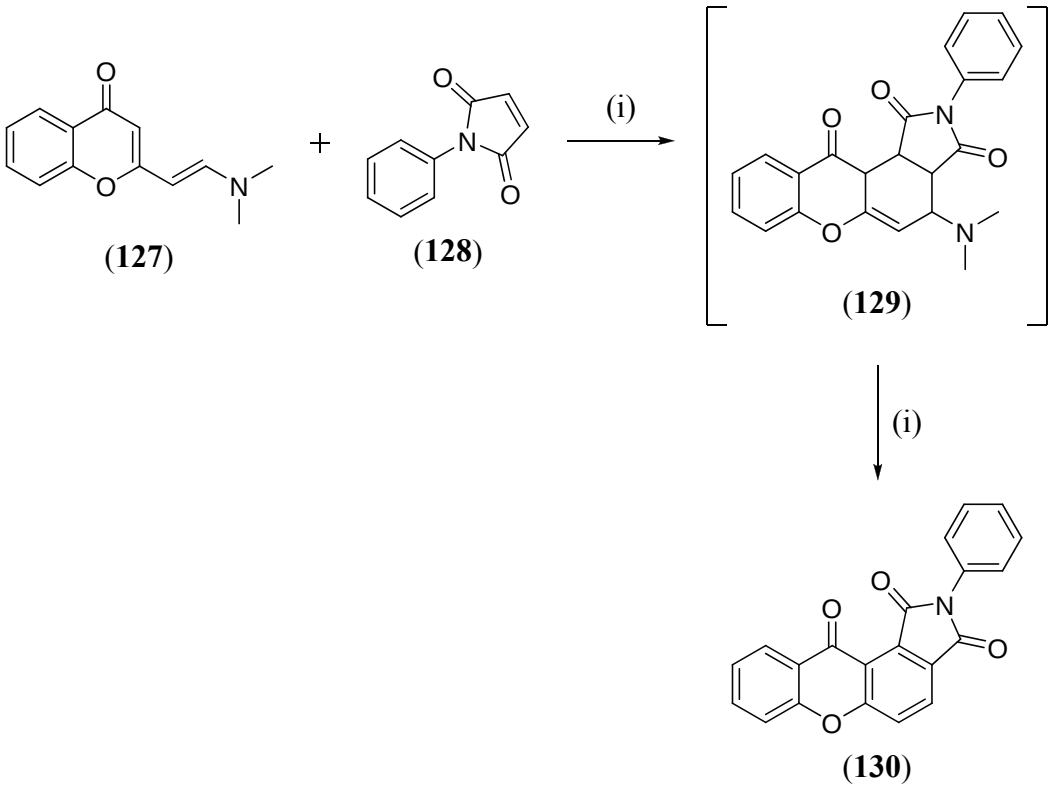

(**127**) (**128**) (**129**) (**130**)

Scheme 26: (i) reflux, DMF, 8 h.

A similar reaction was carried out on an alkyne system[79]. The dimethyl acetylene dicarboxylate (**131**) with benzopyrone (**127**) was subjected to Diels Alder conditions to give xanthone (**134**) (***Scheme 27***).

The formation of the xanthone is due to the benzopyrone (**127**) behaving like an unconjugated amine in undergoing [2+2] cycloaddition with the alkyne (**131**) to give adduct (**133**) which undergoes ring opening and isomerizes to (**132**). The ring opened intermediate (**133**) incorporating a pre-existing double bond at the pyran 2,3 position, behaves as a hexatriene system and by electrocyclization and subsequent elimination of dimethylamine affords xanthone (**134**).

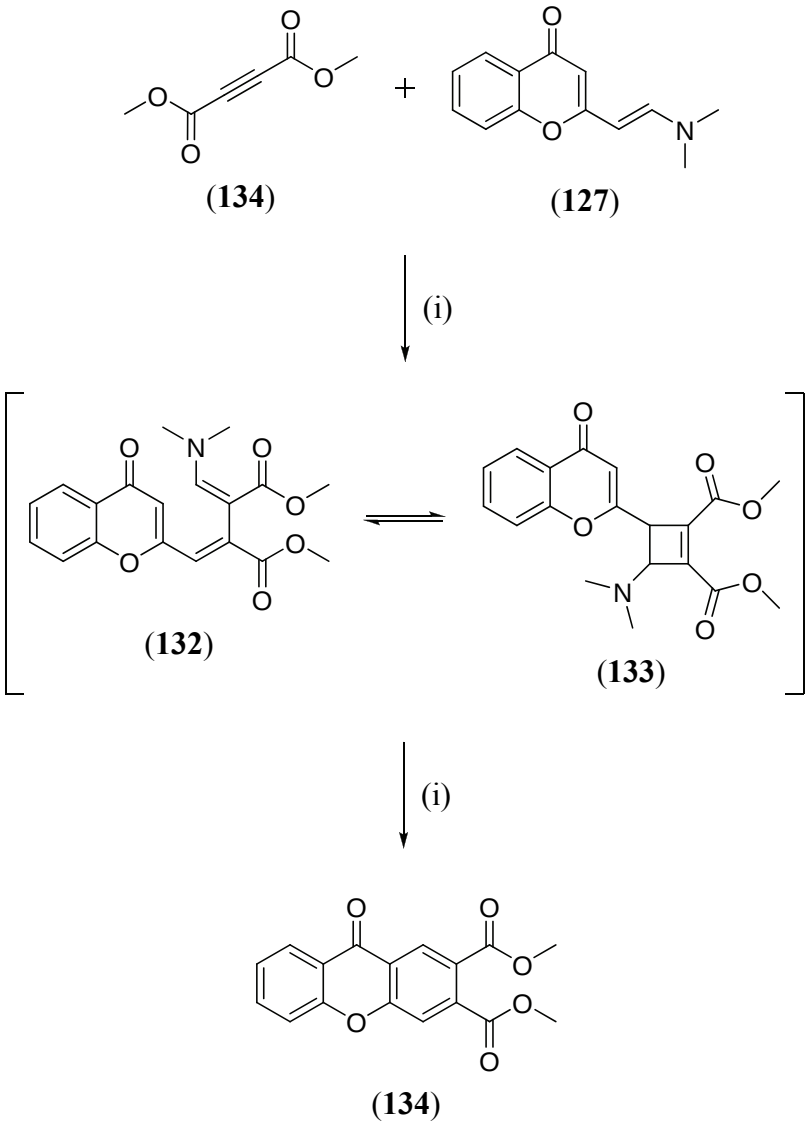

Scheme 27: (i) reflux, DMF, 8 h.

These reactions are successful with both weak and reactive dienophiles and provide another useful route of accessing highly substituted xanthones, which ultimately could lead to attractive syntheses of more complex naturally occurring xanthones.

These are only a few examples of the new methods that are being used to synthesize xanthones. As appealing as many of these methods are, some are limited to availability of starting materials and the synthesis of their precursors thus there is room for new and other more versatile methods towards the synthesis of xanthone containing compounds.

AIMS OF PROJECT

Xanthones are an important class of organic compounds. They have diverse biological properties, many of which are potential leads to pharmaceuticals against diseases such as malaria, HIV-AIDS and various cancers. These pharmacological properties have led to many groups researching the synthesis and biological properties of naturally occurring and synthetic xanthones, which have been discussed in the previous section.

Earlier in the introduction, the synthesis of bikaverin (**2**) using a novel route by de Koning and co-workers was discussed[4]. The University of the Witwatersrand (WITS) interest for this dissertation was to synthesize other xanthone containing compounds using the same route employed in the synthesis of bikaverin (**2**) by de Koning *et al.*[4]. We wished to test the flexibility of the methodology towards the synthesis of simple xanthone compounds and if successful to apply the methodology to more complex xanthones. The synthetic route we initially wished to attempt is illustrated in ***Scheme 28***.

As a starting point we wished to assemble the simple xanthones such as (**140**). For this approach salicylic acid and 1,4-naphthoquinone would be our initial starting materials. We believed that using a number of simple synthetic steps we would gain access to the bridged carbonyl compound (**135**). This would represent a key intermediate on which hydrogenolysis could be performed to afford (**136**). We would now be in a position to attempt our DDQ mediated reaction. Hence, phenol (**136**) would be treated with DDQ in an analogous manner to that described by de Koning to form spiro-compound (**137**). Compound (**137**) would subsequently be hydrolyzed to the trione (**138**) using TFA. The trione (**138**) we hoped would then undergo pyrolytic isomerization at 200^{o}C under reduced pressure to afford the desired xanthone (**139**), which will be oxidized to xanthone (**140**) using silver(I)oxide in the presence of air.

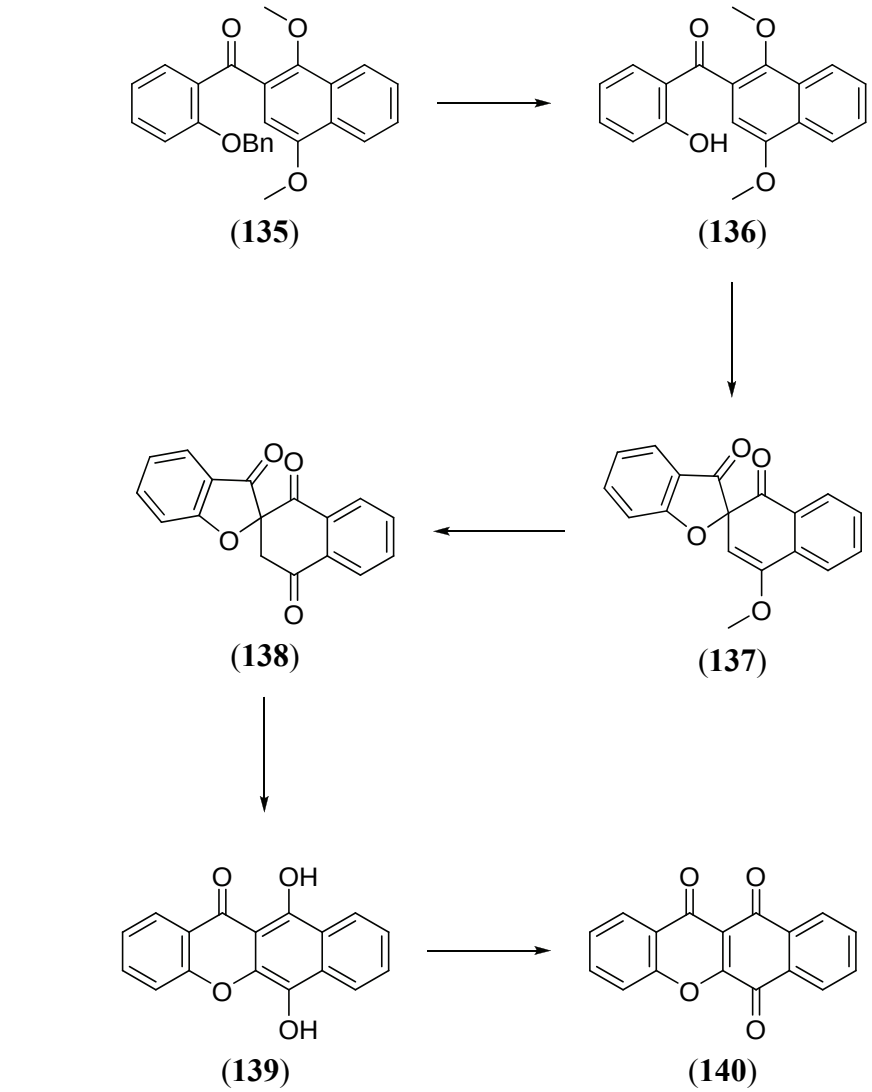

(**135**) (**136**) (**137**) (**138**) (**139**) (**140**)

Scheme 28

After applying the methodology to hopefully afford simple xanthones, the methodology would then be applied to assemble more complex systems such as (**143**) with more complex starting materials such as highly substituted 1,4-naphthoquinones (**141**) and substituted salicylic acids (**142**) as shown in ***Scheme 29***.

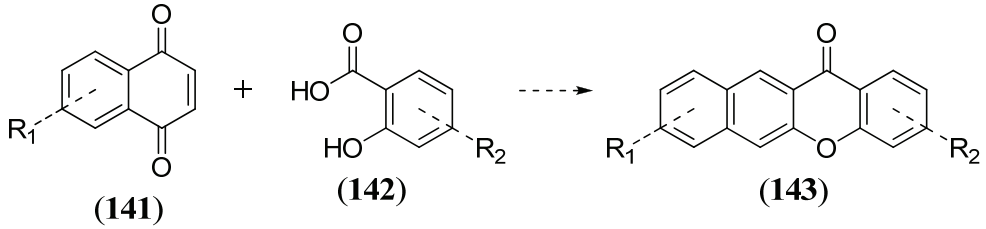

(**141**) (**142**) (**143**)

Scheme 29

The work that was carried out in this MSc using the proposed methodology was partially successful but as will be discussed later led to some novel and unexpected results, which has opened the door to wider research into this area. These results will be discussed in the next chapter.

RESULTS AND DISCUSSION

SYNTHESIS OF 12a-METHOXY-5*H*-BENZO[c]XANTHENE-5,7(12a*H*)-DIONE

PREPARATION OF BENZYL 2(BENZYLOXY)BENZOATE

As a starting point the reactive functional groups on the starting material, salicylic acid (**144**) needed to be masked hence, similar to the procedure used by de Koning *et al.*[4], salicylic acid (**144**) was treated with potassium carbonate in order to deprotonate both the phenol and carboxylic acid functional groups. The addition of benzyl bromide (**146**) then resulted in the formation of the desired product (**147**) as shown below in ***Scheme 30***.

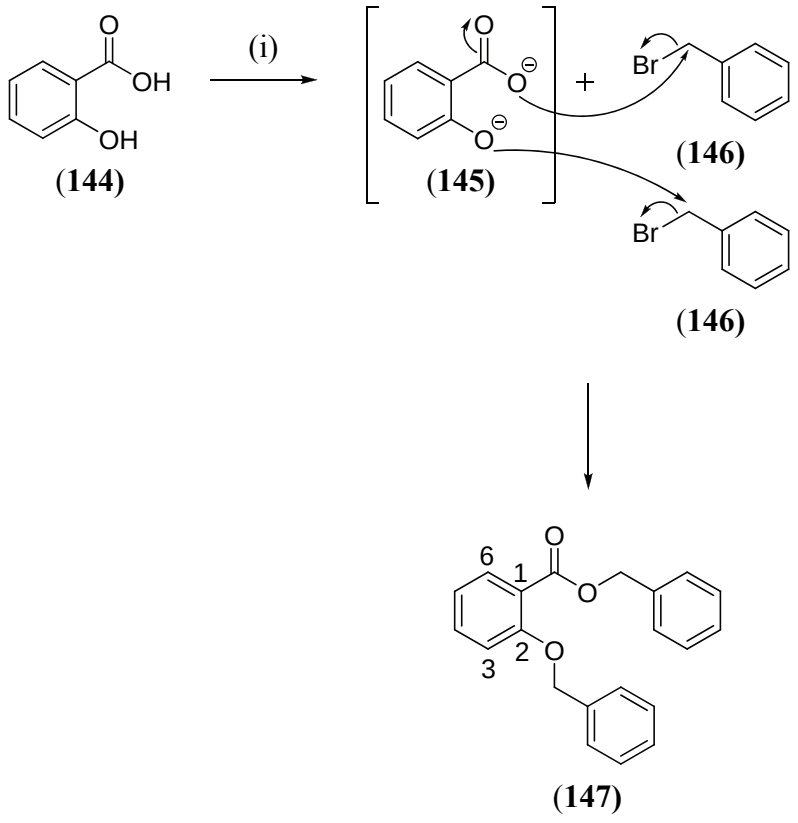

Scheme 30: (i) K_2CO_3, acetone, benzyl bromide, reflux, 18 h, $N_{2(g)}$, 87%.

The reaction is a classic electrophilic substitution reaction via an S_N2 mechanism hence substitution occurred via a transition state rather than an intermediate. The base, potassium carbonate, deprotonated both the acid and the phenol and formed an

alkoxide ion (**145**), while the benzyl bromide (**146**) acted as a suitable electrophile. The reaction occurred quite rapidly via the S_N2 mechanism.

The ^1H NMR spectrum showed two singlets with a chemical shift (δ) at 5.33 ppm and 5.13 ppm both integrating for 2 protons. These signals are for the methylene groups and the peak at 5.33 ppm is slightly deshielded from the peak at 5.13 ppm indicating that it is the methylene group bonded to the ester functionality. *Inter alia*, a doublet of doublets is seen at 7.85 ppm integrating for 1 proton. This is hydrogen in the 6-position of (**147**). The doublet of doublets was due to *ortho*- and *meta*- coupling of the hydrogen in the 6-position with the coupling with the hydrogens in the 5- and 4-position of (**147**) respectively. This was indicated by the coupling constants of 7.7 Hz and 1.7 Hz which corresponded to the hydrogen coupling to the hydrogen in the *ortho*- and *meta*- positions of the aromatic ring respectively. The ^{13}C NMR spectrum showed, *inter alia*, two signals at 66.6 ppm and 70.5 ppm which corresponded to the two methylene carbons. The signal at 70.5 ppm appeared further downfield because it was bonded to the ester moiety. Another characteristic peak was at 166.2 ppm which was due to the carbonyl functional group from the ester moiety. There were also four quaternary aromatic carbons at 158.1 ppm, 136.5 ppm, 136.0 ppm and 128.4 ppm that are unique to our protected salicylic acid (**147**). The IR spectrum showed a strong signal at 1716 cm^{-1} that was characteristic of a carbonyl stretching and two strong signals at 1233 cm^{-1} and 1072 cm^{-1} which were characteristic of a carbon single bonded to oxygen. The absence of a strong broad signal around 3300 cm^{-1}, which was representative of a hydroxy group of the salicylic acid (**144**), suggests that both the carboxylic acid and phenol had been converted into an ester and ether respectively. The melting point of 47 ˚C - 49 ˚C was close to that of the literature melting point of 50 ^oC - 51 ^oC[80]. The product was confirmed as benzyl 2-(benzyloxy)benzoate (**147**).

PREPARATION OF 1,4-DIMETHOXYNAPHTHALENE

In a parallel synthesis the reactive carbonyls of the 1,4-naphthoquinone (**148**) needed to be protected (***Scheme 31***). To this effect 1,4-naphthoquinone (**148**) was first reduced to hydroquinone (**150**) using sodium dithionite via what is believed to be an anionic radical mechanism[81]. The radical anion initially formed was very basic and in

the presence of a proton and a reducing agent, a radical (**149**) is formed. The radical intermediate (**149**) is then provided with another electron and forms an anion, which ultimately obtains a second proton and forms hydroquinone (**150**). The key to the reduction is that electrons can reduce any functional group with a low energy π antibonding orbital, such as carbonyls, into which electrons could enter. The product (**150**) was immediately used in the next step of the reaction because the hydroquinone (**150**) would be oxidized back to the 1,4-naphthoquinone (**148**) by air.

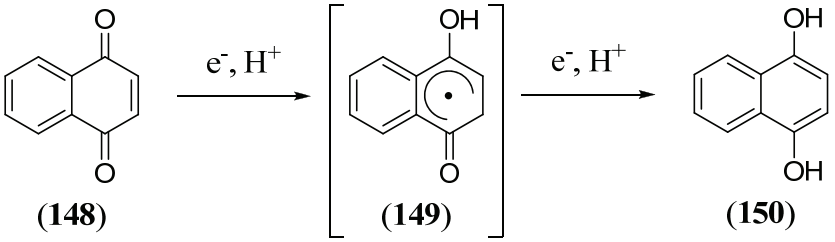

(148) **(149)** **(150)**

Scheme 31

The reaction of dimethyl sulfate (**152**) with hydroquinone (**150**) is essentially an electrophilic substitution similar to that of benzyl bromide (**146**) with salicylic acid (**144**) (***Scheme 30***). The potassium carbonate abstracts the acidic phenolic proton to form the hydroquinone anion (**151**). This reacts with the electrophilic methyl substituent of dimethyl sulfate (**152**) to ultimately form 1,4-dimethoxynaphthalene (**153**) as shown in ***Scheme 32***.

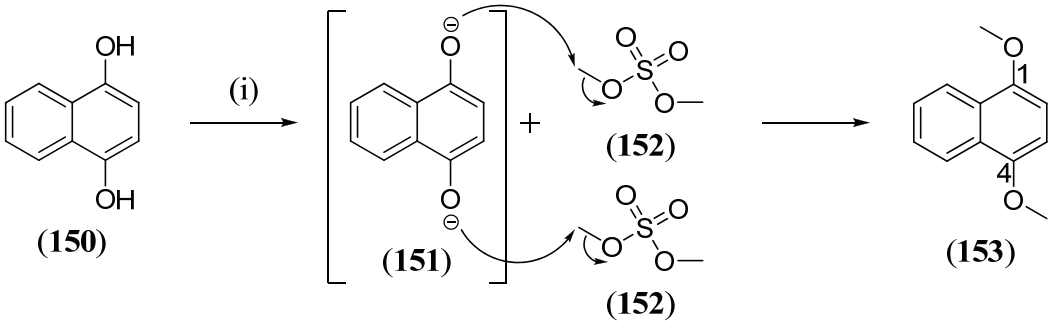

(150) **(151)** **(152)** **(152)** **(153)**

Scheme 32: (i) $(CH_3)_2SO_4$, acetone, K_2CO_3, reflux, 18 h, $N_{2(g)}$, 85%.

The reaction proceeded smoothly to give (**153**) in 85% yield.

The ^{1}H NMR spectrum showed a singlet at 4.00 ppm which integrated for 6 protons, characteristic of the two methoxy groups at the 1- and 4-positions of (**153**). Another singlet occurred at a chemical shift of 6.73 ppm for the hydrogens in the 2- and 3-position of (**153**). These singlets occurred due to the symmetry of the molecule thus there is no coupling between these two hydrogens. The ^{13}C NMR spectrum showed two quaternary signals at 149.5 ppm and 126.4 ppm. The peak at 149.5 ppm corresponded to the carbon attached to the methoxy groups at the 1- and 4-positions therefore it is further downfield from the other quaternary peak at 126.4 ppm, which is due to the bridging carbons. Another signal at 55.7 ppm was characteristic of a methoxy group. The absence of quaternary signals around 160-180 ppm indicated the absence of the quinone carbonyl. The IR spectrum showed the absence of a sharp peak around 1700 cm^{-1} which was characteristic of ketone vibrational stretching but showed two strong signals at 1058 cm^{-1} and 1231 cm^{-1} which are due to a carbon single bonded to oxygen, which suggests that the quinone has successfully been converted into an aromatic ether. The product was confirmed as 1,4-dimethoxynaphthalene (**153**).

SYNTHESIS OF 2-(BENZYLOXY)BENZOIC ACID

The ester (**147**) was selectively deprotected by base catalyzed hydrolysis of the ester moiety to its corresponding carboxylic acid (**155**). The base catalyzed hydrolysis of the ester was irreversible (***Scheme 33***). The tetrahedral intermediate (**154**) could give back the ester (**147**) or go in a forward sense to the carboxylic acid (**155**). Under basic conditions the formation of the acid was irreversible as it was deprotonated to form the carboxylate salt (**156**) that was hydrolysed in a separate reaction to the corresponding benzoic acid (**155**) upon work up with acid. Due to the formation of the carboxylate salt (**156**), at least one mole equivalent of base was required.

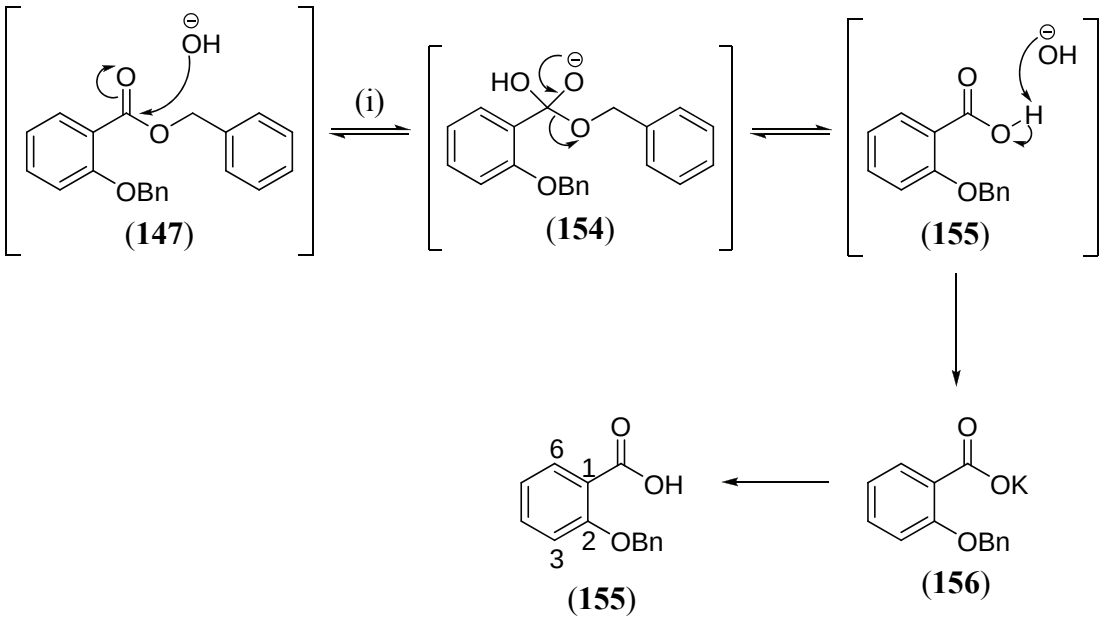

Scheme 33: (i) 12% KOH/methanol, reflux, 18 h, $N_{2(g)}$, HCl, 86%.

The ^{1}H NMR spectrum showed a broad singlet at 10.71 ppm, which integrated for 1 proton that corresponded to the hydroxy group. A singlet at 5.48 ppm was characteristic of the methylene group from the remaining benzyl ether. The doublet of doublets has shifted downfield from 7.85 ppm to 8.14 ppm was assigned to the proton on the aromatic ring in the 6-position of (**155**), since it was adjacent to a carbon at the carboxylic acid rather than an ester. The absence of second singlet at about 5.00 ppm suggested that the benzyl group attached to the ester moiety had been cleaved and the ester successfully hydrolyzed to the carboxylic acid (**155**) without the removal the second benzyl group. The ^{13}C NMR spectrum showed four quaternary peaks at 166.2 ppm, 157.6 ppm, 134.7 ppm and 118.1 ppm, one less than the starting material. The peak at 166.2 ppm corresponded with the carbonyl group of the carboxylic acid (**155**) while the peak at 118.1 ppm corresponded to the quaternary aryl carbon of the benzyl group. A characteristic peak in the ^{13}C NMR spectrum at 72.02ppm was due to a methylene group. The absence of a second peak in the region suggested that the second benzyl substituent had been successfully hydrolyzed. The IR spectrum showed a strong broad peak at 2970 cm^{-1} which was due to a hydroxy bond stretching band. The broad peak was due to the hydroxy peak hydrogen bonding to the carbonyl group of another molecule. The strong sharp peaks at 1674 cm^{-1} and 1232 cm^{-1} are characteristic of carbonyl stretching and a carbon single bonded to oxygen respectively. The melting point of 72˚C - 75˚C was identical to that of the literature

value of 73.5˚C – 74.5˚C and suggested that the reaction was successful[82]. The product was confirmed as 2-(benzyloxy)benzoic acid (**155**).

SYNTHESIS OF (2-(BENZYLOXY)PHENYL)(1,4-DIMETHOXYNAPHTHALEN-2-YL)METHANONE USING TFAA

The building of the carbonyl bridge of the xanthone nucleus was one of the key reactions of our synthesis. de Koning *et al.*[4] used trifluoroacetic anhydride (TFAA) (**160**) together with 2-benzyloxy-4-methoxy-6-methylbenzoic acid (**5**) and 1,2,4,5,8-pentamethoxynaphthalene (**4**) to form the carbonyl bridge between the two compounds in reasonable yield (***Scheme 34***).

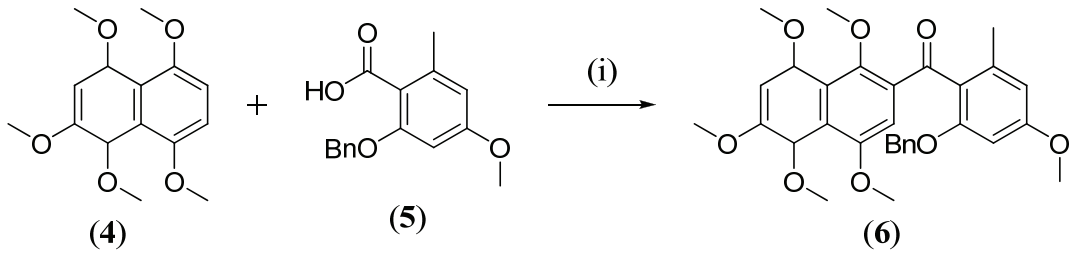

(**4**) (**5**) (**6**)

Scheme 34: (i) TFAA, dry CH_2Cl_2, rt, 90 h, 51%.

Sundholm[83] had shown that aromatic acylation using an oxygenated benzene compound such as 1,3,5-tris(benzyloxy) benzene (**158**) and a substituted benzoic acid (**157**) in the presence of TFAA also proceeded to give the carbonyl bridged compound (**159**) in very high yield (***Scheme 35***).

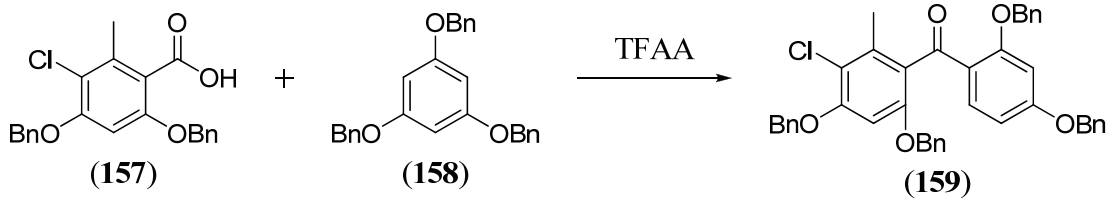

(**157**) (**158**) (**159**)

Scheme 35

The 1,4-dimethoxynaphthalene (**153**) is not as electron rich as the 1,2,4,5,8-pentamethoxynaphthalene (**4**) and the Friedel-Crafts type reaction with TFAA proceeds best with highly oxygenated systems. Thus the 1,4-dimethoxynaphthalene (**153**) used in the reaction was a poorer nucleophile than 1,2,4,5,8-

pentamethoxynaphthalene (**4**) used by de Koning *et al*.[4] and this was a possible reason attributed to the poor yield of 30% obtained in this reaction.

The first step in this reaction was to form the mixed anhydride (**162**) which was pivotal to the Friedel Crafts reaction between the 1,4-dimethoxynaphthalene (**153**) and the 2-(benzyloxy)benzoic acid (**155**) (***Scheme 36***). The nucleophilic oxygen from the carboxylic acid (**155**) added to the electrophilic carbonyl group of the trifluoroacetic anhydride (**160**) and formed a tetrahedral intermediate (**161**). The tetrahedral intermediate (**161**) was highly unstable and underwent an elimination of trifluoroacetic acid (TFA). The elimination of the trifluoroacetate anion and the proton resulted in the formation of the desired mixed anhydride (**162**).

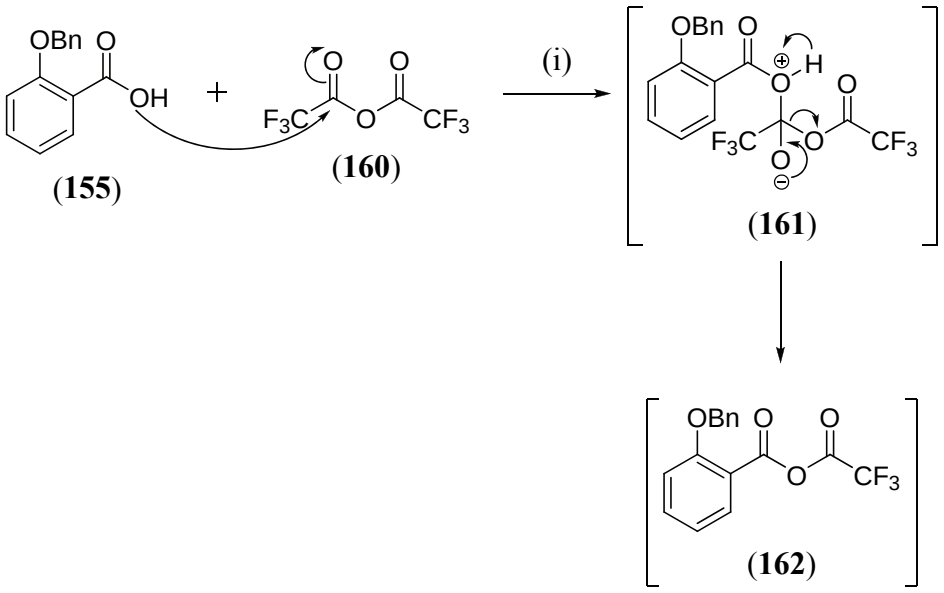

Scheme 36: (i) TFAA, dry CH_2Cl_2, rt, 48 h.

As fluorine is very electronegative the carbonyl adjacent to the aromatic ring is more susceptible to nucleophilic attack hence the 1,4-dimethoxynaphthalene (**153**) acted as the nucleophile to initially form the intermediate (**163**), which aromatized to afford the required ketone (**135**) (***Scheme 37***).

The diacylated and triacylated products reported by de Koning *et al*.[4] in their synthesis were not produced. Only the starting materials and the desired ketone (**135**) formed in 30% yield were recovered through column chromatography.

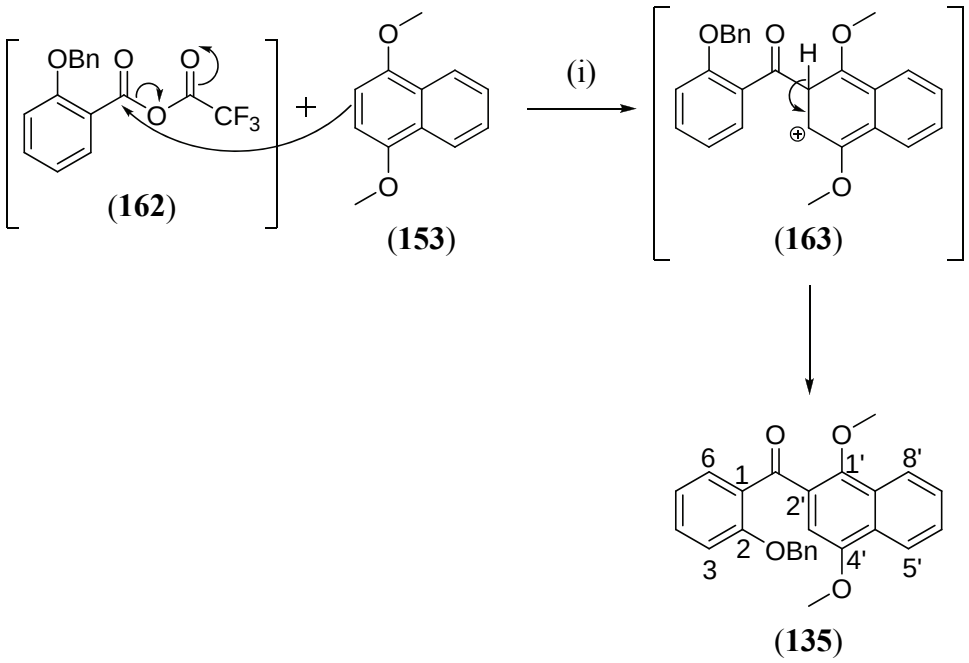

Scheme 37: (i) TFAA, dry CH_2Cl_2, rt, 48 h, 30%.

The ^{1}H NMR spectrum showed singlets at a chemical shift of 3.91 ppm and 3.59 ppm. These singlets corresponded to the methoxy groups at the 1'- and 4'-positions of (**135**) as they integrated for 3 protons each. The singlet at 3.91 ppm appeared downfield because of the presence of the carbonyl group attached to the 2'-position which deshielded the methoxy group. Another singlet with a chemical shift of 4.89 ppm was characteristic of the methylene group from the benzyloxy substituent (**155**) as it integrated for 2 protons. A doublet appeared at 6.74 ppm and was due to the hydrogen at the 3-position coupling with the hydrogen at the 4-position as the signal integrated for 1 proton. Another doublet appeared at 7.69ppm and was due to the hydrogens at the 8'-positions as well as the 5'-positions of (**135**). The molecule is symmetrical in the region therefore the doublet integrated for 2 protons. The doublet formed by the hydrogen in the 5'-position coupling with the hydrogen in the 6'-position and the hydrogen in the 7'-position coupling with the hydrogen in the 8'-position exhibited identical shifts. A characteristic shift was the singlet at 6.87 ppm which was due to the isolated hydrogen in the 3'-position of (**135**). These shifts verified that the 1,4-dimethoxynaphthalene (**153**) had reacted with the 2-(benzyloxy)benzoic acid (**155**). The ^{13}C NMR spectrum showed a peak at 196.3 ppm which was characteristic of a ketone carbonyl. The peaks at 55.8 ppm and 63.6 ppm corresponded to the carbons of the methoxy groups while the peak at 70.3 ppm was due to the carbon from the

benzyloxy methylene. Two signals at 150.3 ppm and 151.7 ppm were due to the carbons on the naphthalene ring attached to the methoxy substituents, while a signal at 157.5 ppm corresponded to the benzyl ether carbon. These shifts proved that the carbonyl bridge was formed between the 2-(benzyloxy)benzoic acid (**155**) and 1,4-dimethoxynaphthalene (**153**). The IR spectrum showed a strong sharp signal at 1734 cm^{-1} which was characteristic of carbonyl stretching vibrations. The peaks at 1290 cm^{-1} and 1096 cm^{-1} were due to carbon single bonded to oxygen stretching vibrations from the methoxy and benzyloxy groups respectively. There was an absence of a strong broad peak at 3000 cm^{-1} thus the absence of the hydroxyl group from the carboxylic acid also suggested that the carbonyl bridge was formed. The mass spectrum showed an ion of 398.1523 which correlated with the calculated mass, 398.1518 of the desired ketone (**135**). The product was thus confirmed as (2-(benzyloxy)phenyl)(1,4-dimethoxynaphthalen-2-yl)methanone (**135**).

Although the reaction was successful, the yields were poor with a maximum yield of 30%, when the reaction was heated under reflux in chloroform for 90 hours. Apart from the poor yields, separation of the ketone (**135**) from the starting material was arduous involving extensive use of column chromatography. To test the flexibility of the entire synthetic route, another method was sought to form the ketone (**135**).

In their pursuit to successfully synthesize nigrolineaxanthone F (**164**) and osajaxanthone (**165**), Argade and co-workers formed the carbonyl bridge of the xanthone nucleus to yield (**168**) by reacting *n*-butyllithium with 2-bromo-1,3,5-trimethoxybenzene (**166**) followed by methyl-2,5-(dibenzyloxy)benzoate (**167**)[84] (***Scheme 38***).

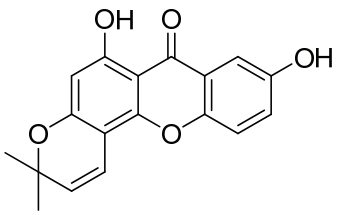

(**164**)

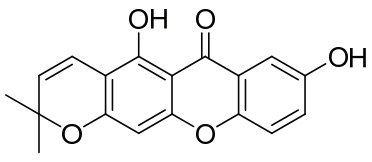

(**165**)

Figure 15: The structure of nigrolineaxanthone F (**164**) and osajaxanthone (**165**).

We therefore decided that the carbonyl bridge could be formed using similar methodology by first brominating 1,4-dimethoxynaphthalene (**153**) and then under the same conditions as described above by reacting it with benzyl 2-(benzyloxy) benzoate (**147**).

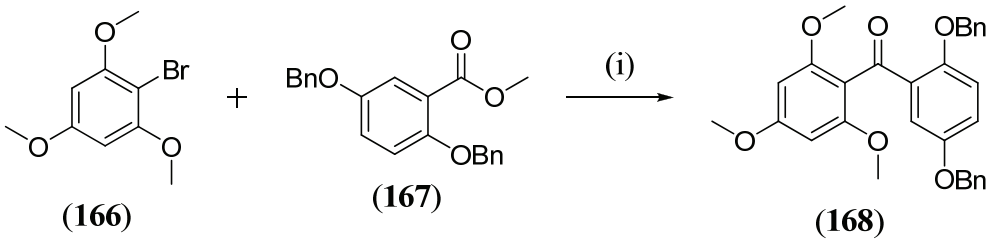

(**166**) (**167**) (**168**)

Scheme 38: (i) *n*-BuLi, dry THF, –78 °C,1.5 h.

SYNTHESIS OF 2-BROMO-1,4-DIMETHOXYNAPHTHALENE

Bloomer *et al.*[85] have used *N*-bromosuccinimide (NBS) (**169**) as a mild brominating reagent for polyalkoxyaromatic systems such as 1,4-dimethoxynaphthalene (**153**) as shown in ***Scheme 39***. The reaction is believed to occur through an electrophilic substitution process. The naphthalene system was not very reactive and would only react with good electrophiles such as cationic bromine. The methoxy groups at the 1- and 4-positions of the naphthalene ring donate electron density into the ring and were thus *ortho*-directors. One mole equivalent of NBS (**169**) was added and due to the symmetry of 1,4-dimethoxynaphthalene (**153**) only one product was formed. The NBS (**169**) provided the electrophilic bromine that reacted with the 1,4-dimethoxynaphthalene (**153**) at the 2-position and produced the cation intermediate (**170**). The loss of the proton from the cation intermediate restored the aromaticity and furnished 2-bromo-1,4-dimethoxynaphthalene (**171**).

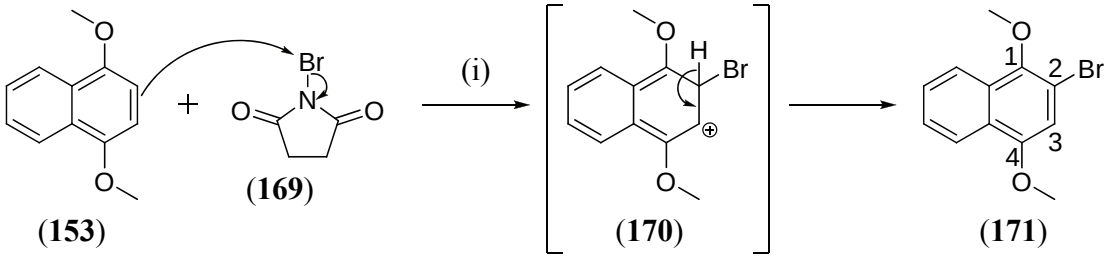

(**153**) (**169**) (**170**) (**171**)

Scheme 39: (i) NBS, dry CH_2Cl_2, rt, 18 h, 90%.

The ^{1}H NMR spectrum showed two singlets at a chemical shift of 3.97 ppm and 3.98 ppm that integrated for 3 protons each. These signals suggested that the symmetry of the 1,4-dimethoxynaphthalene (**153**) was now absent. A singlet appeared at 6.91 ppm and integrated for 1 proton and corresponded to the single proton at the 3-position of (**171**). The ^{13}C NMR spectrum showed five quaternary carbon signals at 152.1 ppm, 146.6 ppm, 128.9 ppm, 125.7 ppm and 111.8 ppm. The signals at 152.1 ppm and 146.6 ppm were characteristic of the carbons bonded to the methoxy groups, while the signal at 111.8 ppm was due to the carbon bonded to the bromine rather than hydrogen. Two signals at 61.3 ppm and 55.7 ppm corresponded to the carbons of the two methoxy groups. The IR spectrum showed a strong sharp peak at 773 cm^{-1} that was due to a carbon single bonded to a halide stretching vibration. The strong signal at 1105 cm^{-1} was characteristic of a carbon single bonded to oxygen stretching vibration and was attributed to the methoxy group. The melting point of 56˚C - 58˚C was very close to that reported in the literature of 54˚C - 55˚C and suggested that the desired product was formed[86]. The product was confirmed as 2-bromo-1,4-dimethoxynaphthalene (**171**).

SYNTHESIS OF (2-(BENZYLOXY)PHENYL)(1,4-DIMETHOXYNAPHTHALEN-2-YL)METHANONE USING *n*-BUTYL LITHIUM

The carbonyl bridge of the xanthone nucleus of (**135**) was synthesized in two steps from naphthalene (**171**). Firstly, the organometallic reagent (**173**) needed to be synthesized (***Scheme 40***). The methoxy functional group guided the butyllithium, so that it attacked the adjacent bromine. This was done via a presumed complex (**172**) formed between the oxygen from the methoxy group and the electron deficient lithium atom. The complexation facilitates lithium-halogen exchange.

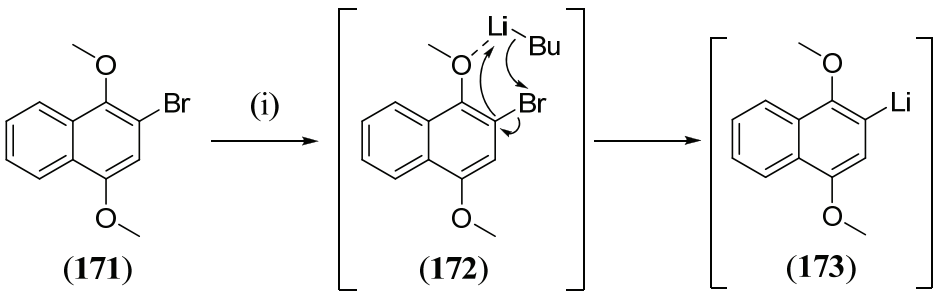

(171) **(172)** **(173)**

Scheme 40: (i) *n*-BuLi, dry THF, –78 ˚C, $N_{2(g)}$, 1.5 h.

The 2-bromo-1,4-dimethoxynaphthalene (**171**) underwent lithium-halogen exchange to form the lithiated product (**173**). The second step was then the slow addition of the lithiated product (**173**) to the benzyl 2-(benzyloxy)benzoate (**147**) (***Scheme 41***).

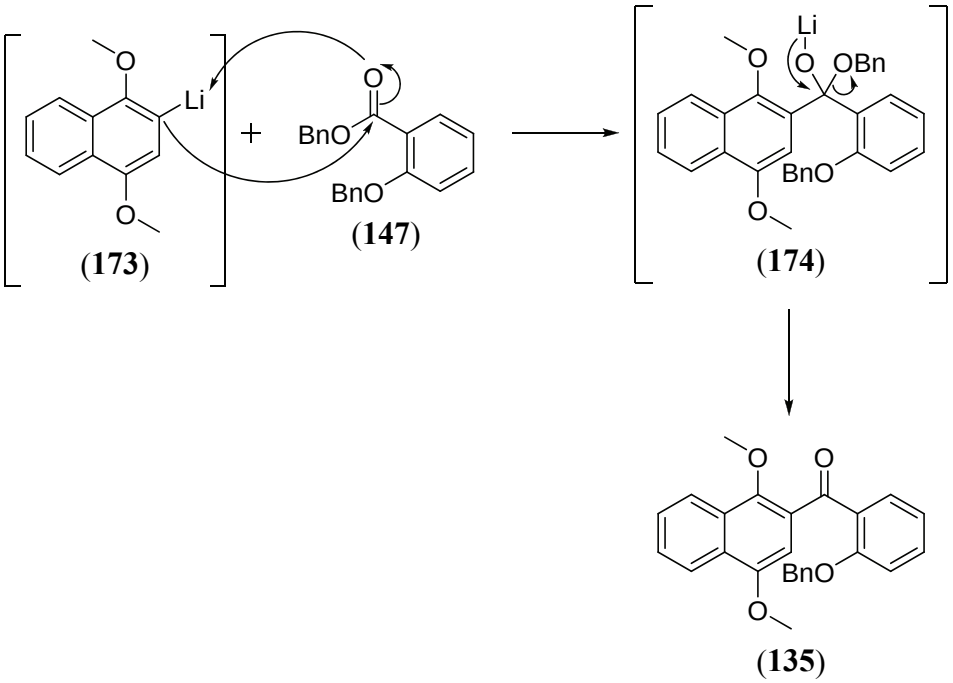

Scheme 41: (i) *n*-BuLi, dry THF, –78 ˚C, $N_{2(g)}$, 1.5 h, 89%.

It was important that the organolithiated compound (**173**) as added slowly to the benzyl 2-(benzyloxy)benzoate (**147**) to prevent the very reactive lithiated 1,4-dimethoxynaphthalene (**173**) from adding twice to the ester (**147**). Another factor that prevented the second addition was the presence of the bulky benzyloxy group that could have caused steric hindrance and worked in the favour of a single addition. The nucleophilic lithiated 1,4-dimethoxynaphthalene (**173**) attacked the carbonyl and formed the tetrahedral intermediate (**174**) that readily eliminated the benzyloxy anion and furnished the desired protected ketone (**135**) in 89% yield.

The ^{1}H NMR, ^{13}C NMR and IR spectra all correlated exactly to that of the product (**135**) formed using TFAA in the Friedel-Crafts reaction.

SYNTHESIS OF (1,4-DIMETHOXYNAPHTHALEN-2YL)(2-HYDROXYPHENYL) METHANONE

The benzyl group had to be removed to prepare the compound for the next step that involved utilizing DDQ. Palladium on carbon under a hydrogen atmosphere of 4.5 bars was chosen as it is a clean and efficient method for the removal of *O*-benzyl groups in our laboratories and therefore should provide the same results for our benzyl substituent (**135**). The palladium was precipitated onto the carbon. The palladium provided maximum surface area for the reaction it catalysed. The hydrogen was adsorbed onto the surface of the metal.

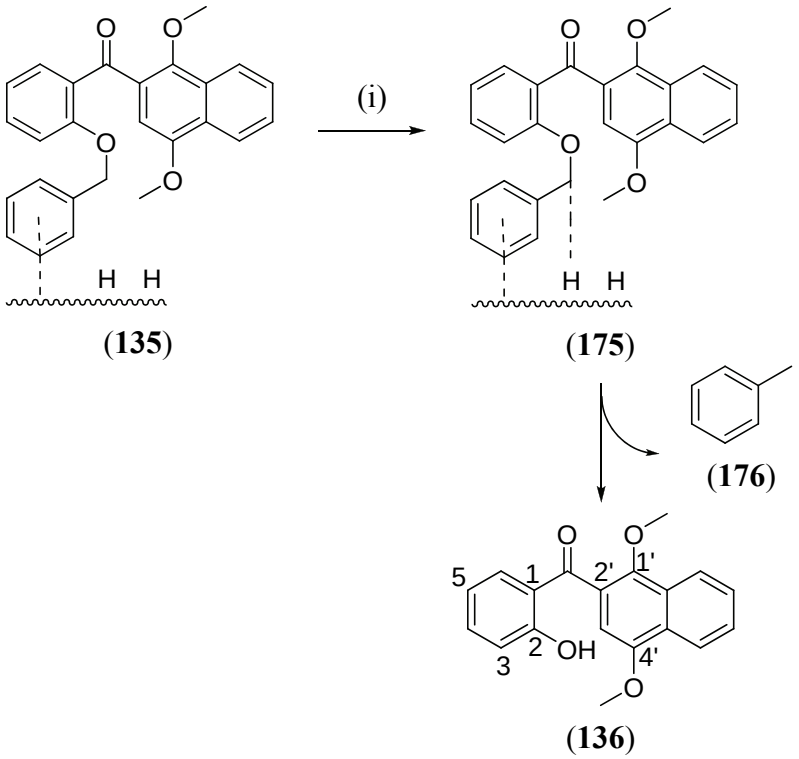

Scheme 42: (i) 5% Pd/C, $H_{2(g)}$, dry methanol, 5 atm, 18 h, 97%

It is believed that the benzyloxy group is co-ordinated to the metal catalyst via the electron rich aromatic ring. The carbon oxygen bond was now in close proximity to the palladium and under these conditions furnished the required phenol (**136**) and toluene (**176**) (***Scheme 42***). Initial co-ordination with the catalyst was needed therefore only benzylic or allylic carbon oxygen bonds can be reduced. Due to the high pressures the reaction was carried out in a Parr hydrogenator.

The ^{1}H NMR spectrum showed two singlets at 3.94 ppm and 3.81 ppm which correlated to the two methoxy groups at the 1'- and 4'-positions of (**136**). The absence of the singlet at around 5.00 ppm was noteworthy as this was characteristic of the methylene group from the benzyl substituent and suggested that the benzyl protection group was removed. There was a singlet that integrated for 1 proton downfield at 12.25 ppm and was assigned to the hydroxyl group at the 2-position of (**136**). The hydroxyl group exhibited a sharp signal rather than the characteristic broad signal associated which the hydroxyl group that appeared around 9.00 ppm, in 2-(benzyloxy)benzoic acid (**155**). This was due to the intramolecular hydrogen bonding between the hydrogen of the hydroxyl group and oxygen of the carbonyl group of the product (**136**). The singlet at 6.68 ppm in the spectrum was assigned to the proton at the 3'-position as it is flanked by the carbonyl functionality and the methoxy group at the 4'-position. The doublet at 7.05 ppm corresponded to the proton adjacent to the hydroxyl group in the 3-position, while the triplet at 6.78 ppm was due to the proton at the 5-position of (**136**). The ^{13}C NMR spectrum showed a peak at 202.4 ppm which indicative of a carbonyl signal while the peaks at 63.7 ppm and 55.8 ppm were due to the carbons attached to the methoxy groups while the absence of the peak at around 70 ppm, characteristic of a methylene group suggested the removal of the benzyl protecting group. A quaternary carbon signal at 163.1 ppm appeared while a quaternary signal at 157.2 ppm disappeared indicating that an aromatic carbon was still bonded to an oxygen atom and hence a phenolic substituent could be present. The IR spectrum showed a broad peak at 2970 cm^{-1} that correlated to a phenol group while the characteristic sharp peak at 1739 cm^{-1} was indicative of carbonyl stretching vibrations. The mass spectrum showed an ion of 308.1048 which correlated with the calculated mass, 308, 1049 of the desired ketone (**136**). The product was confirmed as (1,4-dimethoxynaphthalen-2-yl)(2-hydroxyphenyl)methanone (**136**) by X-ray crystallography.

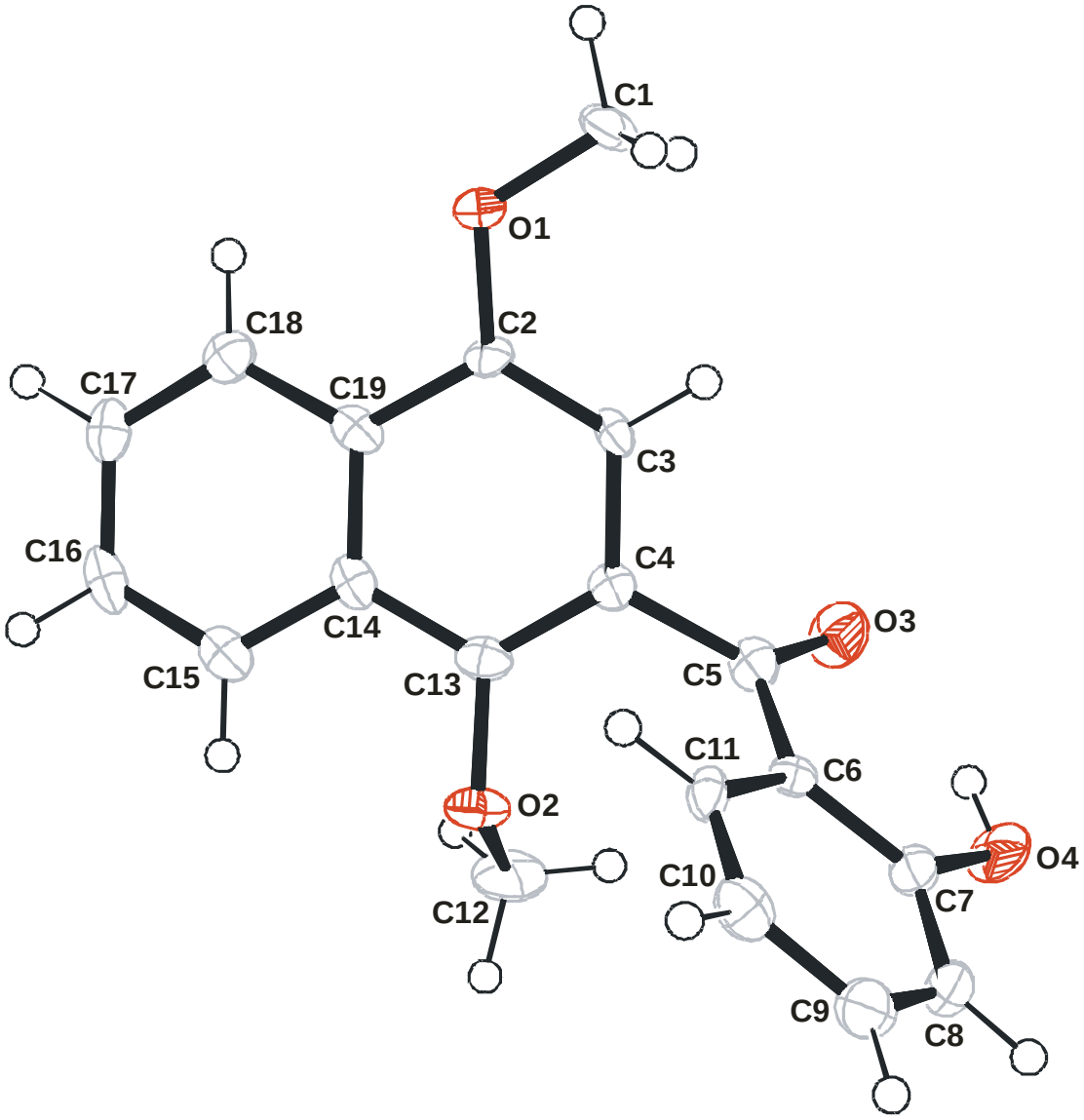

Figure 16: ORTEP diagram for the crystal structure of the (1,4-dimethoxynaphthalen-2-yl)(2-hydroxyphenyl)methanone (**136**)

The crystal structure of (**136**) (***Figure 16***) showed the hydrogen bonding between the hydrogen connected to O4 from the phenol group with the oxygen O3 from the carbonyl group. It was clear that free rotation around the bond between C4 and C5 as well as C5 and C6 occurred in solution. As will be discussed later, this was important as the molecule can arrange itself in a manner to allow for one the methoxy group of the naphthalene ring to be in close proximity to the phenolic substituent which would prove strategically vital in the formation of our final product as shown schematically in ***Scheme 43***.

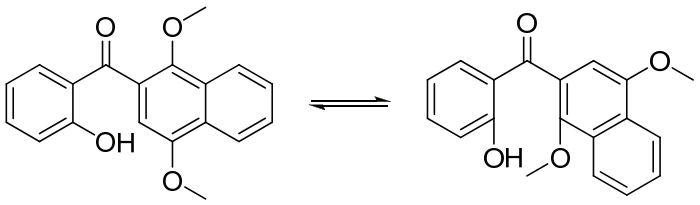

(136) **(136)**

Scheme 43

ATTEMPTED SYNTHESIS OF 4'-METHOXY-1'*H*,3*H*-SPIRO[BENZOFURAN-2,2'-NAPHTHALENE]-1',3(3'*H*,8a'*H*)-DIONE

The formation of the spiro-compound with the use of DDQ (**186**) as an oxidizing agent was a key step in the synthesis of bikaverin (**2**) by de Koning *et al.*[4]. Lewis and co-workers showed that 2-hydoxy-3-methoxybenzophenones (**177**) underwent intramolecular oxidative cyclization with 2,3-dichloro-5,6-dicyanobenzoquinone (DDQ) (**186**) to form corresponding methoxyxanthones (**178**) and (**179**)[87], unfortunately as a mixture of products (***Scheme 44***).

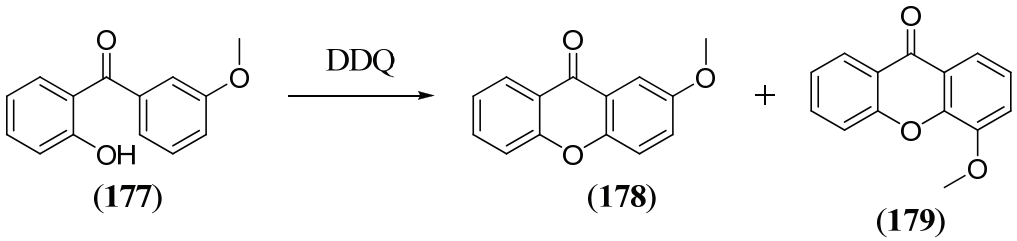

(177) **(178)** **(179)**

Scheme 44

Lewis *et al.*[88] later showed that the benzophenone (**180**) upon oxidation with 2,3-dichloro-5,6-dicyanobenzoquinone (DDQ) (**186**) yielded two products, the xanthone (**181**) and the spiro-compound (**182**) which in turn was converted into the xanthone (**181**) upon heating (***Scheme 45***).

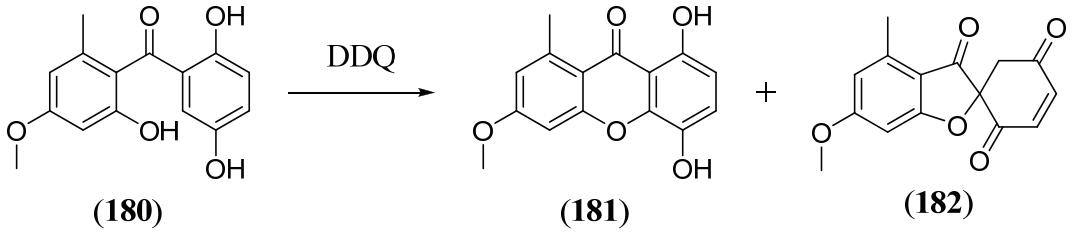

(180) **(181)** **(182)**

Scheme 45

de Koning *et al.*[4] applied the methodology used by Lewis on a more complex system to form the spiro-enol ether (**8**) from the hydroxymethanone (**7**) in a 61% yield (***Scheme 46***). The mechanism postulated for the formation of the spiro-enol ether (**8**) was similar to that described by Becker[89] as shown in ***Scheme 47***.

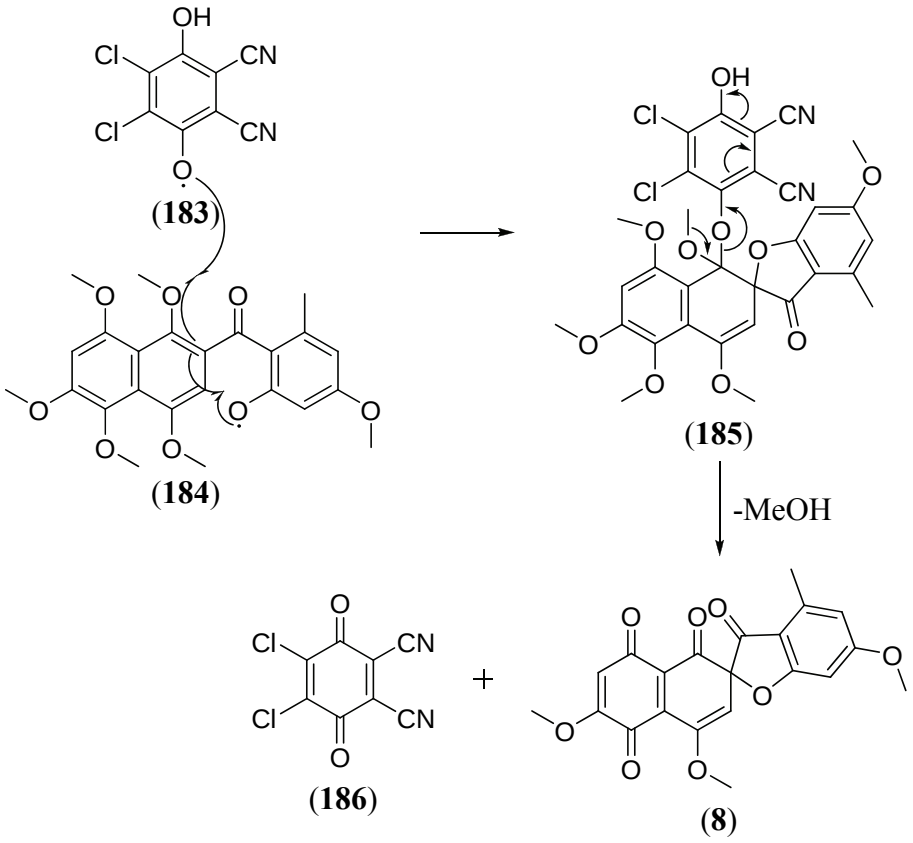

Scheme 46

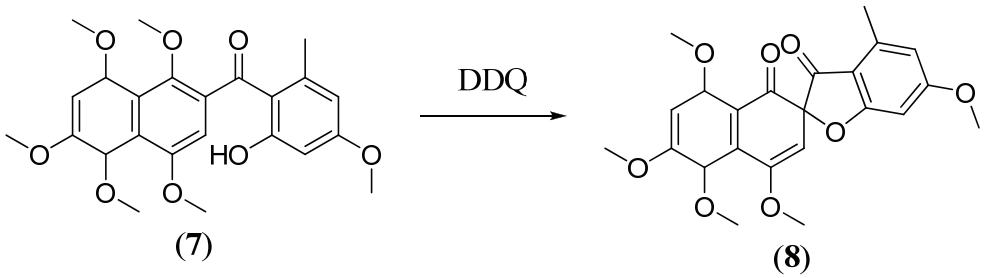

Scheme 47

The naphthol (**7**) underwent transfer of a hydrogen atom to give the phenoxy radical (**184**) and the 2,3-dichloro-5,6-dihydroquinone radical (**183**). The two radicals combined to yield the 2,3-dichloro-5,6-dicyanobenzoquinone phenol adduct (**185**)

under the reaction conditions, the ketal (**185**) collapsed and formed the spiro-enol ether (**8**).

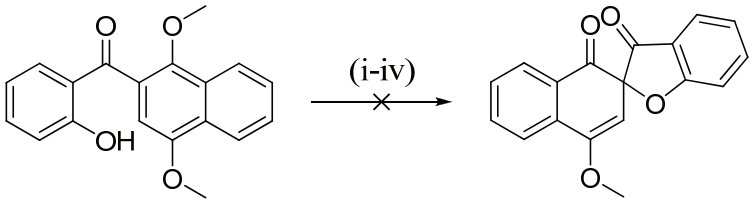

(**136**) (**137**)

Scheme 48: (i) dry benzene, DDQ, rt, 72 h; (ii) dry benzene, DDQ, reflux, 72 h; (iii) dry chloroform, DDQ, rt, 72 h; (iv) dry chloroform, DDQ, reflux, 72 h

Hence the reaction of (**136**) with DDQ (**186**) was a pivotal step in this project for the formation of the ether linkage of the xanthone. Our intermediate (**136**) was subjected to the same conditions used by de Koning and Lewis but this only gave back starting material. The solvent was changed to chloroform and the reaction was brought to reflux for the 72 hours but only starting material was recovered (***Scheme 48***). Therefore we had to change the direction of the project and pursue other leads.

.

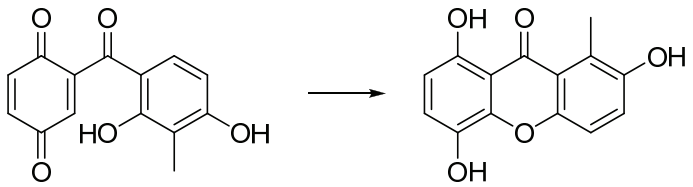

(**187**) (**188**)

Scheme 49

Whalley and co-workers have found that 1,4-benzoquinones such as (**187**) undergo 1,4 Michael addition to afford the xanthone for example (**188**)[90] (***Scheme 49***).

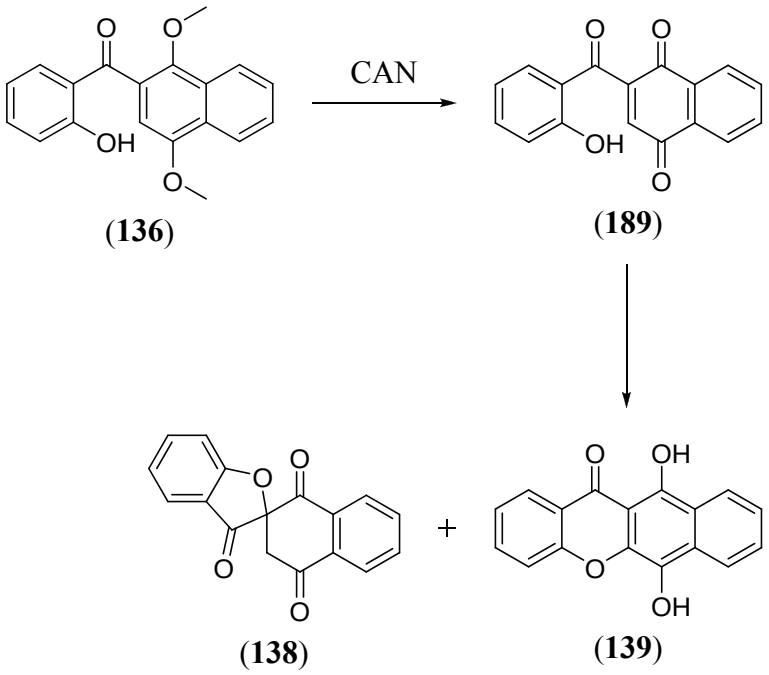

(**136**) (**189**)

(**138**) (**139**)

Scheme 50

After the lack of success using DDQ (**186**) as a reagent, a decision was made to oxidize the methoxy groups using another oxidizing agent such as ceric ammonium nitrate (CAN), to hopefully form the quinone (**189**) which would undergo either the 1,4-addition or the formation of the spiro-compound (**138**) which could be transformed to the xanthone (**139**) upon heating (***Scheme 50***).

SYNTHESIS OF 12a-METHOXY-5*H*-BENZO[c]XANTHENE-5,7(12a*H*)-DIONE USING CERIC AMMONIUM NITRATE

Ceric ammonium nitrate is an excellent oxidizing agent for hydroquinone dimethyl ethers due to its selectivity, efficiency and mildness of reaction conditions. Castagnoli Jnr and co-workers successfully showed the application of CAN as an oxidizing agent and even formulated a basic mechanism for the reaction[91]. The reaction mechanism was exactly opposite to that reported earlier on by Waldhor *et al*.[81] and occurred via a cationic radical mechanism. Oxidation of 1,4-dimethoxy-2,3,5,6-tetramethylbenzene (**190**) in the presence of 95% isotopically rich H_2O (O^{18}) provided doubly labelled deuterated benzoquinone (**191**). Consequently the reaction proceeded by aryl-oxygen bond cleavage with a net formation of the quinone and 2 moles of methanol. CAN acted as a one electron transfer reagent by producing hydroxyl radicals from the

water. The oxidation allows the hydroxyl radical to attack (**192**)[92]. As shown in ***Scheme 51*** this process occurs twice.

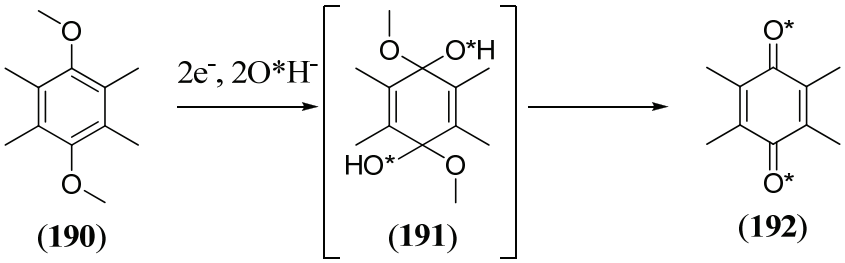

(**190**) (**191**) (**192**)

Scheme 51

When (**136**) was treated with ceric ammonium nitrate in aqueous acetonitrile, it was monitored by TLC over an hour. After an hour all the starting material had been consumed as shown by TLC and a new fluorescent spot appeared below the starting material spot when irradiated with UV light. We expected the product to be (**189**) or possibly the xanthone (**139**) or the oxidized xanthone (**140**) (***Scheme 52***).

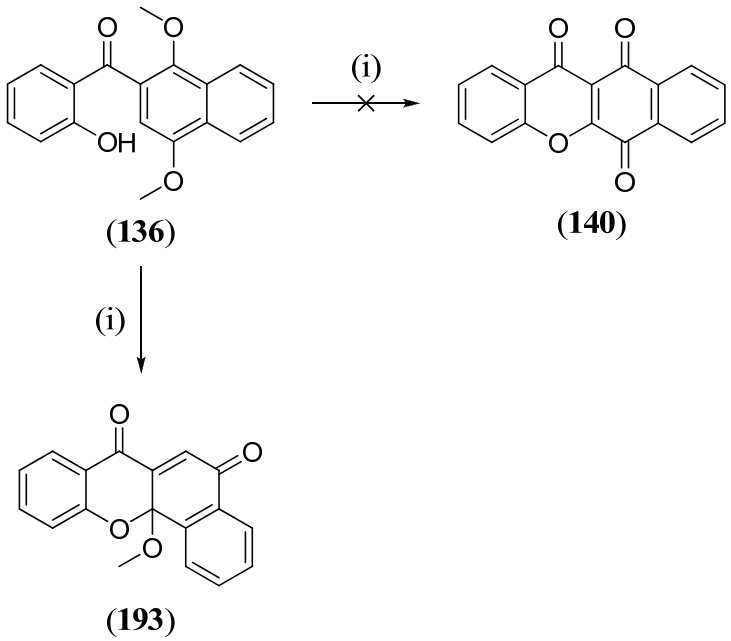

(**136**) (**140**) (**193**)

Scheme 52: (i) CAN, acetonitrile, rt, 1.5 h, 72%.

Surprisingly the ^{1}H NMR spectrum still showed a singlet at 3.03 ppm that integrated for 3 protons. This corresponded to one methoxy group, while the absence of another singlet in the region suggested that neither (**139**), (**140**) nor (**189**) had been formed.

The methoxy group at 3.03 ppm appeared further upfield than its usual chemical shift around 3.50 - 4.00 ppm. It was discovered later that the unusual chemical shift was due to the methoxy group being a constituent of a hemiacetal. A puzzling signal appeared as a singlet at 7.26 ppm which integrated for 1 proton which was consistent for a quinone proton. Furthermore the doublet at 8.16 ppm was characteristic of the hydrogen adjacent to the carbonyl bridge of a xanthone as it was deshielded by the carbonyl. The absence of the singlet at around 12.00 ppm combined with the unusual shift of the methoxy group suggested that probably the ether linkage of the xanthone was formed. The ^{13}C NMR spectrum showed two quaternary signals at 184.0 ppm and 181.0 ppm that corresponded to carbonyl chemical shifts. This suggested that the one methoxy substituent was oxidised to the carbonyl. A signal at 51.4 ppm was characteristic of a methoxy group while a confusing quaternary signal at 96.4 ppm suggested that an acetal could be present. A quaternary signal at 157.8 ppm was characteristic of a carbon single bonded to oxygen was also evident. The IR spectrum showed a sharp signal at 1738 cm^{-1} that was due to carbonyl stretching vibrations. The absence of a broad band around 3000 cm^{-1} corresponded to the absence of the hydroxyl group in the product while there were three sharp signals at 1129 cm^{-1}, 1099 cm^{-1} and 1023 cm^{-1} that corresponded to carbon singly bonded to oxygen stretching vibrations.

The spectroscopy data was still very inconclusive and unexpected thus a crystal structure was obtained on the unknown product and it revealed an unexpected structure indicating that the acetal had been formed containing two carbonyl substituents (***Figure 17***). The mass spectrum showed an ion of 276.0778 which correlated with the calculated mass, 292.0736 of the crystal product (**193)** minus an oxygen. The product was confirmed as the angular fused xanthone 12a-methoxy-5*H*-benzo[*c*]xanthene-5,7(12a*H*)-dione (**193**) . An optical rotation was carried out on the crystal revealing a rotation of -7.2 which confirmed the stereogenic centre at C2.

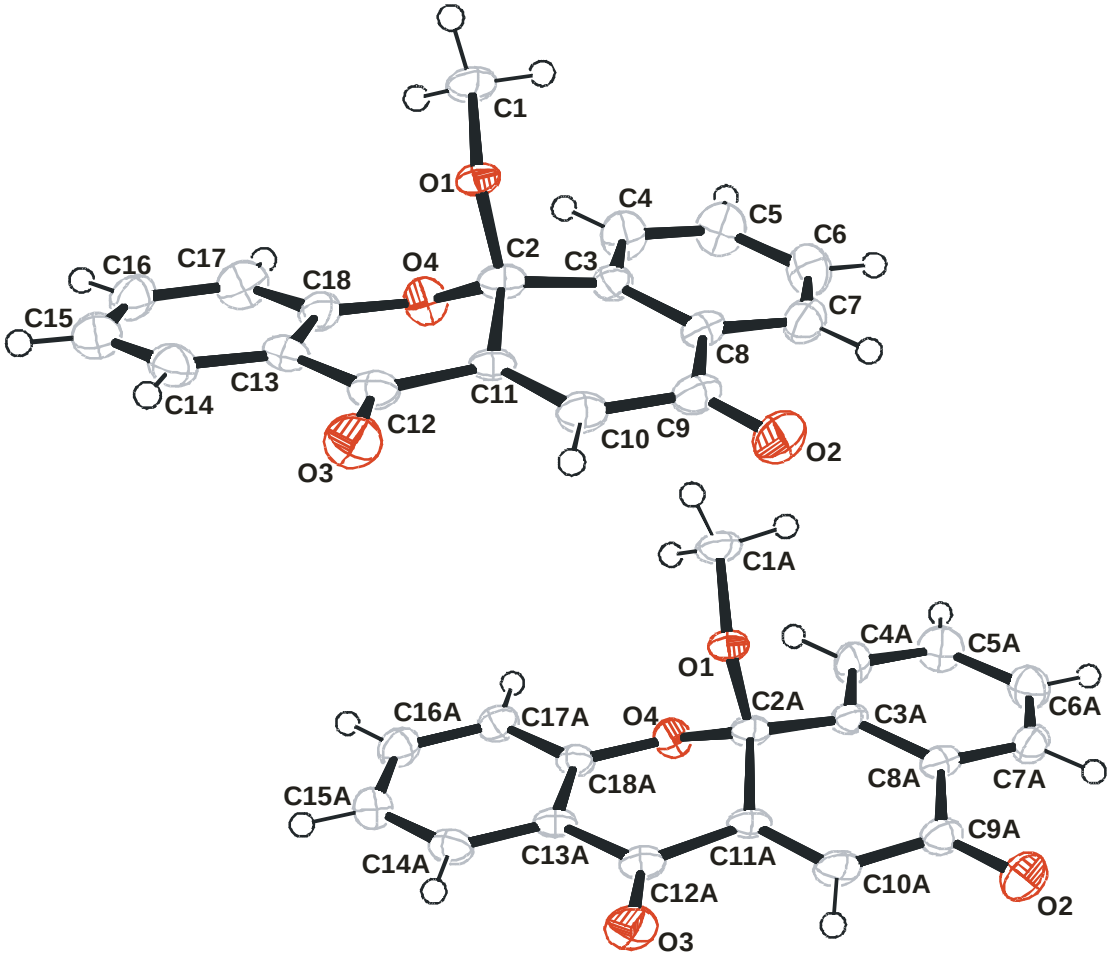

Figure 17: ORTEP diagram for the crystal structure of the 12a-methoxy-5*H*-benzo[*c*]xanthene-5,7(12a*H*)-dione (**193**)

The following mechanism was proposed. The hydroxyketone (**136**) is oxidized to intermediate (**194**) consistent with the proposed mechanism. The intermediate (**194**) undergoes elimination of water by way of the nucleophilic oxygen attacking the electrophilic carbon attached to the hemiacetal and thus a xanthone like compound (**195**) was produced. The hemiacetal of the xanthone (**195**) then undergoes the elimination of methanol to furnish our product (**193**) in good yield as the only product (***Scheme 53***).

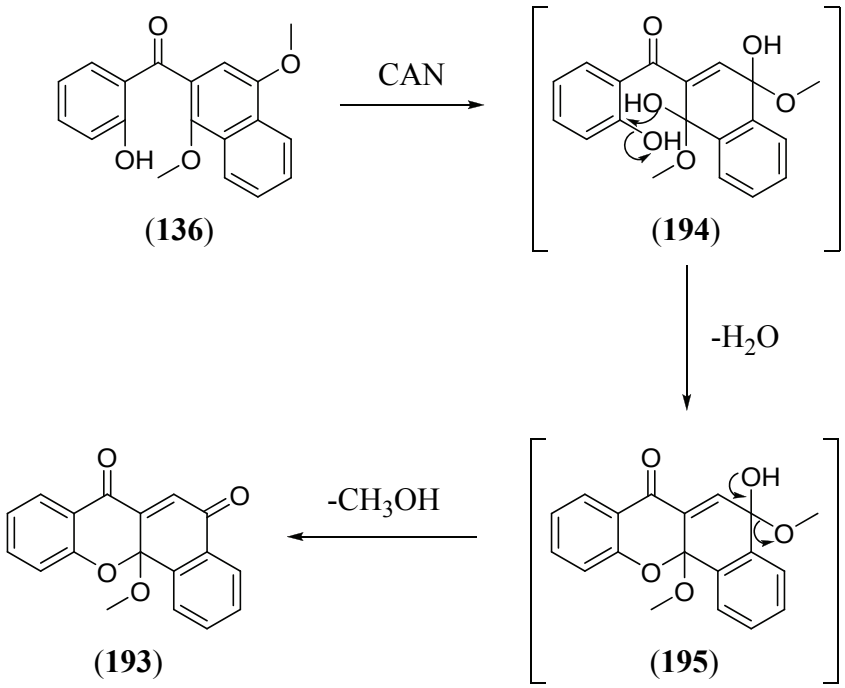

(**136**) (**194**) (**195**) (**193**)

Scheme 53

After the surprising results obtained, the decision was made to try the reaction on related substrates to gauge the versatility of this novel reaction. 1,4-Dimethoxybenzene (**196**) could be used instead of 1,4-dimethoxynaphthalene (**153**) in this investigation since it is commercially available.

SYNTHESIS OF 2-METHOXY-9*H*-XANTHENE-9-ONE AND 4a-METHOXY-2*H*-XANTHENE-2,9(4a*H*)-DIONE

The decision was made to further explore the efficiency and flexibility of the reaction after the surprising results obtained with the use of ceric ammonium nitrate. 1,4-Dimethoxybenzene (**196**) which was commercially available was used instead of 1,4-dimethoxynaphthalene (**153**) as a starting point.

1,4-Dimethoxybenzene (**196**) was brominated with NBS by way of an electrophilic substitution reaction to furnish 2-bromo-1,4-dimethoxybenzene (**197**) as a colourless liquid in excellent yields via the method used by Bloomer and co-workers[85] (***Scheme 54***).

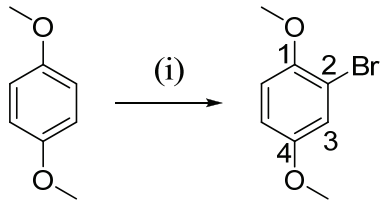

(**196**) (**197**)

Scheme 54: (i) NBS, dry CH_2Cl_2, reflux, 24 h, 89%.

The ^{1}H NMR spectrum showed two singlets at 3.74 ppm and 3.82 ppm respectively that integrated for 3 protons each. These signals corresponded to the two methoxy groups at the 1- and 4-position of (**197**), which suggested that the symmetry of the compound was now absent. A singlet at 7.11 ppm which was due to the hydrogen in the 3-position was also evident. The ^{13}C NMR spectrum showed three quaternary signals at 154.0 ppm, 150.3 ppm and 113.6 ppm. The peaks at 154.0 ppm and 150.3 ppm were characteristic of aromatic carbons bonded to methoxy groups, while the peak at 113.6 ppm suggested that a halogen was attached to an aromatic carbon. The IR spectrum showed a strong sharp signal at 730 cm^{-1} which was due to carbon single bonded to bromide stretching vibrations. The compound was confirmed to be 2-bromo-1,4-dimethoxybenzene (**197**).

The next step was to form the carbonyl bridge between 2-bromo-1,4-dimethoxy benzene (**197**) and benzyl 2-(benzyloxy)benzoate (**147**) to furnish the benzyloxy ketone (**201**) (***Scheme 55***). The 2-bromo-1,4-dimethoxybenzene (**197**) was lithiated and then added to the benzyl 2-(benzyloxy)benzoate (**147**) to form the tetrahedral intermediate (**199**), which immediately eliminated the benzyloxy anion and furnished the desired product (**200**) as shown in ***Scheme 56***.

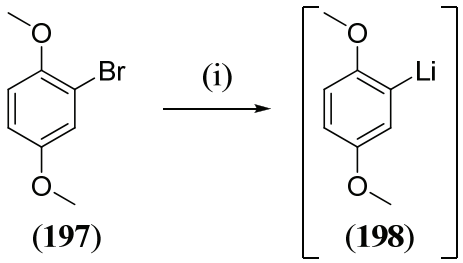

(**197**) (**198**)

Scheme 55: (i) *n*BuLi, dry THF, –78°C, 30 min

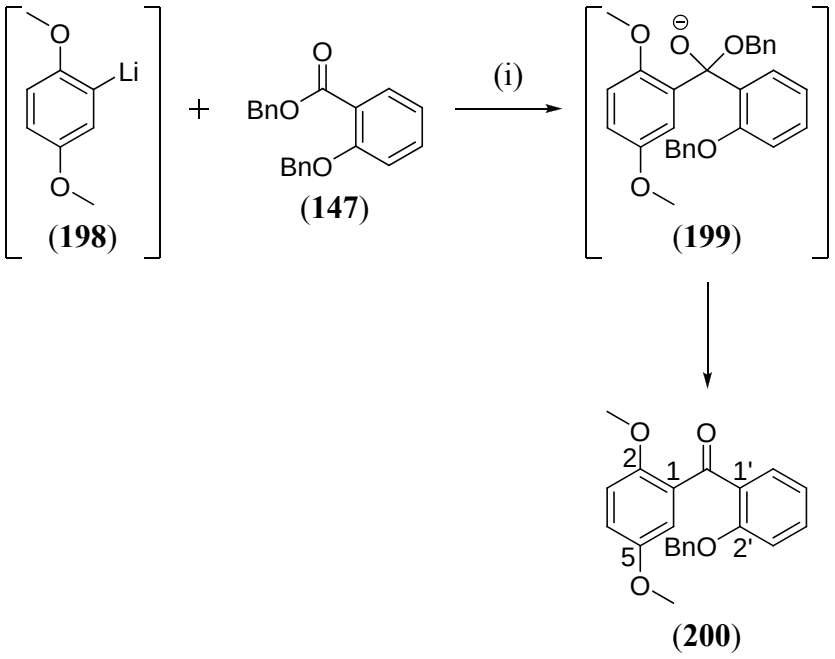

Scheme 56: (i) dry THF, –78 °C, 45 min, 72%.

The ^{1}H NMR spectrum showed two singlets at 3.75 ppm and 3.52 ppm which integrated for 3 protons each and corresponded to the two methoxy groups at the 2- and 5-positions of (**200**). The singlet 3.75 ppm appeared slightly downfield because it was deshielded by the adjacent carbonyl group attached at the 1-position. A singlet at 4.94 ppm which was characteristic of a methylene group as it integrated for two protons. The singlet was due to the benzyl substituent and suggested that the carbonyl bridge was formed. The doublet of doublets at 7.59 ppm was due to the hydrogen at the 6'-position of (**200**). The signal appeared as a doublet of doublets due to *ortho*-coupling with the hydrogen in the 5'-position that was verified by a coupling constant of 7.6Hz and *meta*-coupling with the hydrogen in the 4'-position that was verified by a coupling constant of 1.7Hz. Another doublet appeared at 6.76 ppm and was due to the hydrogens at the 3- and 4-positions of (**200**) coupling with one another. The signal appeared as one doublet integrating for 2 protons because the molecule was symmetrical in this region and thus the hydrogens are in similar environments. The ^{13}C NMR spectrum showed a quaternary peak at 195.4 ppm which was due to the carbonyl carbon. The three quaternary signals at 157.2 ppm, 153.5 ppm and 152.8 ppm corresponded to the carbons bonded to the benzyloxy and two methoxy groups respectively. Two peaks at 56.5 ppm and 55.9 ppm were characteristic of methoxy groups while the peak at 70.1 ppm was due to the methylene group. The IR

spectrum showed a peak at 1738 cm^{-1} that was indicative of carbonyl stretching vibrations. The mass spectrum showed an ion of 348.1346 which correlated with the calculated mass, 348.1362 of the desired ketone (**200**). The product was confirmed as (2-(benzyloxy)phenyl)(2,5-dimethoxyphenyl)methanone (**200**).

The next step was the removal of the benzyl protection group using hydrogenolysis. The benzyloxymethanone (**200**) was treated with 5% palladium on carbon at 5 atmospheres in the presence of hydrogen gas for 24 hours and furnished the required product (**201**) in good yield as shown in ***Scheme 57***.

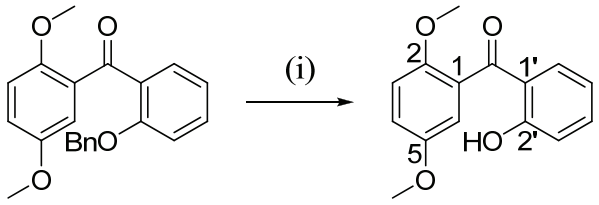

(**200**) (**201**)

Scheme 57: (i) 5% Pd/C, 5 atm, $H_{2(g)}$, rt, 24 h, 90%.

The ^{1}H NMR spectrum showed two singlets at 3.60 ppm and 3.67 ppm that integrated for 3 protons each. These singlets corresponded to the two methoxy groups at the 2- and 5-positions of (**201**). The absence of the singlet at around 5.00 ppm and the appearance of the singlet that integrated for 1 proton at 12.04 ppm suggested that the benzyl substituent was no longer present. As before the peak appeared downfield and as a sharp signal because of internal hydrogen bonding between the hydroxy group at the 2'-position and the carbonyl group attached at the 1'-position of (**201**). The singlet at 6.85 ppm corresponded to the hydrogen at the 6-position of (**201**). There was a doublet of doublets at 7.26 ppm which was due to the hydrogen at the 6'-position of *ortho*-coupling with the hydrogen in the 5'-position that was verified with the coupling constant of 8.0Hz and *meta*-coupling with the hydrogen in the 4'-position that was verified with a coupling constant of 1.5Hz. The ^{13}C NMR spectrum showed two signals at 55.2 ppm and 54.8 ppm which were characteristic of methoxy carbons. A quaternary signal at 200.7 ppm correlated to that of the carbonyl carbon. The disappearance of the peak at around 70 ppm, which was due to a methylene carbon, suggested that the benzyl group was removed. The quaternary signal at 161.8 ppm corresponded to a carbon bonded to an alcohol. The IR spectrum showed a broad

band at 2970 cm^{-1} which was characteristic of a hydroxyl group as well as a sharp strong signal at 1738 cm^{-1} which was indicative of carbonyl bond stretching vibrations. The mass spectrum showed an ion of 258.0883 which correlated with the calculated mass, 258.0892 of (**201**). The product was confirmed as (2,5-dimethoxyphenyl)(2-hydroxyphenyl)methanone (**201**).

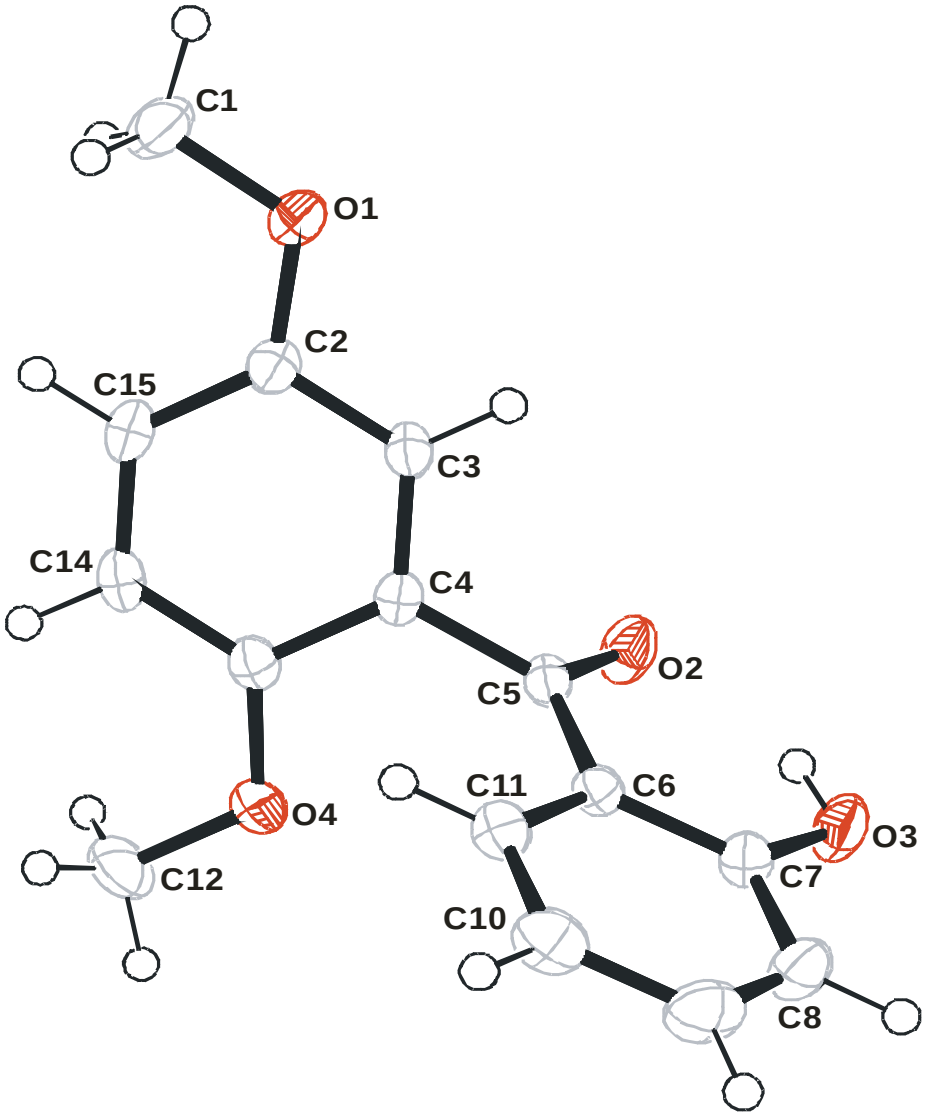

Figure 18: ORTEP diagram for the crystal structure of the (2,5-dimethoxyphenyl)(2-hydroxyphenyl)methanone (**201**).

The crystal structure clearly showed the internal hydrogen bonding between the hydroxyl group and the carbonyl group (***Figure 18***). The crystal structure of (**201**) also showed the possibility of free rotation around the C4- and C5-positions and the

C6- and C5-positions which was vital if we were to expect the formation of products like the unexpected xanthone (**193**) (***Scheme 58***).

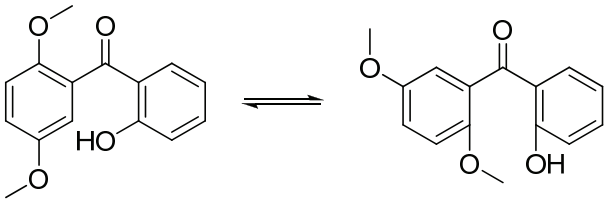

(**201**) (**201**)

Scheme 58

Finally the hydroxybenzophenone (**201**) was oxidized with ceric ammonium nitrate. The reaction was monitored over 30 minutes. After 15 minutes the starting material had mostly been consumed. The reaction was left for a further 15 minutes and another spot appeared on the TLC plate furnishing two products. The reaction was left overnight and furnished two surprising products after purification of the reaction mixture (***Scheme 59***). The first and major product was the unexpected 2-methoxyxanthone (**202**) while the second and minor product was the expected dione (**203**).

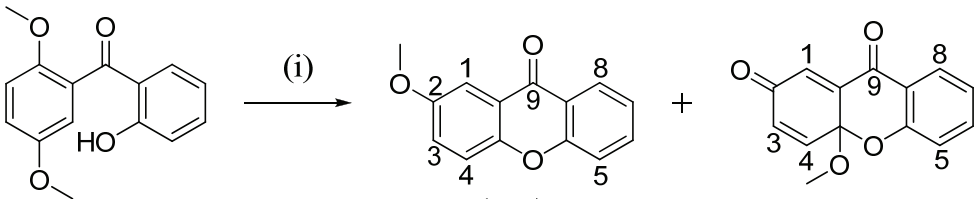

(**201**) (**202**) (**203**)

Scheme 59: (i) CAN, acetonitrile, rt, 1.5 h, (**202**) 74%, (**203**) 15%.

The ^{1}H NMR spectrum for the major product showed a singlet at 3.83 ppm which integrated for 3 protons was due to the methoxy group in the 2-position of (**202**). The usual chemical shift for the methoxy group suggested that the methoxy group was not part of a hemiacetal. There was a doublet of doublets at 8.25 ppm that corresponded to the hydrogen at the 8-position of (**202**). The hydrogen displayed *ortho*-coupling with the hydrogen at the 7-position which was verified with a coupling constant of 8.0 Hz and *meta*-coupling with the hydrogen at the 6-position which was verified with a coupling constant of 1.6 Hz. There was a singlet at 7.28 ppm which corresponded to

the proton in the 1-position of (**202**). The ^{13}C NMR spectrum showed a quaternary signal at 176.0 ppm that was characteristic of a carbonyl carbon. The two quaternary signals at 155.0 ppm and 154.9 ppm were due to a carbon single bonded to oxygen and suggested the formation of the ether linkage. A quaternary peak at 150.0 ppm was indicative of a carbon bonded to a methoxy group. The peak at 54.9 ppm was due to the methoxy group. The absence of a quaternary signal at around 90 ppm suggested that the acetal had not formed as was previously seen. The IR spectrum showed a sharp peak at 1738 ppm that was characteristic of carbonyl bond stretching vibrations. The mass spectrum showed an ion of 226.06120 which correlated with the calculated mass, 226.0630 of 2-methoxy-9*H*-xanthen-9-one (**202**)

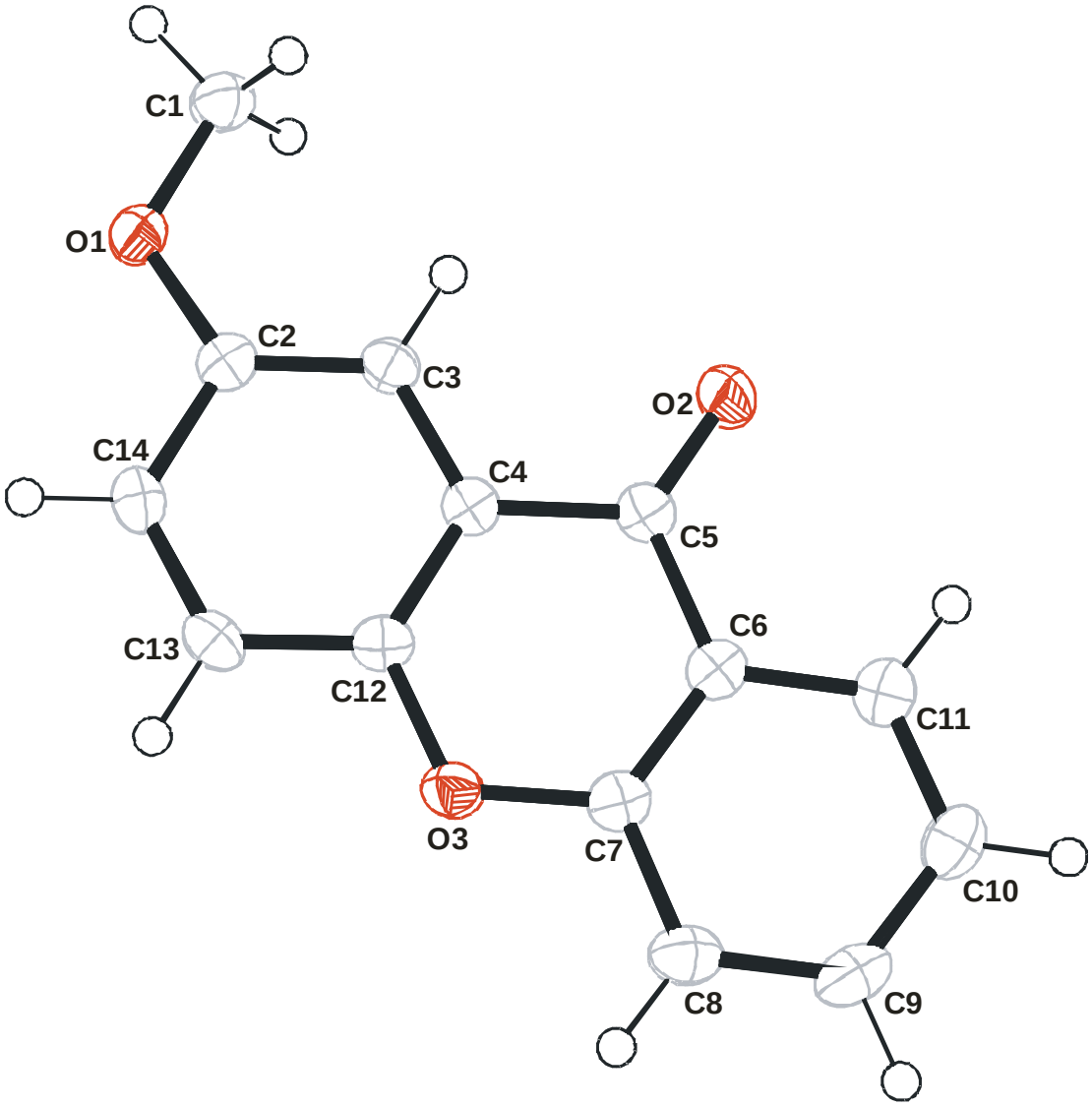

Figure 19: ORTEP diagram for the crystal structure of the 2-methoxy-9*H*-xanthen-9-one (**202**)

A crystal structure was obtained and the product was confirmed as 2-methoxy-9*H*-xanthen-9-one (**202**) (***Figure 19***). The crystal structure clearly showed the carbonyl bridge and ether linkage of the xanthone flanked by the two aromatic rings.

The ^{1}H NMR spectrum for the minor product (**203**) showed a singlet that integrated for 3 protons at 3.25 ppm that was characteristic of a methoxy group in the 4a-position. The unusual chemical shift of 3.25 ppm which was upfield of the 3.83 ppm reported for the major product suggested an acetal had been formed. A singlet at 6.81 ppm that integrated for 1 proton was the hydrogen in the 1-position of (**203**) which was sandwiched between the two carbonyl groups at the 2- and 9-positions. The two triplets were due to the hydrogens on the 6- and 7-positions of (**203**). The ^{13}C NMR spectrum showed two quaternary peaks at 185.0 ppm and 180.9 ppm that corresponded to carbonyl carbons. The absence of one quaternary signal at around 155 ppm and the appearance of a quaternary signal at 95.1 ppm suggested that an acetal was formed as had been seen previously. The peak at 51.3 ppm was indicative of a methoxy group. The IR spectrum showed a strong sharp signal at 1738 cm^{-1} that was due to carbonyl bond stretching vibrations. The mass spectrum showed an ion of 242.0568 which correlated with the calculated mass, 242.0892 of dione (**203**). The product was confirmed to be 4a-methoxy-2*H*-xanthene-2,9(4a*H*)-dione (**203**).

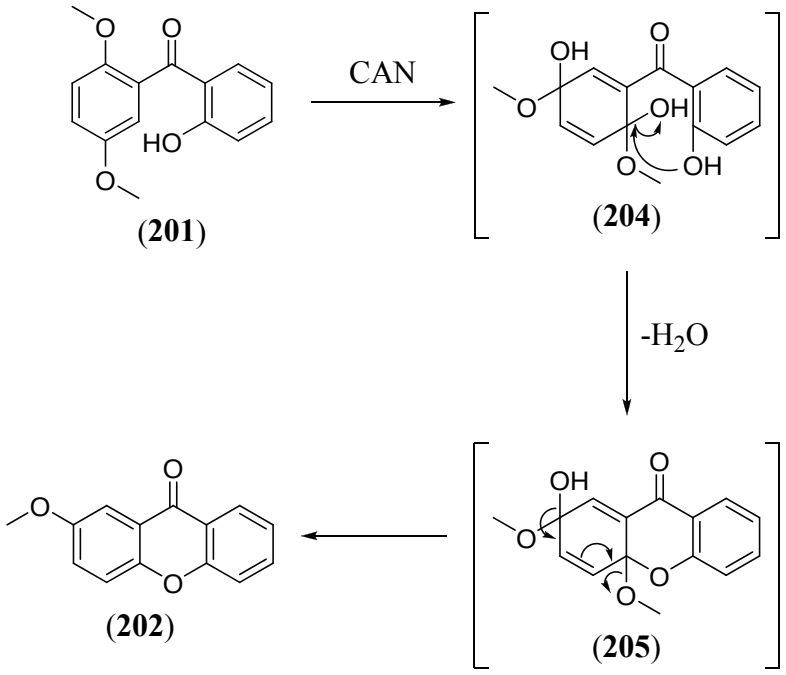

Scheme 60

It was thought that the xanthone (**202**) was the majority product because the compound could regain aromaticity unlike the dione. The following mechanism was postulated for the formation of the xanthone (***Scheme 60***).

The hydroxybenzophenone (**201**) underwent the normal CAN addition reaction to afford (**203**). The intermediate (**203**) underwent the elimination of water and formed intermediate (**205**) and rearranged to maintain the aromaticity of the ring and furnished the xanthone (**202**). The dione (**203**) was formed by the other postulated mechanism mentioned earlier with the elimination of water and then methanol (***Scheme 61***).

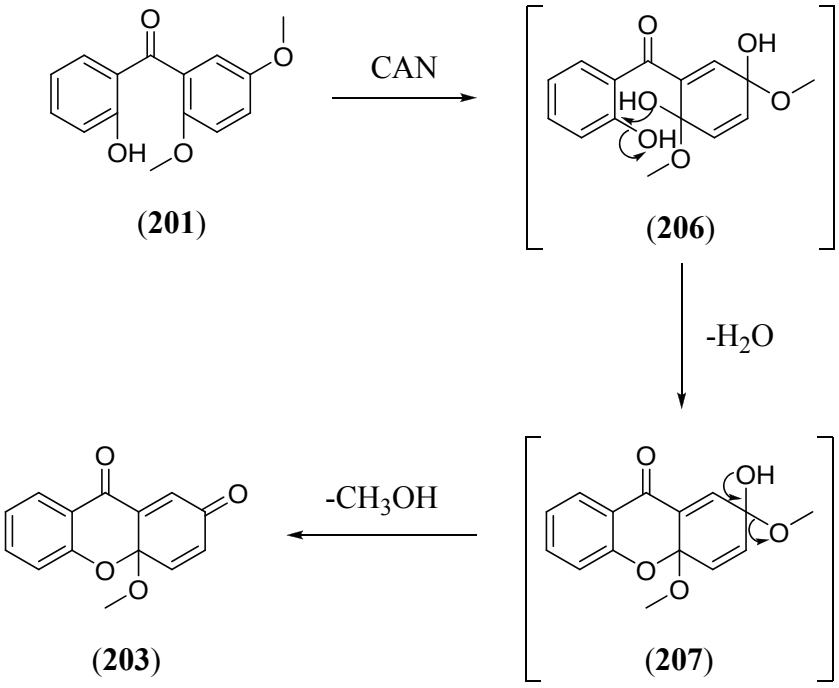

Scheme 61

CONCLUSION

Our main aim was to explore the flexibility and efficiency of the synthetic route used by de Koning et al.[4] in the total synthesis of the naturally occurring xanthone bikaverin (**2**).

The proposed synthetic route mentioned in the aims section of this dissertation was accomplished to a certain extent. Salicylic acid (**144**) was successfully protected with benzyl groups to furnish benzyl 2-(benzyloxy)benzoate (**147**) in an excellent yield of 87%. Benzyl 2-(benzyloxy)benzoate (**147**) was selectively deprotected by base catalysed ester hydrolysis with potassium hydroxide in a methanolic solution and afforded 2-(benzyloxy)benzoic acid (**155**) in good yields of 86%. 1,4-Naphthoquinone (**148**) was protected by first reducing to 1,4-hydroxynaphthalene (**150**) and then protecting the phenolic groups using dimethyl sulfate furnishing 1,4-dimethoxynaphthalene (**153**) in a good yield of 85%. The Friedel Crafts type reaction with the 1,4-dimethoxynaphthalene (**153**) and 2-(benzyloxy)benzoic acid (**155**) had limited success. The trifluoroacetic anhydride (**160**) reacted with the 2-(benzyloxy)benzoic acid (**155**) and formed the mixed anhydride that immediately reacted with the 1,4-dimethoxynaphthalene (**153**) and produced (2-(benzyloxy)phenyl)(1,4-dimethoxynaphthalen-2-yl)methanone (**135**) in a poor maximum yield of 30%. The (2-(benzyloxy)phenyl)(1,4-dimethoxynaphthalen-2-yl)methanone (**135**) was successfully deprotected with palladium on carbon under a hydrogen atmosphere using a hydrogenolysis reaction to remove the remaining benzyl group giving (1,4-dimethoxynaphthalen-2-yl)(2-hydroxyphenyl)methanone (**136**) in an excellent yield of 97%. The reaction with the DDQ to form the spiro-compound (**147**) was unsuccessful. The reaction only furnished starting material no matter how the conditions were varied.

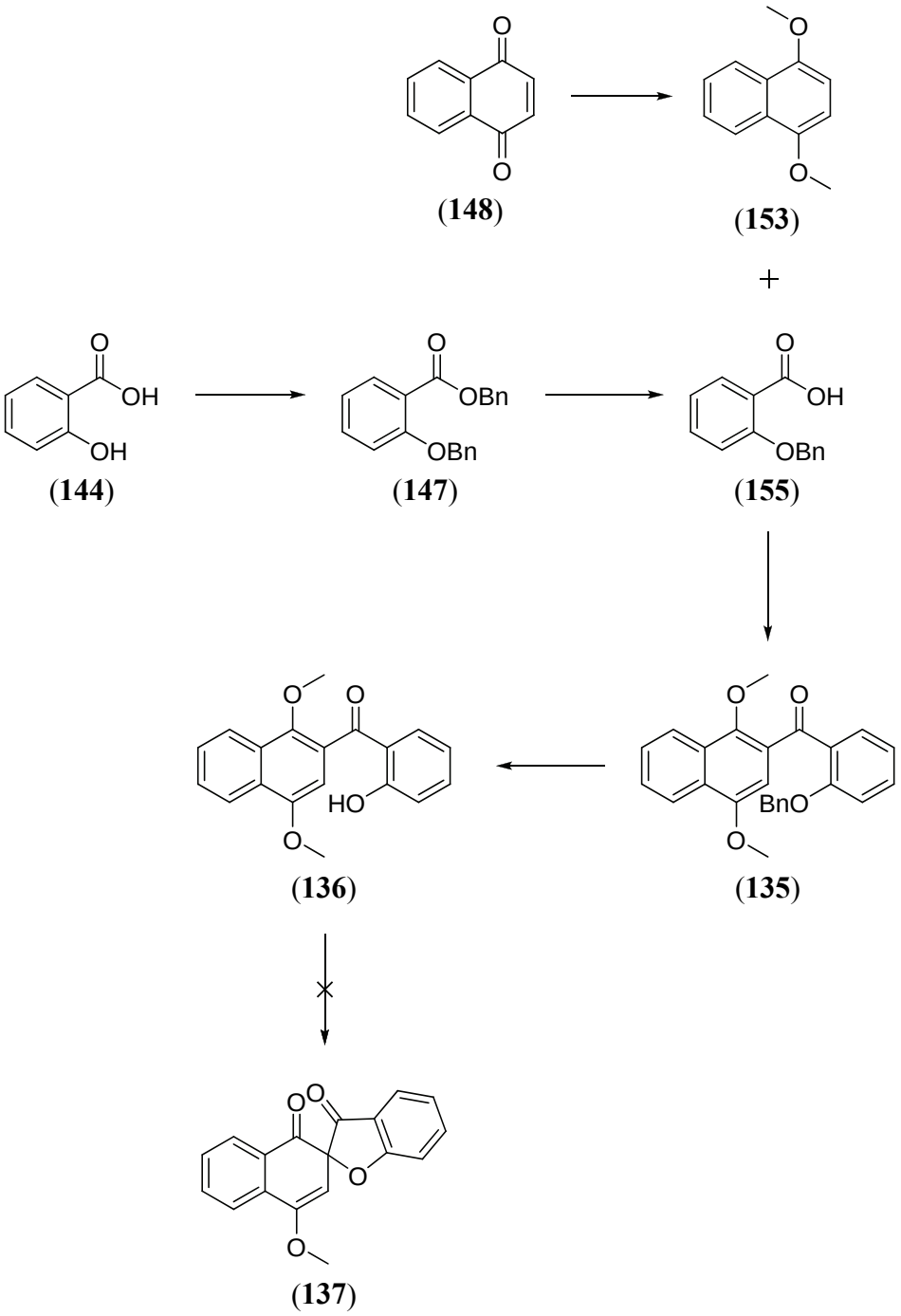

Scheme 62

This was when the synthesis deviated from the original aim. The first deviation came whereby the TFAA Friedel Crafts reaction was replaced with a higher yielding organometallic addition reaction. Due to the reaction being so early in the synthesis, more material was required to successfully test the outcomes of the following reactions in the sequence. The 1,4-dimethoxynaphthalene (**153**) was brominated via an electrophilic substitution using NBS under mild condition and gave the product 2-

bromo-1,4-dimethoxynaphthalene (**171**) in excellent yields of 90%. The 2-bromo-1,4-dimethoxynaphthalene (**171**) was lithiated at the 2-position using butyl lithium and added to the benzyl-2-(benzyloxy)benzoate (**147**) and furnished the (2-(benzyloxy)phenyl)(1,4-dimethoxynaphthalen-2-yl)methanone (**135**) in good yields of 89% (***Scheme 63***).

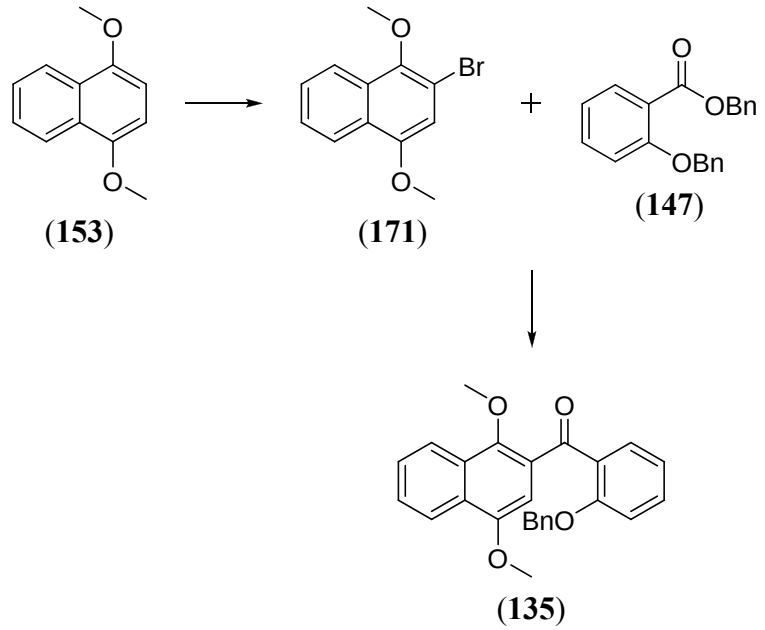

Scheme 63

The Friedel Crafts reaction with TFAA was a pivotal reaction in the synthesis of bikaverin due to the formation of the carbonyl bridge which was an important structural feature of the xanthone nucleus. The one pot synthesis proved to have limited success but further investigation is necessary to improve this step. For example Basavaiah *et al.*[93] used this reaction in their synthesis of alonimid derivatives (**208**) by first forming the mixed anhydride.

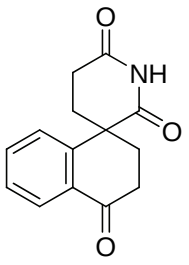

(**208**)

Figure 20: The structure of alominid (**208**)

The reaction should be tried by reacting the 2-(benzyloxy) benzoic acid (**155**) with the TFAA for 6 hours under reflux forming the mixed anhydride and then the 1,4-dimethoxynaphthalene (**153**) could be added as was done by Basavaiah *et al.*[93].

The second deviation was due to the failure of the key reaction with DDQ. Instead of the use of DDQ, the decision was made to use CAN. The idea was that the CAN would oxidize the aromatic methyl ether to the quinone and a 1,4 addition with the free phenol would occur or the spiro compound would result. The (1,4-dimethoxynaphthalen-2-yl)(2-hydroxyphenyl)methanone (**136**) was treated with CAN and furnished 12a-methoxy-12a*H*-benzo[*c*]xanthene-5,7-dione (**193**) in a moderately good yield of 76% (***Scheme 64***). This provided an unexpected result and a mechanism was postulated. Further investigation would need to be done to verify the mechanism.

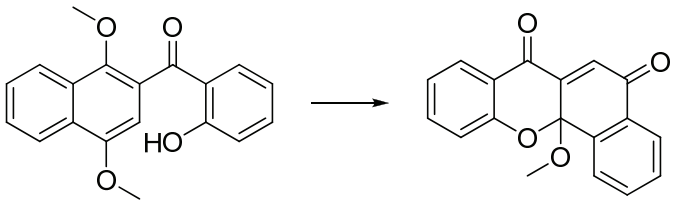

(136) **(193)**

Scheme 64

Due to the unexpected but very interesting development, the decision was made to further explore the reaction with CAN on a single ring system of benzene rather than naphthalene. (2,5-Dimethoxyphenyl)(2-hydroxyphenyl)methanone (**201**) was synthesized via the exact same procedure detailed above and treated with CAN and furnished two products 2-methoxy-9*H*-xanthen-9-one (**202**) in a 80% yield and 4a-methoxy-4a*H*-xanthene-2,9-dione (**203**) in 17% yield (***Scheme 65***).

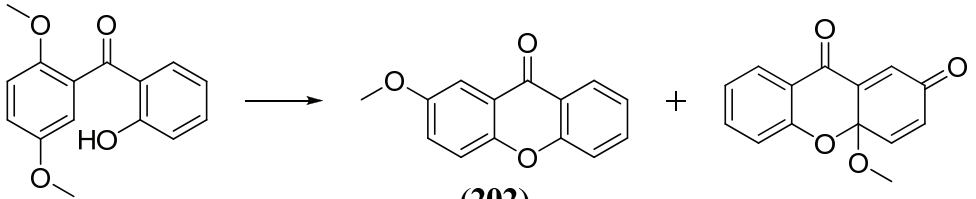

(201) **(202)** **(203)**

Scheme 65

These results proved that the reaction was reproducible to a certain extent due to the expected product being the minor product. Further exploration of this process would need to be done on different ring systems such as 1,4-dimethoxyanthracene (**209**) as well as exploring more substituted ring systems with either electron withdrawing or electron donating groups and monitor the effects on the reaction.

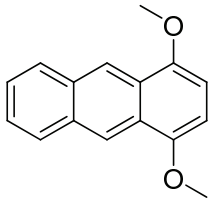

(**209**)

Figure 21: The structure of 1,4 dimethoxyanthracene (**209**).

These reactions with CAN could prove useful because the reaction could provide another novel route to attempt the synthesis of, for example, the complex angular fused xanthones cervinomycin A2 (**210**).

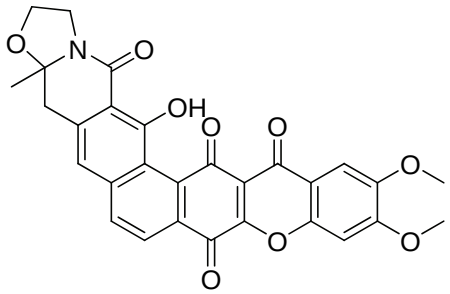

(**210**)

Figure 22: The structure of cervinomycin A2 (**210**).

In summary, the goal of this work was to examine the flexibility of the xanthone synthesis proposed by de Koning *et al.*[4] in their synthesis of bikaverin (**2**). This aim was achieved to a certain extent but more importantly a novel route to xanthones was discovered utilizing CAN as a key reagent in the synthesis.

EXPERIMENTAL

GENERAL DETAILS

PURIFICATION OF SOLVENTS AND REAGENTS

All solvents used for reactions and preparative column chromatography were distilled. Solvents used in reactions were pre-dried in their reagent bottles and then distilled over the appropriate drying mediums under a nitrogen atmosphere.

Tetrahydrofuran (THF) was pre-dried over sodium wire and distilled from sodium metal wire and benzophenone. Dichloromethane and methanol were distilled from calcium hydride. Triethylamine was distilled from, and stored over potassium hydroxide.

EXPERIMENTAL TECHNIQUES

Some reactions were performed under an inert atmosphere (nitrogen) using a standard manifold line connected to a vacuum pump. The nitrogen was dehydrated by passing the gas through silica gel.

The Parr hydrogenator used was the Buchiglasuster Picoclave and was employed at the conditions outlined in the experimental procedures.

CHROMATOGRAPHIC SEPARATION

The R_f values quoted are for thin layer chromatography (TLC) on aluminium-backed Machery-Nagel ALUGRAMSil G/UV_{254} plates pre-coated with 0.25mm silica gel 60 or Aldrich TLC plates, silica gel on aluminium.

Machery-Nagel Silica gel 60 (particle size 0.063-0.200mm) was used as the adsorbent for conventional preparative column chromatography, with a silica to product ratio of 30:1. The silica was packed into a suitable column, and the indicated solvent was passed through several times under pressure, until no bubbles were visible in the column. The crude product was adsorbed onto silica, loaded onto the silica surface and covered with a plug of cotton wool. The elution process was performed using the indicated solvent mixtures either under gravity or air pump pressure conditions.

SPECTROSCOPIC AND PHYSICAL DATA

All melting points were obtained on a Reichert hot-stage microscope, and are uncorrected.

Optical rotations were obtained on a Jasco DIP-370 Digital Polarimeter. The values reported each represent an average of several consistent measurements.

Infrared spectra were obtained on a Bruker Vector 22 spectrometer. The absorptions are reported on the wavenumber (cm^{-1}) scale, in the range 400-4000cm^{-1}. The signals are reported: value (assignment).

Hydrogen (^{1}H NMR) and carbon (^{13}C NMR) nuclear magnetic resonance spectra were recorded on Bruker Avance-300 at 300.13MHz respectively using standard pulse sequences. The probe temperature for all experiments was 300±1K. All spectra were recorded in deuterated chloroform ($CDCl_3$) in 5mm NMR tubes. Chemical shifts are reported in parts per million (ppm) relative to tetramethylsilane as internal standard, in the case of ^{1}H NMR spectra and relative to the central signal of deuterated chloroform taken at δ 77.00 for the ^{13}C NMR spectra. The ^{1}H NMR spectra chemical shifts are reported: value (number of hydrogens, splitting pattern, coupling constant(s) in Hertz were applicable, assignment). ^{13}C NMR chemical shifts are reported value (assignment).

Intensity data were collected on a Bruker APEX II CCD area detector diffractometer with graphite monochromated Mo K_α radiation (50kV, 30mA) using the APEX 2 data collection software. The collection method involved ω-scans of width 0.5° and 512x512 bit data frames. Data reduction was carried out using the program *SAINT+* (Bruker, 2005b) and face indexed absorption corrections were made using the program *XPREP*. The crystal structure was solved by direct methods using *SHELXTL*. Non-hydrogen atoms were first refined isotropically followed by anisotropic refinement by full matrix least-squares calculations based on F^2 using *SHELXTL*. Hydrogen atoms were first located in the difference map then positioned geometrically and allowed to ride on their respective parent atoms. Diagrams and publication material were generated using SHELXTL, PLATON[94] and ORTEP-3[95].

OTHER GENERAL PROCEDURES

Concentration of evaporation *in vacuo* refers to the removal of solvent under reduced pressure (~20mm Hg, 45^{o}C) on a rotary evaporator and final drying on an oil pump (~1-2 mm Hg) at room temperature.

Yields are calculated from the mass of the immediate synthetic precursor used, unless otherwise specified.

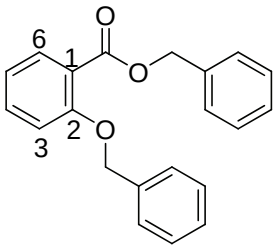

(**147**)

benzyl 2-(benzyloxy)benzoate

2-Hydroxybenzoic acid (5.00 g, 0.0362 moles) was dissolved in dry acetone (120 ml). Dry potassium carbonate (15.00 g, 0.109 moles) was added and the mixture left to stir at room temperature for 10 minutes. Benzyl bromide (12.9 ml, 0109 moles) was added to the stirring mixture and the solution was heated under reflux for 18 hour under nitrogen atmosphere. The cooled reaction mixture was filtered through Celite, which was washed with dry acetone (3 × 50 ml). The solvent was removed under reduced pressure and the residue dissolved in dichloromethane (25 ml). The organic layer was washed consecutively with 5% aqueous NaOH (25 ml), brine (20 ml) and distilled water (20 ml). The organic layer was dried over magnesium sulfate and the solvent removed under reduced pressure. The residue was purified by column chromatography with 5%-20% ethyl acetate/hexane as eluent to afford the product (**147**) as a white crystalline solid (10.04 g, 0.0315 moles, 87%). M.p. 47 ^{o}C - 49 ^{o}C, lit. M.p.[80] 50 ^{o}C - 51 ^{o}C; ^{1}H NMR ($CDCl_3$, 300 MHz) δ 7.85 (dd, *J* = 7.7, 1.7, 1H, Ar-*H*, 6-H), 7.52 - 7.23 (m, 11H, Ar-*H*), 6.93 - 6.99 (m, 2H, Ar-*H*), 5.33 (s, 2H, C*H*$_2$), 5.13 (s, 2H, C*H*$_2$); ^{13}C NMR ($CDCl_3$, 75 MHz) δ 166.2 (*C*=O)^{q}, 158.1 (Ar*C*-C=O)^{q}, 136.5 (Ar*C*-O-CH$_2$)^{q}, 136.0 (Ar*C*-C)^{q} , 133.4 (Ar*C*H), 131.8 (Ar*C*H), 128.4 (2Ar*C*H), 128.4 (2Ar*C*H), 128.1 (2Ar*C*H), 128.0 (Ar*C*H), 127.7 (Ar*C*H), 127.0 (2Ar*C*H), 120.6 (Ar*C*-C)^{q}, 120.4 (Ar*C*H), 113.6 (Ar*C*H), 70.5 (*C*H$_2$), 66.6 (*C*H$_2$); IR ν_{max}. 1716 (C=O), 1598 (C=C), 1580 (C=C), 1233 (C-O), 1072 (C-O) cm^{-1}; LRMS (*m/z*) calculated for $C_{21}H_{18}O_3$ 318.13, found (M^+, 100%), 319.20.

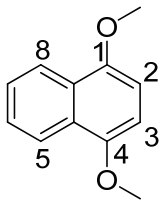

(**153**)

1,4-dimethoxynaphthalene

1,4-Naphthoquinone (5.00 g, 0.0316 moles), sodium dithionite (35.86 g) in distilled water (300 ml) and diethyl ether (500 ml) were added to a 1 liter separatory funnel. The mixture was shaken every 10 minutes over an hour. The organic layer was separated and washed with brine (50 ml) and dried over magnesium sulfate. The solvent was removed under reduced pressure. The brown solid was immediately dissolved in dry acetone (100 ml) followed by successive additions of dry potassium carbonate (10.90 g, 0.0790 moles) and dimethyl sulfate (7.50 ml, 0.0790 moles). The stirring mixture was heated under reflux in an inert atmosphere for 18 hours. The cooled reaction mixture was filtered through Celite and was washed with dry acetone (3 × 50 ml). The solvent was removed under reduced pressure and the residue dissolved in diethyl ether (50 ml). The organic layer was washed consecutively with 25% ammonia (25 ml), distilled water (25 ml), 10% HCl (25 ml), brine (25 ml) and distilled water (25 ml) again. The organic layer was dried over magnesium sulfate and the solvent removed under reduced pressure. The residue was purified by column chromatography with 5% ethyl acetate/hexane as eluent to afford the product (**153**) as white needle crystals (5.05 g, 0.0269 moles, 85%). M.p. 85 ^{o}C - 88 ^{o}C, lit. M.p.[96] 87 ^{o}C - 88 ^{o}C; ^{1}H NMR ($CDCl_3$, 300 MHz) δ 8.48 - 8.09 (m, 2H Ar-*H*), 7.68 - 7.41 (m, 2H, Ar-*H*), 6.73 (s, 2H, Ar-*H*, 2-H, 3-H), 4.00 (s, 6H, 2OC*H*$_3$); ^{13}C NMR ($CDCl_3$, 75 MHz) δ 149.5 (2Ar*C*-OCH_3)^{q}, 126..4 (2Ar*C*=C)^{q}, 125.9 (2Ar*C*H), 121.8 (2Ar*C*H), 103.2 (2Ar*C*H), 55.7 (2O*C*H_3); IR ν_{max}. 1630 (C=C), 1592 (C=C), 1231 (C-O), 1058 (C-O) cm^{-1}; LRMS (*m/z*) calculated for $C_{12}H_{12}O_2$ 188.08, found (M^+, 100%), 189.09.

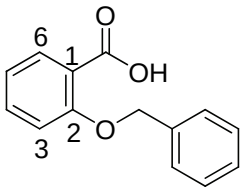

(**155**)

2-(benzyloxy)benzoic acid

Benzyl 2-(benzyloxy)benzoate (**147**) (9.00 g, 0.0283 moles) was added to the 12% potassium hydroxide in methanol (5.00 g in 60 ml) and heated under reflux in an inert atmosphere for 18 hours. The reaction mixture was subsequently cooled and quenched with ice cold concentrated HCl (50 ml). The mixture was filtered through Celite and was washed with diethyl ether (3 × 50 ml). The organic layer was dried over magnesium sulfate and the solvent removed under reduced pressure. The residue was purified by column chromatography with 20% ethyl acetate/hexane as eluent to afford the product (**155**) as white cube crystals (5.55 g, 0.0243 moles, 86%). M.p. 72 ^{o}C - 75 ^{o}C, lit. M.p.[82] 73.5 ^{o}C - 74.5 ^{o}C; ^{1}H NMR ($CDCl_3$, 300 MHz) δ 10.71 (s, 1H Ar-O*H*), 8.14 (dd, *J* = 7.8, 1.7 1H, Ar-*H*, 6-H), 7.60 - 7.29 (m, 6H, Ar-*H*), 7.15 - 7.03 (m, 2H, Ar-*H*), 5.48 (s, 2H, C*H*$_2$); ^{13}C NMR ($CDCl_3$, 75 MHz) δ 166.2 (HO*C*=O)^{q}, 157.6 (Ar*C*-C=O)^{q}, 135.1 (Ar*C*H), 134.7 (Ar*C*-O-CH_2)^{q}, 133.6 (Ar*C*H), 129.0 (2Ar*C*H), 129.0 (Ar*C*H), 127.8 (2Ar*C*H), 122.2 (Ar*C*H), 118.1 (Ar*C*-C)^{q}, 113.3 (Ar*C*H), 72.0 (*C*H_2); IR ν_{max}. 2970 (C-OH), 1674 (C=O), 1599 (C=C), 1232 (C-O) cm^{-1}; LRMS (*m/z*) calculated for $C_{14}H_{12}O_3$ 228.08, found (M^+, 100%), 229.15

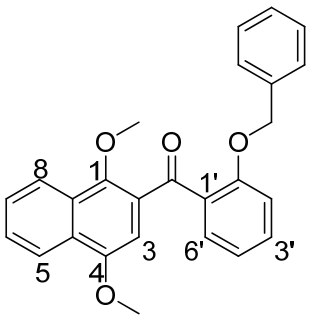

(**135**)

(2-(benzyloxy)phenyl)(1,4-dimethoxynaphthalen-2-yl)methanone

2-(Benzyloxy)benzoic acid (**155**) (3.64 g, 0.0160 moles) was premixed with the trifluoroacetic anhydride (2.25 ml, 0.0160 moles) in dry dichloromethane (10 ml) and was rapidly added to the 1,4-dimethoxynaphthalene (3.00 g, 0.0160 moles) dissolved in dry dichloromethane (10 ml). The stirring mixture was heated under reflux for 92 hours with the addition of further trifluoroacetic anhydride (2.25 ml, 0.0160 moles) at 6 hours, 24 hours and 48 hours. The mixture was allowed to cool and was quenched with successive additions of methanol (50 ml) and saturated sodium hydrogen carbonate solution (50 ml). The organic material was extracted into dichloromethane (4 × 25ml) and dried over magnesium sulfate. The solvent was removed under reduced pressure and the residue was purified by column chromatography with 5% ethyl acetate/hexane as eluent to afford the product (**135**) as pale green plate crystals (1.14 g, 0.00455 moles, 30%) from methanol. M.p. 105 ^{o}C - 107 ^{o}C; ^{1}H NMR ($CDCl_3$, 300 MHz) δ 8.33 - 7.99 (m, 2H Ar-*H*), 7.69 (d, 1H, *J* = 7.5, Ar-*H*, 6'-H), 7.61 - 7.42 (m, 3H, Ar-*H*), 7.15 – 6.96 (m, 3H, Ar-*H*), 6.96 - 6.84 (m, 2H, Ar-*H*), 6.82 (s, 1H, Ar-*H*, 3-H), 6.74 (d, *J* = 7.6, 2H, Ar-*H*, 5-H, 8-H), 4.89 (s, 2H, CH_2), 3.91 (s, 3H, OCH_3), 3.59 ((s, 3H, OCH_3); ^{13}C NMR ($CDCl_3$, 75 MHz) δ 196.3 (*C*=O)^{q}, 157.5 (Ar*C*-OCH_2)^{q}, 151.7 (Ar*C*-OCH_3)^{q}, 150.3 (Ar*C*-OCH_3)^{q}, 135.9 (Ar*C*-C=O)^{q}, 132.9 (Ar*C*H), 130.7 (Ar*C*-C=O)^{q}, 130.2 (Ar*C*H), 129.0 (Ar*C*=C)^{q}, 128.8 (Ar*C*=C)^{q} , 128.4 (Ar*C*-CH_2)^{q}, 127.9 (2Ar*C*H), 127.5 (Ar*C*H) , 127.2 (Ar*C*H), 126.8 (Ar*C*H), 126.8 (2Ar*C*H), 123.1 (Ar*C*H), 122.4 (Ar*C*H), 120.7 (Ar*C*H), 112.3 (Ar*C*H), 103.0 (Ar*C*H), 70.3 (*C*H_2), 63.6 (O*C*H_3), 55.8 (O*C*H_3); IR ν_{max}. 1734 (C=O), 1594 (C=C), 1290 (C-O), 1096 (C-O) cm^{-1}; HRMS (*m/z*) calculated for $C_{26}H_{22}O_4$ 398.1518, found 398.1523.

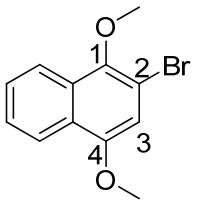

(**171**)

2-bromo-1,4-dimethoxynaphthalene

N-Bromosuccinimide (3.80 g, 0.0214 moles) was added to the 1,4-dimethoxynaphthalene (4.00 g, 0.0213 moles) in dry dichloromethane (30 ml). The mixture was stirred for 18 hours at room temperature. The mixture was washed with saturated sodium sulfite solution (25 ml) and extracted into dichloromethane (3 × 50 ml). The organic layer was dried over magnesium sulfate. The solvent was removed under reduced pressure and the residue was purified by column chromatography with 5% ethyl acetate/hexane as eluent to afford the product (**171**) as white grains (5.12 g, 0.0192 moles, 90%). M.p. 56 ^{o}C - 58 ^{o}C, lit. M.p.[86] 54 ^{o}C - 55 ^{o}C; ^{1}H NMR ($CDCl_3$, 300 MHz) δ 8.28 - 8.05 (m, 2H Ar-*H*), 7.63 - 7.48 (m, 2H, Ar-*H*), 6.91 (s, 1H, Ar-*H*, 1-H), 3.97 (s, 3H, OC*H*$_3$), 3.98 (s, 3H, OC*H*$_3$); ^{13}C NMR ($CDCl_3$, 75 MHz) δ 152.1 (Ar*C*-OCH_3)^{q}, 146.6 (Ar*C*-OCH_3)^{q}, 128..9 (Ar*C*=C)^{q}, 127.3 (Ar*C*H), 125.5 (Ar*C*H), 125.5 (Ar*C*=C)^{q} 122.2 (Ar*C*H), 121.7 (Ar*C*H), 111.8 (Ar*C*Br), 107.8 (Ar*C*H), 61.3 (O*C*H_3), 55.7 (O*C*H_3); IR ν_{max}. 1615 (C=C), 1575 (C=C), 1105 (C-O), 773 (C-Br) cm^{-1}; LRMS (*m/z*) calculated for $C_{12}H_{11}BrO_2$, 265.99, found (M^+, 100%), 267.03

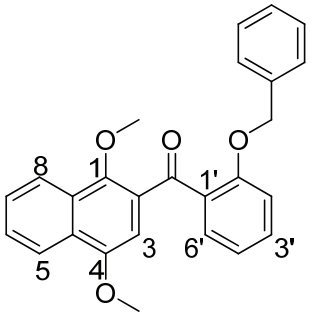

(**135**)

(2-(benzyloxy)phenyl)(1,4-dimethoxynaphthalen-2-yl)methanone

2-Bromo-1,4-dimethoxynaphthalene (**171**) (4.00 g, 0.0148 moles) was dissolved in dry tetrahydrofuran (20 ml) and stirred at –78 ^{o}C for 5 minutes under an inert

atmosphere. The *N*-butyl lithium (1.2M, 0.0150moles, 18ml) was added dropwise at –78 ^{o}C and the mixture stirred at 78^{o}C for 45 minutes in an inert atmosphere. The lithiated mixture was added dropwise to the benzyl 2-(benzyloxy)benzoate (**147**) (4.78 g, 0.0143 moles) in dry tetrahydrofuran (20 ml) at –78 ^{o}C. The mixture was stirred for an additional 30 minutes at –78 ^{o}C in an inert atmosphere. The mixture was quenched with a saturated solution of ammonium chloride (25 ml) at –78 ^{o}C and allowed to reach room temperature. The tetrahydrofuran was removed under reduced pressure and ethyl acetate (50 ml) was added. The organic layer was washed consecutively with water (25 ml) and brine (25 ml) and dried over magnesium sulfate. The solvent was removed under reduced pressure and the residue was purified by column chromatography with 5% - 20% ethyl acetate/hexane as eluent to afford the product (**135**) as pale green plate crystals (5.07 g, 0.0127 moles, 89%) in methanol. M.p. 105 ^{o}C - 107 ^{o}C; ^{1}H NMR ($CDCl_3$, 300 MHz) δ 8.33 - 7.99 (m, 2H Ar-*H*), 7.69 (d, 1H, *J* = 7.5, Ar-*H*, 6'-H), 7.61 - 7.42 (m, 3H, Ar-*H*), 7.15 – 6.96 (m, 3H, Ar-*H*), 6.96 - 6.84 (m, 2H, Ar-*H*), 6.82 (s, 1H, Ar-*H*, 3-H), 6.74 (d, *J* = 7.6, 2H, Ar-*H*, 5-H, 8-H), 4.89 (s, 2H, C*H*$_2$), 3.91 (s, 3H, OC*H*$_3$), 3.59 ((s, 3H, OC*H*$_3$); ^{13}C NMR ($CDCl_3$, 75 MHz) δ 196.3 (*C*=O)^{q}, 157.5 (Ar*C*-OCH$_2$)^{q}, 151.7 (Ar*C*-OCH$_3$)^{q}, 150.3 (Ar*C*-OCH$_3$)^{q}, 135.9 (Ar*C*-C=O)^{q}, 132.9 (Ar*C*H), 130.7 (Ar*C*-C=O)^{q}, 130.2 (Ar*C*H), 129.0 (Ar*C*=C)^{q}, 128.8 (Ar*C*=C)^{q} , 128.4 (Ar*C*-CH$_2$)^{q}, 127.9 (2Ar*C*H), 127.5 (Ar*C*H) , 127.2 (Ar*C*H), 126.8 (Ar*C*H), 126.8 (2Ar*C*H), 123.1 (Ar*C*H), 122.4 (Ar*C*H), 120.7 (Ar*C*H), 112.3 (Ar*C*H), 103.0 (Ar*C*H), 70.3 (*C*H$_2$), 63.6 (O*C*H$_3$), 55.8 (O*C*H$_3$); IR ν_{max}. 1734 (C=O), 1594 (C=C), 1290 (C-O), 1096 (C-O) cm^{-1}; HRMS (*m/z*) calculated for $C_{26}H_{22}O_4$, 398.1518, found 398.1523.

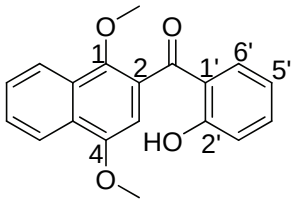

(**136**)

(1,4-dimethoxynaphthalen-2-yl)(2-hydroxyphenyl)methanone

5% Palladium on carbon (0.25 g) was added to (2-(benzyloxy)phenyl)(1,4-dimethoxynaphthalen-2-yl)methanone (**135**) (2.50 g, 0.00627 moles) in dry methanol

(30 ml). The mixture was submitted to a hydrogen atmosphere at a pressure of 4.5 bars for 24 hours. The mixture was filtered through Celite and washed with dichloromethane (3 × 50 ml). The organic layer was dried over magnesium sulphate. The solvent was removed under reduced pressure and the residue was purified by column chromatography with 10% ethyl acetate/hexane as eluent to afford the product (**136**) as pale green needles (1.88 g, 0.00608 moles, 97%) in methanol. M.p. 116 ^{o}C - 118 ^{o}C; ^{1}H NMR ($CDCl_3$, 300 MHz) δ 12.25 (s, 1H, Ar-O*H*) 8.31 - 8.13 (m, 2H Ar-*H*), 7.69 - 7.39 (m, 4H, Ar-*H*), 7.05 (d, *J* = 8.7, 1H, Ar-*H*, 6'-H), 6.78 (t, *J* = 7.6 1H, Ar-*H*, 5'-H), 6.68 (s, 1H, Ar-*H*, 3-H), 3.94 (s, 3H, OC*H*$_3$), 3.81 ((s, 3H, OC*H*$_3$); ^{13}C NMR ($CDCl_3$, 75 MHz) δ 202.4 (*C*=O)^{q}, 163.1 (Ar*C*-OH)^{q}, 151.8 (Ar*C*-OCH_3)^{q}, 147.5 (Ar*C*-OCH_3)^{q}, 136.9 (Ar*C*H), 134.2 (Ar*C*H), 128.5 (Ar*C*-C=O)^{q}, 127.7 (Ar*C*-C=O)^{q}, 127.4 (Ar*C*H), 127.2 (Ar*C*H), 126.4 (Ar*C*=C)^{q}, 122.7 (Ar*C*H), 122.6 (Ar*C*H), 120.0 (Ar*C*=C)^{q}, 119.1 (Ar*C*H), 118.1 (Ar*C*H), 102.3 (Ar*C*H), 63.7 (O*C*H_3), 55.8 (O*C*H_3); IR ν_{max}. 2970 (C-OH), 1739 (C=O), 1592 (C=C), 1216 (C-O) cm^{-1}; HRMS (*m/z*) calculated for $C_{19}H_{16}O_4$, 308,1049, found 308.1048.

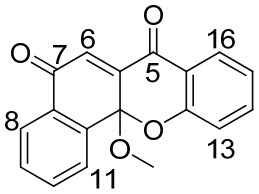

(**193**)

12a-methoxy-5H-benzo[c]xanthene-5,7(12aH)-dione

Ceric ammonium nitrate (13.3 g, 0.0243 moles) in water (25 ml) was added dropwise to a stirring mixture of (1,4-dimethoxynaphthalene-2-yl)(2-hydroxyphenyl)methanone (**136**) (1.50 g, 0.00486 moles) in acetonitrile (25 ml) and chloroform (5 ml). The mixture was stirred at room temperature for 90 minutes. The reaction mixture was filtered through Celite and washed with ethyl acetate (3 × 25 ml). The organic layer was washed consecutively with saturated sodium hydrogen carbonate solution (25 ml), brine (25 ml) and water (25 ml). The organic layer was dried over magnesium sulphate. The solvent was removed under reduced pressure and the residue was purified by column chromatography with 5% ethyl acetate/hexane as eluent to afford the product (**193**) as orange rod crystals (1.02 g, 0.00348 moles, 72%) in ethyl acetate.

M.p. 111 °C - 113 °C; [α] = -7.2; ^{1}H NMR ($CDCl_3$, 300 MHz) δ 8.16 (d, *J* = 7.8, 1H, Ar-*H*, 8-H), 8.07 - 8.02 (m, 2H, Ar-*H*), 7.83 - 7.57 (m, 3H, Ar-*H*), 7.26 (s, 1H, Ar-*H*, 6-H), 7.24 - 7.08 (m, 2H, Ar-*H*), 3.03 (s, 3H, OC*H*$_3$); ^{13}C NMR ($CDCl_3$, 75 MHz) δ 184.0 (*C*=O)^{q}, 181.0 (*C*=O)^{q}, 157.8 (Ar*C*-OCAr)^{q}, 143.8 (Ar*C*-C=O)^{q}, 137.0 (Ar*C*H), 136.6 (Ar*C*-C=O)^{q}, 133.9 (Ar*C*H), 130.8 (Ar*C*=C)^{q}, 130.6 (Ar*C*H), 130.2 (Ar*C*H), 127.6 (Ar*C*H), 126.9 (Ar*C*H), 126.5 (Ar*C*H), 123.2 (Ar*C*H), 121.5 (Ar*C*=C)^{q}, 118.6 (Ar*C*H), 96.4 (ArCO-*C*-OCH$_3$), 51.5 (O*C*H$_3$); IR ν_{max}. 1738 (C=O), 1637 (C=C), 1605 (C=C), 1226 (C-O), 1129 (C-O), 1099 (C-O) cm^{-1}; HRMS (*m/z*) calculated for $C_{18}H_{12}O_4$, 292.0736, found 308.1048, found 276.0778 (100%).

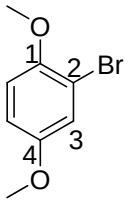

(**197**)

2-bromo-1,4-dimethoxybenzene

N-Bromosuccinimide (6.65 g, 0.0373 moles) was added to the 1,4-dimethoxybenzene (5.02 g, 0.0363 moles) in dry dichloromethane (30 ml). The stirring mixture was heated under reflux for 48 hours. The mixture was allowed to cool to room temperature and was washed with saturated sodium sulfite solution (25 ml). The mixture was extracted into dichloromethane (3 × 50 ml). The organic layer was dried over magnesium sulfate. The solvent was removed under reduced pressure and the residue was purified by column chromatography with 5% ethyl acetate/hexane as eluent to afford the product (**197**) as a colorless oil (7.01 g, 0.0323 moles, 89%). ^{1}H NMR ($CDCl_3$, 300 MHz) δ 7.11 (s, 1H Ar-*H*, 1-H), 6.91 - 6.74 (m, 2H, Ar-*H*), 3.82 (s, 3H, OC*H*$_3$), 3.74 (s, 3H, OC*H*$_3$); ^{13}C NMR ($CDCl_3$, 75 MHz) δ 154.0 (Ar*C*-OCH$_3$)^{q}, 150.3 (Ar*C*-OCH$_3$)^{q}, 119.0 (Ar*C*H), 113.6 (Ar*C*Br)^{q}, 112.9 (Ar*C*H), 111.9 (Ar*C*H), 56.8 (O*C*H$_3$), 55.9 (O*C*H$_3$); IR ν_{max}. 1607 (C=C), 1575 (C=C), 1036 (C-O), 730 (C-Br) cm^{-1}; LRMS (*m/z*) calculated for $C_8H_9BrO_2$, 225.98, found (M^{+}, 100%), 227.05.

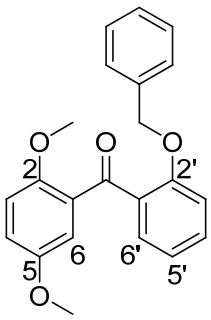

(**200**)

(2-(benzyloxy)phenyl)(2,5-dimethoxyphenyl)methanone

2-Bromo-1,4-dimethoxy benzene (2.50 g, 0.0115 moles) was dissolved in dry tetrahydrofuran (15 ml) and stirred at –78 ^{o}C for 5 minutes in an inert atmosphere. *N*-Butyl lithium (1.2 M, 0.0115 moles, 14 ml) was added dropwise at –78 ^{o}C and the mixture stirred at –78 ^{o}C for 45 minutes in an inert atmosphere. The lithiated mixture was added dropwise to the benzyl 2-(benzyloxy)benzoate (**147**) (3.67 g, 0.0115 moles) in dry tetrahydrofuran (20 ml) at –78 ^{o}C over 30 minutes. The mixture was stirred for an additional 30 minutes at –78^{o}C in an inert atmosphere and thereafter was quenched with a saturated solution of ammonium chloride (25 ml) at –78 ^{o}C and allowed to reach room temperature. The tetrahydrofuran was removed under reduced pressure and ethyl acetate (50 ml) was added to dissolve the residue and was washed consecutively with water (25 ml) and brine (25 ml) and dried over magnesium sulfate. The solvent was removed under reduced pressure and the residue was purified by column chromatography with 5% - 20% ethyl acetate/hexane as eluent to afford the product (**200**) as a light yellow oil (2.85 g, 0.00819 moles, 72%). ^{1}H NMR ($CDCl_3$, 300 MHz) δ 7.59 (dd, *J* = 7.6, 1.7 1H Ar-*H*, 6'-H), 7.48 - 7.32 (m, 2H, Ar-*H*), 7.22 - 7.15 (m, 2H, Ar-*H*), 7.12 - 7.6.88 (m, 6H, Ar-*H*), 6.76 (d, *J* = 7.4 , 1H, Ar-*H*, 3-H) 4.94 (s, 2H, C*H*$_2$), 3.75 (s, 3H, OC*H*$_3$), 3.52 (s, 3H, OC*H*$_3$); ^{13}C NMR ($CDCl_3$, 75 MHz) δ 195.4 (*C*=O)^{q}, 157.2 (Ar*C*-OCH$_2$)^{q}, 153.5 (Ar*C*-OCH$_3$)^{q}, 152.8 (Ar*C*-OCH$_3$)^{q}, 136.4 (Ar*C*-C=O)^{q}, 132.6 (Ar*C*H), 130.8 (Ar*C*-C=O)^{q}, 130.4 (Ar*C*=C)^{q} 130.2 (Ar*C*H), 129.0 (Ar*C*=C)^{q}, 128.8 (Ar*C*=C)^{q} , 128.4 (Ar*C*-CH$_2$)^{q}, 128.2 (Ar*C*H) , 127.5 (2Ar*C*H), 127.0 (Ar*C*H), 126.7 (2Ar*C*H), 120.8 (Ar*C*H), 118.5 (Ar*C*H), 114.5 (Ar*C*H), 113.4 (Ar*C*H), 112.3 (Ar*C*H), 70.1 (*C*H$_2$), 56.5 (O*C*H$_3$), 55.9 (O*C*H$_3$); IR ν_{max}. 1738 (C=O), 1644 (C=C), 1595 (C=C), 1217 (C-O), 1042 (C-O) cm^{-1}; HRMS (*m/z*) calculated for $C_{22}H_{20}O_4$, 348.1362, found 348.1346.

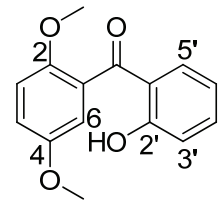

(**201**)

(2,5-dimethoxyphenyl)(2-hydroxyphenyl)methanone

5% Palladium on carbon (0.05 g) was added to (2-(benzyloxy)phenyl)(2,5-dimethoxyphenyl)methanone (**200**) (1.00 g, 0.00287 moles) in dry methanol (30 ml). The mixture was submitted to a hydrogen atmosphere at a pressure of 4.5 bars for 24 hours. The mixture was filtered through Celite and washed with dichloromethane (3 × 50 ml). The organic layer was dried over magnesium sulphate. The solvent was removed reduced pressure and the residue was purified by column chromatography with 10% ethyl acetate/hexane as eluent to afford the product (**200**) as white needles (0.66 g, 0.00258 moles) in methanol. M.p. 95 ^{o}C - 98 ^{o}C, lit. M.p.[97] 98 ^{o}C - 100 ^{o}C ^{1}H NMR ($CDCl_3$, 300 MHz) δ 12.04 (s, 1H, Ar-O*H*) 7.41 - 7.31 (m, 1H Ar-*H*), 7.26 (dd, *J* = 8.0, 1.5, 1H, Ar-*H*, 5'-H), 6.96 – 6.87 (m, 2H, Ar-*H*), 6.85 (s, 1H, Ar-*H*, 6-H), 6.78 - 6.55 (m, 2H, Ar-*H*), 3.67 (s, 3H, OCH_3), 3.60 ((s, 3H, OCH_3); ^{13}C NMR ($CDCl_3$, 75 MHz) δ 200.7 (*C*=O)^{q}, 161.8 (Ar*C*-OH)^{q}, 152.4 (Ar*C*-OCH_3)^{q}, 149.5 (Ar*C*-OCH_3)^{q}, 135.5 (Ar*C*H), 132.8 (Ar*C*H), 127.2 (Ar*C*-C=O)^{q}, 119.0 (Ar*C*-C=O)^{q}, 117.8 (Ar*C*H), 117.0 (Ar*C*H), 116.0 (Ar*C*H), 112.9 (Ar*C*H), 111.9 (Ar*C*H), 55.2 (O*C*H_3), 54.7 (O*C*H_3); IR ν_{max}. 2941 (C-OH), 1738 (C=O), 1575 (C=C), 1221 (C-O) cm^{-1}; HRMS (*m/z*) calculated for $C_{15}H_{14}O_4$, 258.0892, found 258.0883

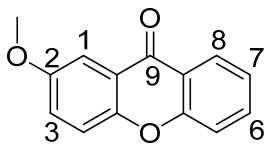

(**202**)

2-methoxy-9H-xanthen-9-one

Ceric ammonium nitrate (1.06 g, 0.00194 moles) in water (5 ml) was added dropwise to a stirring mixture of (2,5-dimethoxyphenyl)(2-hydroxyphenyl)methanone (**201**)

(0.100 g, 0.000388 moles) in acetonitrile (10 ml) and chloroform (2.5 ml). The mixture was stirred at room temperature for 24 hours. The reaction mixture was filtered through Celite and washed with ethyl acetate (3 × 25 ml). The organic layer was washed consecutively with saturated sodium hydrogen carbonate solution (25 ml), brine (25 ml) and water (25 ml) and was dried over magnesium sulfate. The solvent was removed under reduced pressure and the residue was purified by column chromatography with 5% ethyl acetate/hexane as eluent to afford the products (**202**) as white needles (0.065 g, 0.00288 moles, 74%) and (**203**) as orange grains (0.015 g, 0.0000620 moles, 15%). M.p. 130 ^{o}C - 133 ^{o}C, lit. M.p.[98] 134 ^{o}C - 135 ^{o}C; ^{1}H NMR ($CDCl_3$, 300MHz) δ 8.25 (dd, *J* = 8.0, 1.6, 1H Ar-*H*, 8-H), 7.65 - 7.55 (m, 2H, Ar-*H*), 7.42 - 7.31 (dd, *J* = 7.8, 1.4, 1H, Ar-*H*, 5-H), 7.29 (s, 1H, Ar-*H*, 1-H), 7.28 - 7.14 (m, 2H, Ar-*H*), 3.83 (s, 3H, OC*H*$_3$); ^{13}C NMR ($CDCl_3$, 75MHz) δ 176.0 (*C*=O)^{q}, 155.0 (Ar*C*-OCAr)^{q}, 154.9 (Ar*C*-OCAr)^{q} 149.9 (Ar*C*-OCH$_3$)^{q}, 133.5 (Ar*C*H), 125.6 (Ar*C*H), 123.8 (Ar*C*H), 122.6 (Ar*C*H), 121.0 (Ar*C*-C=O)^{q}, 120.2 (Ar*C*-C=O)^{q}, 118.4 (Ar*C*H), 116.9 (Ar*C*H), 104.8 (Ar*C*H), 54.9 (O*C*H$_3$); IR ν_{max}. 1738 (C=O), 1647 (C=C), 1614 (C=C), 1211 (C-O), 1142 (C-O) cm^{-1}; HRMS (*m/z*) calculated for $C_{14}H_{10}O_3$, 226.0630, found 226.0620.

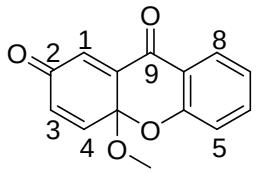

(**203**)

4a-methoxy-2H-xanthene-2,9(4aH)-dione

M.p. 92 ^{o}C - 95 ^{o}C; [α] = -6.111^{o}; ^{1}H NMR ($CDCl_3$, 300 MHz) δ 7.94 (d, *J* = 7.8, 1H Ar-*H*, 3-H), 7.53 (t, *J* = 7.8, 1H, Ar-*H*, 7-H), 7.11 (t, *J* = 7.5, 1H, Ar-*H*, 6-H), 7.03 (d, *J* = 10.0 1H, Ar-*H*, 4-H), 6.81 (s, 1H, Ar-*H*, 1-H), 6.37 (dd, *J* = 10.4, 1.9, 2H, 5-H, 8-H), 3.25 (s, 3H, OC*H*$_3$); ^{13}C NMR ($CDCl_3$, 75 MHz) δ 185.05 (*C*=O)^{q}, 180.94 (*C*=O)^{q}, 157.0 (Ar*C*-OCAr)^{q}, 144.5 (Ar*C*-C=O)^{q}, 140.1 (Ar*C*H), 137.0 (Ar*C*H), 130.7 (Ar*C*H), 128.5 (Ar*C*H), 127.5 (Ar*C*H), 123.3 (Ar*C*H), 121.6 (Ar*C*-C=O)^{q}, 118.5 (Ar*C*H), 95.1 (ArCO-*C*-OCH$_3$)^{q}, 51.3 (O*C*H$_3$); IR ν_{max}. 1738 (C=O), 1645 (C=C),

1604 (C=C), 1217 (C-O), 1140 (C-O), 1098 (C-O) cm^{-1}; HRMS (*m/z*) calculated for $C_{14}H_{10}O_4$, 242.0479, found 242.05676 (100%).

REFERENCES

1. Hepworth, J. D., *In Comprehensive Heterocyclic Chemistry*. Pergamon: Oxford, 1984; Vol. 3.
2. Damas, A. M.; Gales, L., *Curr. Med. Chem.* **2005**, *12*, 2499.
3. Pinto, M. M. M.; Sousa, M. E.; Nascimento, M. S. J., *Curr. Med. Chem.* **2005**, *12*, 2517.
4. de Koning, C. B.; Giles, R. B. F.; Engelhardt, L. M.; White, A. H., *J. Chem. Soc. Perkin Trans. I* **1988**, 3209.
5. Robinson, P. M.; Park, D.; McClure, W. K., *Trans. Br. Mycol. Soc.* **1969**, *52*, 447.
6. Balan, J.; Fuska, J.; Kuhr, I.; Kuhrova, V., *Folia Microbiol.* **1970**, *15*, 479.
7. Fuska, J.; Ivanitskaya, L. P.; Makukho, L. V.; Volkova, L. Y., *Antibiotiki* **1974**, *19*, 890.
8. Kjaer, D.; Kjaer, A.; Pedersen, J. D.; Smith, J. R., *J. Chem. Soc.* **1971**, 2792.
9. Sultanbawa, M. U. S., *Tetrahedron* **1980**, *36*, 1465.
10. Bhattacharya, S. K.; Finnegan, R. A.; Stephani, G. M.; Ganguli, G., *J. Pharm. Sci.* **1968**, *57*, 1039.
11. MacKeen, M. M.; Ali, A. M.; Lajis, N. H.; Kawazu, K.; Hassan, Z.; Amran, M.; Habsah, M.; Mooi, L. Y.; Mohammed, S. M., *J. Ethnopharmacol.* **2000**, *72*, 395.
12. Ito, C.; Itoigawa, M.; Furukawa, H.; Rao, K. S.; Enjo, F.; Bu, P.; Takayasu, J.; Tokuda, H.; Nishino, H., *Cancer Lett.* **1998**, *132*, 113.
13. Saha, P.; Mandal, S.; Das, A.; Das, P. C.; Das, S., *Phytother. Res.* **2004,** *18*, 373.
14. Kupchan, S. M.; Sneden, A. T.; Steelman, D. R., *J. Nat. Prod.* **1980**, *43*, 296.
15. Geran, R. I.; Greenberg, N. H.; McDonald, M. M.; Schumacher, A. M.; Abbot, B. J., *J. Cancer Chemother. Rep.* **1972**, *3*, 1.

16. Cassady, J. M.; Habib, A. M.; Ho, D. K.; Masuda, S.; McCloud, T.; Reddy, K. S.; Aboushoer, M.; McKenzie, A.; Byrn, S. R.; Chang, C. J., *J. Org. Chem.* **1987**, *52*, 413.
17. Cassady, J. M.; Ho, K. K.; McKenzie, A. T.; Byrn, S. R., *J. Org. Chem.* **1987**, *52*, 342.
18. Schwaebe, M. K.; Moran, T. J.; Whitten, J. P., *Tetrahedron Lett.* **2005**, *46*, 827.
19. Nitiss, J. L., *Biochim. Biophys. Acta.* **1998**, *1400*, 63.
20. Hansen, M.; Hurley, L. H.; Lee, S. J.; Cassady, J. M., *J. Am. Chem. Soc.* **1996**, *118*, 5553.
21. Hurley, L. H.; Kim, M. Y.; Younghwa, N.; Vankayalapati, H.; Gleason-Guzman, M., *J. Med. Chem.* **2003**, *46*, 2958.
22. Vladu, B.; Woynarowski, J. M.; Manikumar, G.; Wani, M. C.; Wall, M. E.; Von Hoff, D. D.; Wadkins, R. M., *Mol. Pharmacol.* **2000**, *57*, 243.
23. Tada, M.; Yoshii, T.; Asano, J.; Kazuhiro, C., *Phytochemistry* **1996**, *41*, 815.
24. Nicolaou, K. C.; Xu, H.; Wartmann, M., *Angew. Chem. Int. Ed.* **2005**, *44*, 756.
25. Zhang, H. Z.; Kasibhatla, S.; Wang, Y.; Herich, J.; Guastella, J.; Tseng, B.; Drewe, J.; Cai, S. X., *Bioorg. Med. Chem.* **2004**, *12*, 309.
26. Reed, J. C.; Tomaselli, K. J., *Curr. Opin. Biotechnol.* **2000**, *11*, 586.
27. Thornberry, N. A., *Chem. Biol.* **1998**, *5*, R97.
28. Reed, J. C., *J. Clin. Oncol.* **1999**, *17*, 2941.
29. Cai, S. X.; Kuemmerle, J.; Songchun, J.; Tseng, B.; Kasibhatla, S.; Drewe, J., *Bioorg. Med. Chem.* **2008**, *16*, 4233.
30. Asai, F.; Tosa, H.; Tanaka, T.; Iiunuma, M., *Phytochemistry* **1995**, *39*, 943-944.
31. Iikubo, K.; Ishikawa, Y.; Ando, N.; Umezawa, K.; Nishiyama, S., *Tetrahedron Lett.* **2002**, *43*, 291.
32. Matsumoto, K.; Akao, Y.; Kobayashi, E.; Ohguchi, K.; Ito, T.; Tanaka, T.; Iinuma, M.; Nozawa, Y., *J. Nat. Prod.* **2003**, *66*, 1124.
33. Matsumoto, K.; Akao, Y.; Yi, H.; Ohguchi, K.; Ito, T.; Tanaka, T.; Kobayashi, E.; Iinuma, M.; Nozawa, Y., *Bioorg. Med. Chem.* **2004**, *12*, 5799.
34. Matsumoto, K.; Akao, Y.; Ohguchi, K.; Ito, T.; Tanaka, T.; Iinuma, M.; Nozawa, Y., *Bioorg. Med. Chem.* **2005**, *13*, 6064.

35. Akao, Y.; Nakagawa, Y.; Iinuma, M.; Naoe, T.; Nozawa, Y., *Bioorg. Med. Chem.* **2007**, *15*, 5620.
36. Kuller, L. H.; Matthews, K. A.; Meilahn, E. N., *J. Steroid Biochem. Mol. Biol.* **2000**, *74*, 365.
37. Brueggemeier, R. W.; Richards, J. A.; Petrel, T. A., *J. Steroid Biochem. Mol. Biol.* **2003**, *86*, 501.
38. Kinghorn, A. D.; Brueggemeier, R. W.; Su, B.; Balunas, M. J., *J. Nat. Prod.* **2008**, *71*, 1161.
39. Nuhrich, A.; Moreau, S.; Varache-Lembege, M.; Larrouture, S.; Fall, D.; Neveu, A.; Deffieux, G.; Vercauteren, J., *Eur. J. Med. Chem* **2002**, *37*, 237.
40. Cordell, G. A.; Wang, J. N.; Hou, C. Y.; Liu, Y. L.; Lin, Z. L.; Gil, R. R., *J. Nat. Prod.* **1994**, *57*, 211.
41. Cordell, G. A.; Kinghorn, A. D.; Pengsuparp, T.; Cai, L.; Constant, H.; Fong, H. S.; Lin, Z. L.; Pezutto, J. M.; Ingolfsdottir, K.; Wagner, H.; Hughes, S. H., *J. Nat. Prod.* **1995**, *58*, 1024.
42. Sarin, P. S., *Ann. Rev. Pharmacol. Toxicol.* **1988**, *28*, 411.
43. Boyd, M. R.; Groweiss, A.; Cardellina, J. H., *J. Nat. Prod.* **2000**, *63*, 1537.
44. Riscoe, M.; Kelly, J. X.; Winter, R., *Curr. Med. Chem.* **2005**, *12*, 2539.
45. Riscoe, M.; Winter, R.; Ignatushchenko, M. V.; Bachinger, H. P.; Hinrichs, D. J., *FEBS Lett.* **1997**, *409*, 67.
46. Luzzi, J. A.; Peto, T. E., *Drug Saf.* **1993**, *8*, 295.
47. Riscoe, M.; Winter, R.; Dodean, R. A.; Kelly, J. X.; Peyton, D.; Gard, G. L., *Bioorg. Med. Chem.* **2008**, *16*, 1174.
48. White, W., *In The Porphyrins*. Academic Press: New York, 1978; Vol. 5, p 303.
49. Ampofo, S. A.; Waterman, P. G., *Phytochemistry* **1986**, *25*, 2617.
50. Dharmaratne, H. R. W.; Sotheeswaran, S.; Balasubramaniam, S.; Reischa, J., *Phytochemistry* **1986**, *25*, 1957.
51. Hay, A. E.; Helesbeux, J. J.; Duval, O.; Labaied, M.; Grellier, P.; Richomme, P., *Life Sciences* **2004**, *75*, 3077.
52. Portela, C.; Afonso, C. M. M.; Madalena, M. M.; Pinto, M. M. M.; Ramos, J., *Bioorg. Med. Chem.* **2004**, *12*, 3313.
53. Bringmann, G.; Ochse, M.; Schupp, O.; Tasler, S., *Progress in the Chemistry of Organic Natural Products*. Springer: Wien, Germany, 2001.

54. Sousa, M. E.; Pinto, M. M. M., *Curr. Med. Chem.* **2005**, *12*, 2447.
55. Michael, A., *Amer. Chem. J.* **1883**, *5*, 81.
56. Lespegnol; Betrand; Dupas, *Bull. Soc. Chim. France* **1939**, *6*, 1925.
57. Grover, P. K.; Shah, G. D.; Shah, R. C., *J. Chem. Soc.* **1955**, 3982.
58. Pillai, R. K. M.; Naiksatam, P.; Johnson, F.; Rajagopalan, R.; Watts, P. C.; Cricchio, R.; Borras, S., *J. Org. Chem.* **1986**, *51*, 717.
59. Barton, D. H. R.; Scott, A. I., *J. Chem. Soc.* **1958**, 1767.
60. Scheinmann, F.; Augustus, J. Q., *J. Chem. Soc. Perkin Trans. I* **1973**, *2*, 1329.
61. Elix, J. A.; Gaul, K. L.; Jiang, H., *Aust. J. Chem.* **1993**, *46*, 95.
62. Finnegan, R. A.; Merkel, K. E., *J. Org. Chem.* **1972**, *37*, 2986.
63. Reisch, J.; Mester, I.; El-Moghazy Aly, S. M., *J. Chem. Soc. Perkin Trans. I* **1983**, 219.
64. Atwell, G. J.; Rewcastle, G. W.; Baguley, B. C.; Denny, W. A., *J. Med. Chem.* **1990**, *33*, 1375.
65. Snieckus, V.; Familoni, O. B.; Ionica, I.; Bower, J. F., *Synlett.* **1997**, 1081.
66. Sousa, E. P.; Silva, A. M. A.; Pinto, M. M. M.; Pedro, M. M.; Cerqueira, F. A. M.; Nascimento, M. S. J., *Helv. Chim. Acta.* **2002**, *85*, 2862.
67. Nishikawa, H.; Robinson, R., *J. Chem. Soc.* **1922**, *121*, 839.
68. Bennet, O. F.; Bouchard, M. J.; Malloy, R.; Dervin, P.; Saluti, G., *J. Org. Chem.* **1971**, *37*, 1356.
69. Amstutz, E. D.; Neumeyer, C. R., *J. Am. Chem. Soc.* **1947**, *69*, 1925.
70. Harris, M. H.; Hay, J. V., *J. Am. Chem. Soc.* **1977**, *99*, 1631.
71. Sandifer, R. M.; Bhattacharya, S. K.; Harris, M. H., *J. Org. Chem.* **1981**, *46*, 2260.
72. Hauser, F. M.; Hewawasam, P.; Baghdanov, V. M., *J. Org. Chem.* **1988**, *53*, 223.
73. Hauser, F. M.; Dorsch, W. A., *Org. Lett.* **2003**, *5*, 3753.
74. Liebeskind, L. S.; Sun, L., *J. Am. Chem. Soc.* **1996**, *118*, 12473.
75. Liebeskind, L. S.; Sun, L., *Tetrahedron Lett.* **1997**, *38*, 3663.
76. Casillas, L. K.; Townsend, C. A., *J. Org. Chem.* **1999**, *64*, 4050.
77. Casillas, L. K.; Townsend, C. A.; Udwray, D. W., *J. Am. Chem. Soc.* **2002**, *124*, 5294.
78. Ghosh, C. K.; Bhattacharya, S. K.; Ghosh, C.; Patra, A., *J. Chem. Soc. Perkin Trans. I* **1999**, 3005.

79. Ghosh, C. K.; Bhattacharya, S. K.; Patra, A., *J. Chem. Soc. Perkin Trans. I* **1997**, 2167.
80. Elie; Anderson, *J. Am. Chem. Soc.* **1952,** *74*, 547.
81. Waldhor, E.; Schwederski, B.; Kaim, W., *J. Chem. Soc. Perkin Trans. II* **1993**, 2109.
82. Ye, T.; Garcia, C. F.; McKervey, M. A., *J. Chem. Soc. Perkin Trans. I* **1995,** *11*, 1373.
83. Sundholm, E. G., *Tetrahedron* **1978**, *34*, 577.
84. Argade, N. P.; Mondal, M.; Puranik, V. G., *J. Org. Chem.* **2006**, *71*, 4992.
85. Bloomer, J. L.; Zheng, W., *Synth. Commun.* **1998**, *28*, 2087.
86. Ungnade, H. E.; Hein, H., *J. Org. Chem.* **1949**, *14*, 911.
87. Lewis, J. R.; Findlay, J. W. A.; Gupta, P., *J. Chem. Soc. Chem. Commun.* **1969**, 206.
88. Lewis, J. R.; Paul, J. G., *J. Chem. Soc. Perkin Trans. I* **1981**, 770.
89. Becker, H. D., *J. Org. Chem.* **1969**, *34*, 1207.
90. Whalley, W. B.; Ellis, R. C.; Ball, K., *J. Chem. Soc. Perkin Trans. I* **1976**, 1377.
91. Castagnoli Jnr, N.; Jacob III, P.; Cellery, P. S.; Shulgin, A. T., *J. Org. Chem.* **1976**, *41*, 3627.
92. Chawla, H. M.; Sharma, S. K.; Chakrabarty, K.; Bhanumati, S., *Tetrahedron* **1988**, *44*, 1227.
93. Basavaiah, D.; Reddy, R. J., *Org. Biomol. Chem.* **2008**, *6*, 1034.
94. Spek, A. L., *J. Appl. Cryst.* **2003**, *36*, 7-13.
95. Farrugia, L. J., *J. Appl. Cryst.* **1997**, *30*, 565.
96. Fieser, *J. Am. Chem. Soc.* **1948**, *70*, 3177.
97. Shargi, H.; F, T., *Tetrahedron* **1996**, *52*, 13623.
98. Bennet, *J. Org. Chem.* **1972,** *37*, 1356.

APPENDIX I

Table 1: Crystal data and structure refinement for (1,4-dimethoxy naphthalen-2-yl)(2-hydroxy phenyl) methanone.

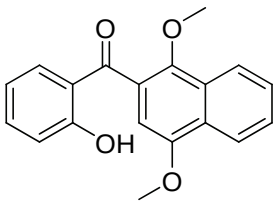

Identification code	8m_jn1_0s
Empirical formula	C18 H12 O4
Formula weight	292.28
Temperature	173(2) K
Wavelength	0.71073 Å
Crystal system	Monoclinic
Space group	P2(1)/n
Unit cell dimensions	a = 13.0183(7) Å □= 90°. b = 13.0356(6) Å □= 98.662(3)°. c = 15.9224(7) Å □= 90°.
Volume	2671.2(2) $Å^3$
Z	8
Density (calculated)	1.454 Mg/m^3
Absorption coefficient	0.103 mm^{-1}
F(000)	1216
Crystal size	0.49 x 0.28 x 0.25 mm^3
Theta range for data collection	1.89 to 28.00°.
Index ranges	-16<=h<=17, -17<=k<=15, -19<=l<=21
Reflections collected	19971
Independent reflections	6440 [R(int) = 0.0773]
Completeness to theta = 28.00°	100.0 %
Absorption correction	None
Max. and min. transmission	0.9747 and 0.9512
Refinement method	Full-matrix least-squares on F^2

Data / restraints / parameters	6440 / 0 / 399
Goodness-of-fit on F2	0.994
Final R indices [I>2sigma(I)]	R1 = 0.0788, wR2 = 0.1969
R indices (all data)	R1 = 0.1306, wR2 = 0.2362
Largest diff. peak and hole	1.128 and -0.307 e.Å^{-3}

Table 1: Crystal data and structure refinement for 12a-methoxy-5H-benzo[c]xanthenes 5,7(12aH)-dione

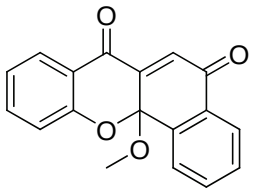

Identification code	8m_jn3_0f
Empirical formula	C19 H16 O4
Formula weight	308.32
Temperature	173(2) K
Wavelength	0.71073 Å
Crystal system	Orthorhombic
Space group	Pbca
Unit cell dimensions	a = 17.551(2) Å
	□= 90°.
	b = 8.1552(12) Å
	□= 90°.
	c = 21.281(3) Å
	□= 90°.
Volume	3046.0(7) Å^3
Z	8
Density (calculated)	1.345 Mg/m^3
Absorption coefficient	0.094 mm^{-1}
F(000)	1296
Crystal size	0.49 x 0.14 x 0.05 mm^3
Theta range for data collection	1.91 to 25.00°.
Index ranges	-20<=h<=19, -9<=k<=8, -15<=l<=25

Reflections collected	12601
Independent reflections	2658 [R(int) = 0.1074]
Completeness to theta = 25.00°	99.1 %
Absorption correction	None
Max. and min. transmission	0.9953 and 0.9553
Refinement method	Full-matrix least-squares on F^2
Data / restraints / parameters	2658 / 0 / 211
Goodness-of-fit on F2	1.303
Final R indices [I>2sigma(I)]	R1 = 0.0981, wR2 = 0.1418
R indices (all data)	R1 = 0.1732, wR2 = 0.1587
Largest diff. peak and hole	0.333 and -0.303 e.$Å^{-3}$

Table 1: Crystal data and structure refinement for (2,5-dimethoxy phenyl)(2-hydroxy phenyl) methanone

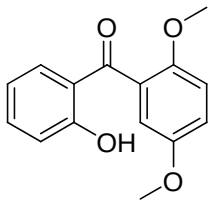

Identification code	8m_jn4_0s
Empirical formula	C15 H14 O4
Formula weight	258.26
Temperature	173(2) K
Wavelength	0.71073 Å
Crystal system	Triclinic
Space group	P-1
Unit cell dimensions	a = 7.4530(2) Å
	□= 80.0310(10)°.
	b = 9.0877(2) Å
	□= 79.7850(10)°.
	c = 9.9834(3) Å
	□ = 74.4330(10)°.
Volume	635.41(3) $Å^3$

Z	2
Density (calculated)	1.350 Mg/m^3
Absorption coefficient	0.098 mm^{-1}
F(000)	272
Crystal size	0.40 x 0.34 x 0.14 mm^3
Theta range for data collection	2.09 to 28.00°.
Index ranges	-9<=h<=9, -11<=k<=11, -13<=l<=13
Reflections collected	13834
Independent reflections	3065 [R(int) = 0.0414]
Completeness to theta = 28.00°	100.0 %
Absorption correction	None
Max. and min. transmission	0.9864 and 0.9619
Refinement method	Full-matrix least-squares on F^2
Data / restraints / parameters	3065 / 0 / 175
Goodness-of-fit on F^2	1.085
Final R indices [I>2sigma(I)]	R1 = 0.0369, wR2 = 0.0983
R indices (all data)	R1 = 0.0456, wR2 = 0.1031
Largest diff. peak and hole	0.283 and -0.208 $e.Å^{-3}$

Table 1: Crystal data and structure refinement for 2-methoxy-9H-xanthen-9-one

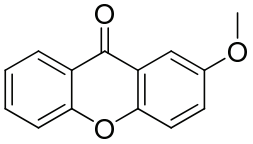

Identification code	8m_jn5_0f
Empirical formula	C14 H10 O3
Formula weight	226.22
Temperature	173(2) K
Wavelength	0.71073 Å
Crystal system	Monoclinic
Space group	P2(1)/n

Unit cell dimensions	a = 4.7765(2) Å □= 90°. b = 14.2280(5) Å □= 93.426(2)°. c = 15.4365(6) Å □ = 90°.
Volume	1047.19(7) $Å^3$
Z	4
Density (calculated)	1.435 Mg/m^3
Absorption coefficient	0.101 mm^{-1}
F(000)	472
Crystal size	0.60 x 0.07 x 0.06 mm^3
Theta range for data collection	1.95 to 28.00°.
Index ranges	-6<=h<=6, -18<=k<=18, -20<=l<=20
Reflections collected	15813
Independent reflections	2533 [R(int) = 0.0446]
Completeness to theta = 28.00°	100.0 %
Absorption correction	None
Max. and min. transmission	0.9940 and 0.9418
Refinement method	Full-matrix least-squares on F^2
Data / restraints / parameters	2533 / 0 / 155
Goodness-of-fit on F^2	1.026
Final R indices [I>2sigma(I)]	R1 = 0.0466, wR2 = 0.1072
R indices (all data)	R1 = 0.0695, wR2 = 0.1178
Largest diff. peak and hole	0.288 and -0.273 $e.Å^{-3}$

APPENDIX II

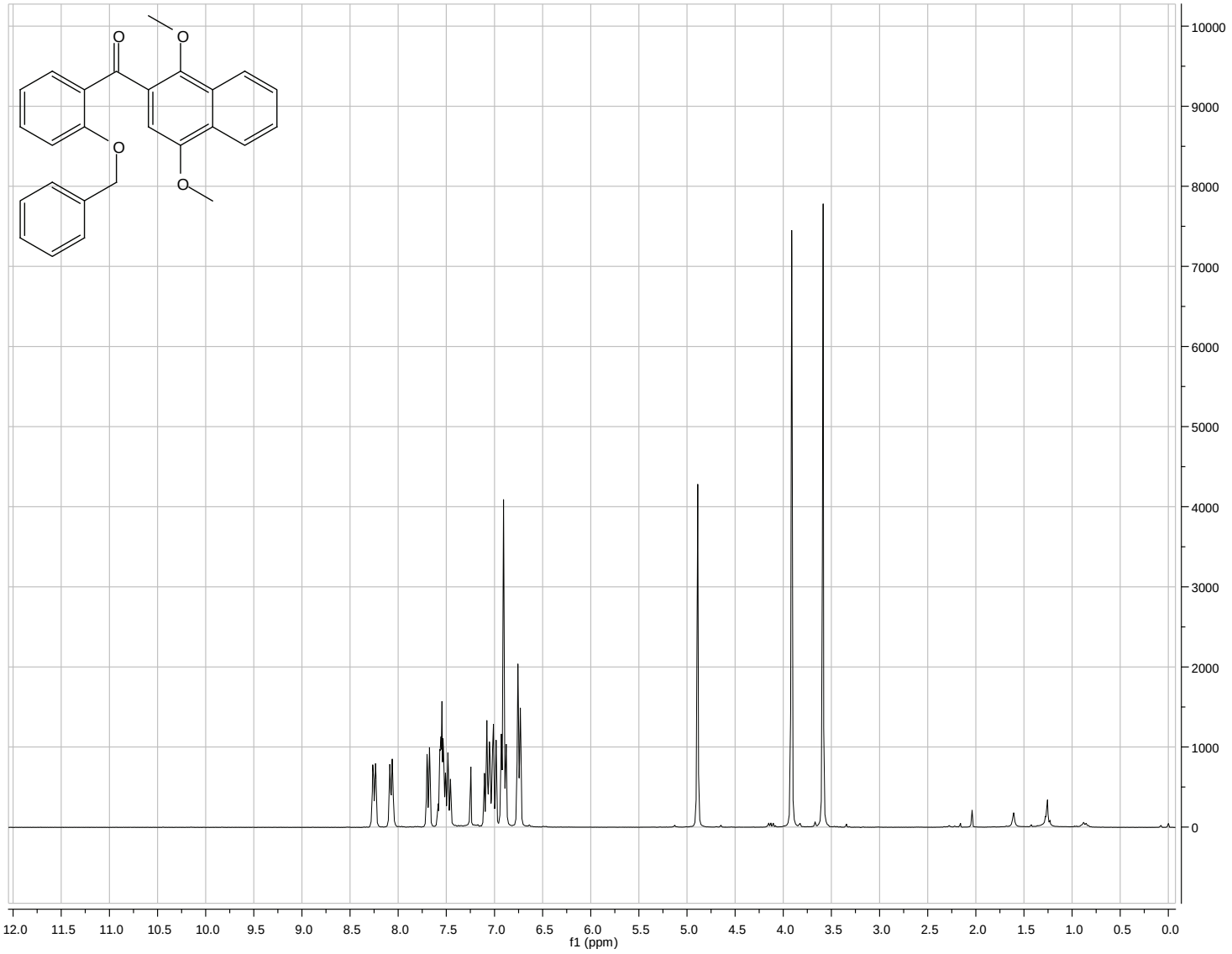
O
O
O
O
10000
9000
8000
7000
6000
5000
4000
3000
2000
1000
0
12.0
11.5
11.0
10.5
10.0
9.5
9.0
8.5
8.0
7.5
7.0
6.5
6.0
5.5
5.0
4.5
4.0
3.5
3.0
2.5
2.0
1.5
1.0
0.5
0.0
f1 (ppm)

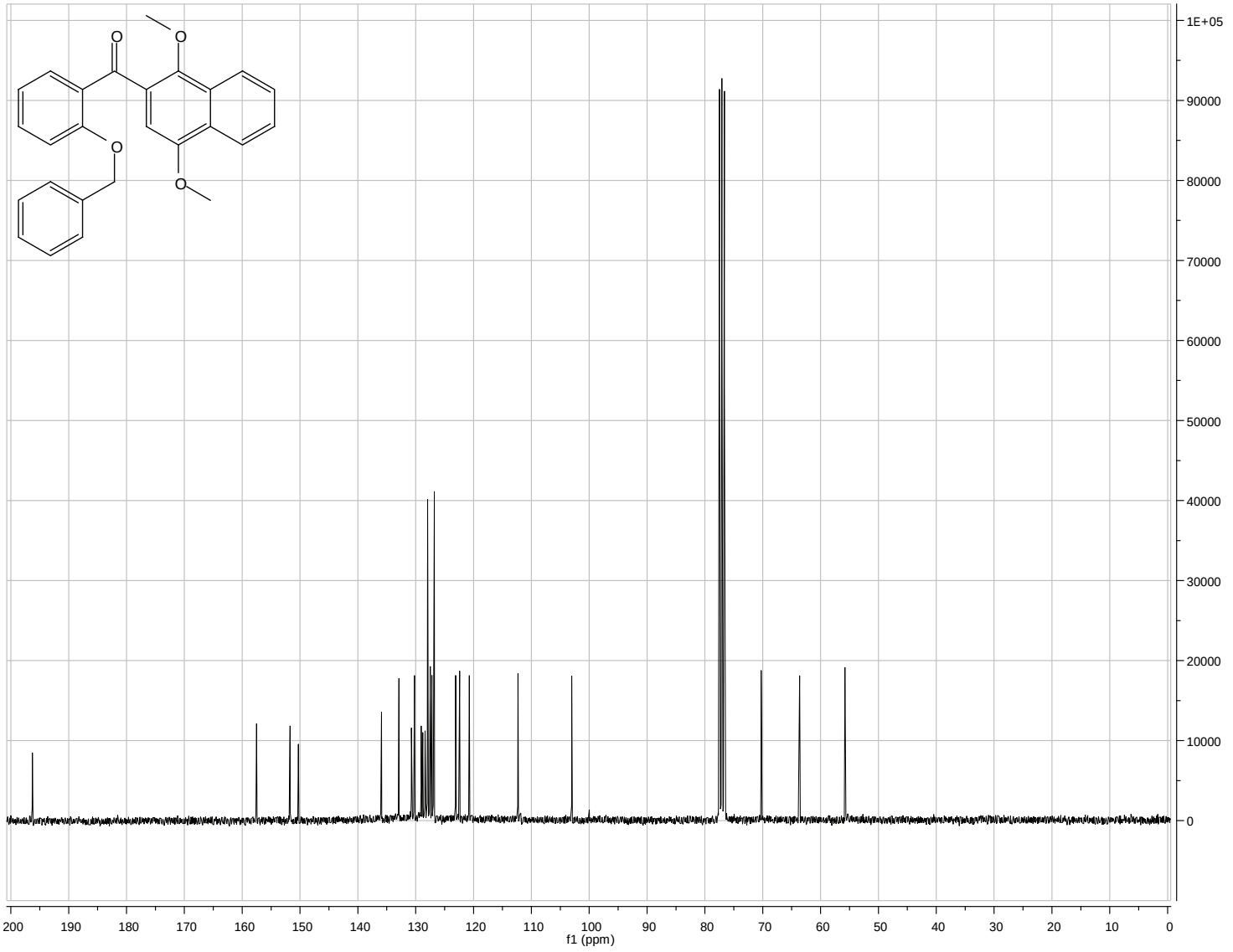
O
O
O
O
1E+05
90000
80000
70000
60000
50000
40000
30000
20000
10000
0
200
190
180
170
160
150
140
130
120
110
100
90
80
70
60
50
40
30
20
10
0
f1 (ppm)

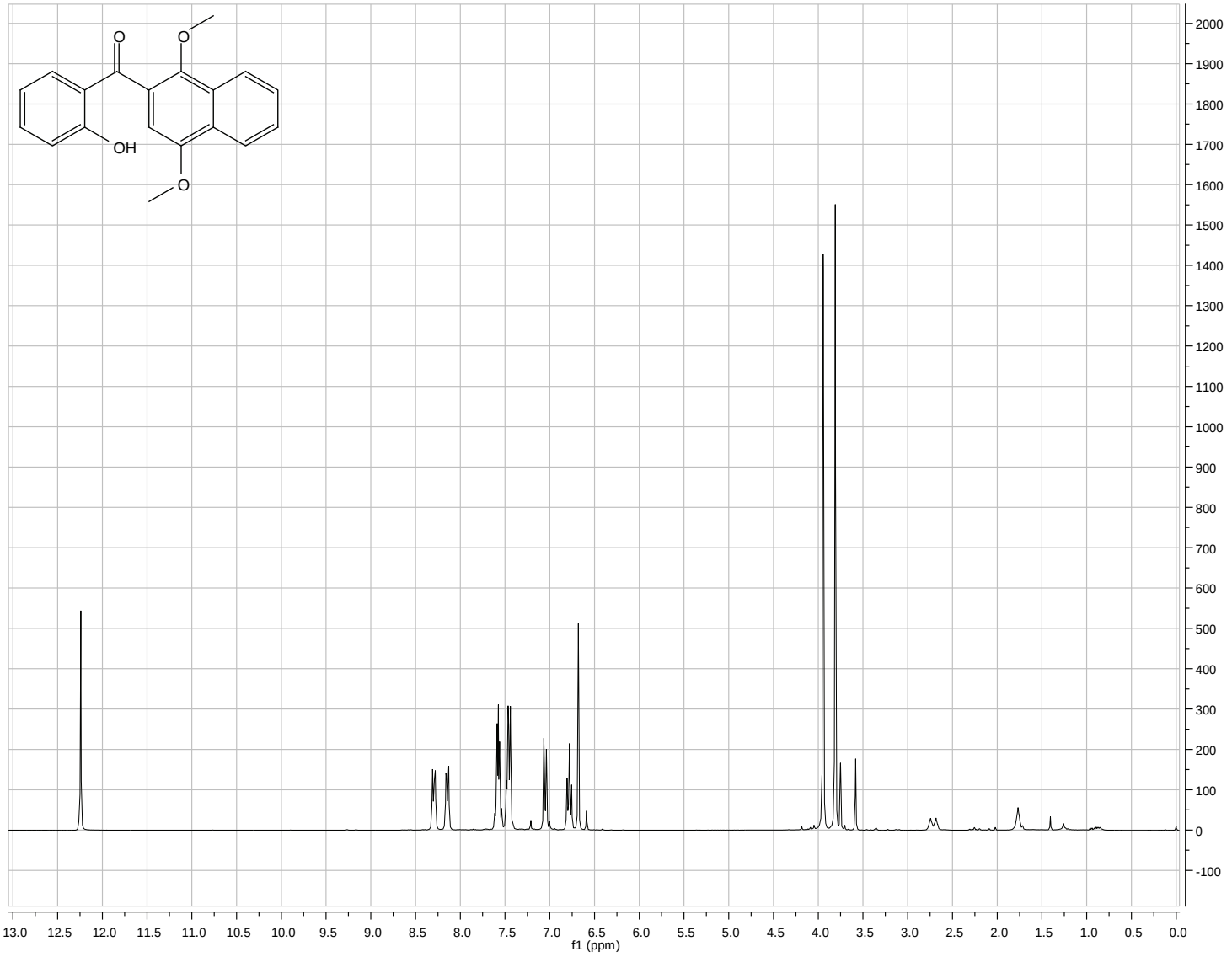
O
O
OH
O
2000
1900
1800
1700
1600
1500
1400
1300
1200
1100
1000
900
800
700
600
500
400
300
200
100
0
-100
13.0 12.5 12.0 11.5 11.0 10.5 10.0 9.5 9.0 8.5 8.0 7.5 7.0 6.5 6.0 5.5 5.0 4.5 4.0 3.5 3.0 2.5 2.0 1.5 1.0 0.5 0.0
f1 (ppm)

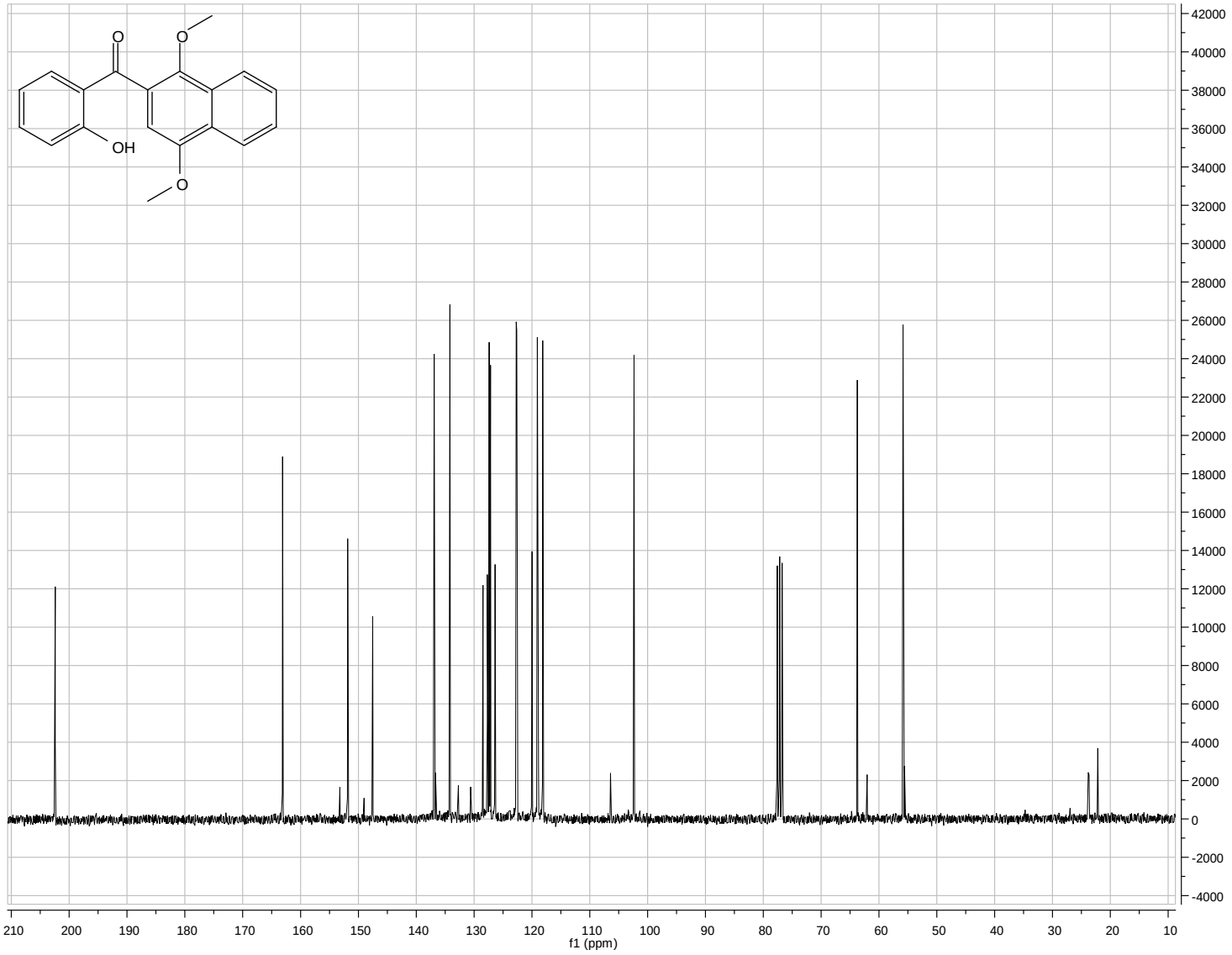
O
O
OH
O
42000
40000
38000
36000
34000
32000
30000
28000
26000
24000
22000
20000
18000
16000
14000
12000
10000
8000
6000
4000
2000
0
-2000
-4000
210
200
190
180
170
160
150
140
130
120
110
100
90
80
70
60
50
40
30
20
10
f1 (ppm)

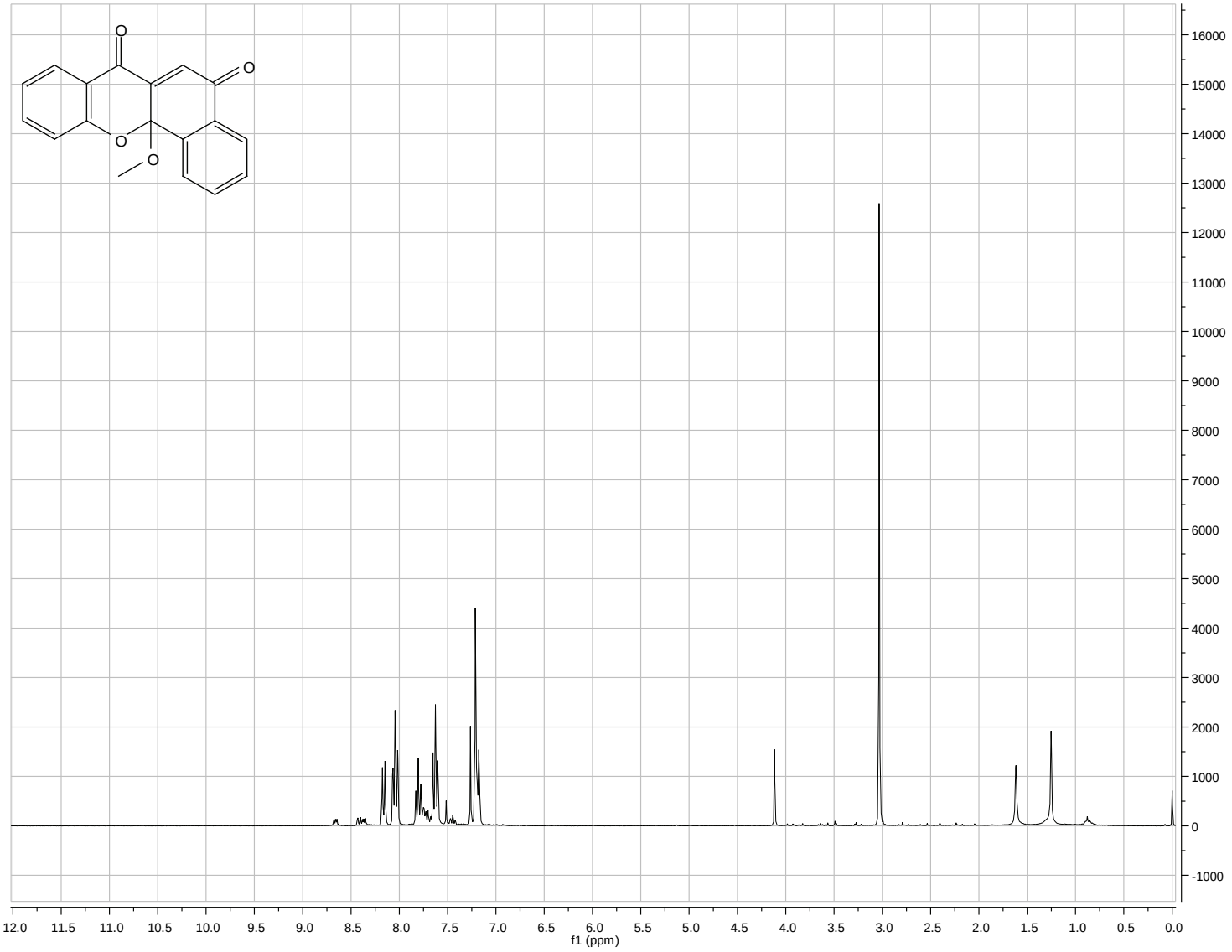
O
O
O
O
16000
15000
14000
13000
12000
11000
10000
9000
8000
7000
6000
5000
4000
3000
2000
1000
0
-1000
12.0
11.5
11.0
10.5
10.0
9.5
9.0
8.5
8.0
7.5
7.0
6.5
6.0
5.5
5.0
4.5
4.0
3.5
3.0
2.5
2.0
1.5
1.0
0.5
0.0
f1 (ppm)

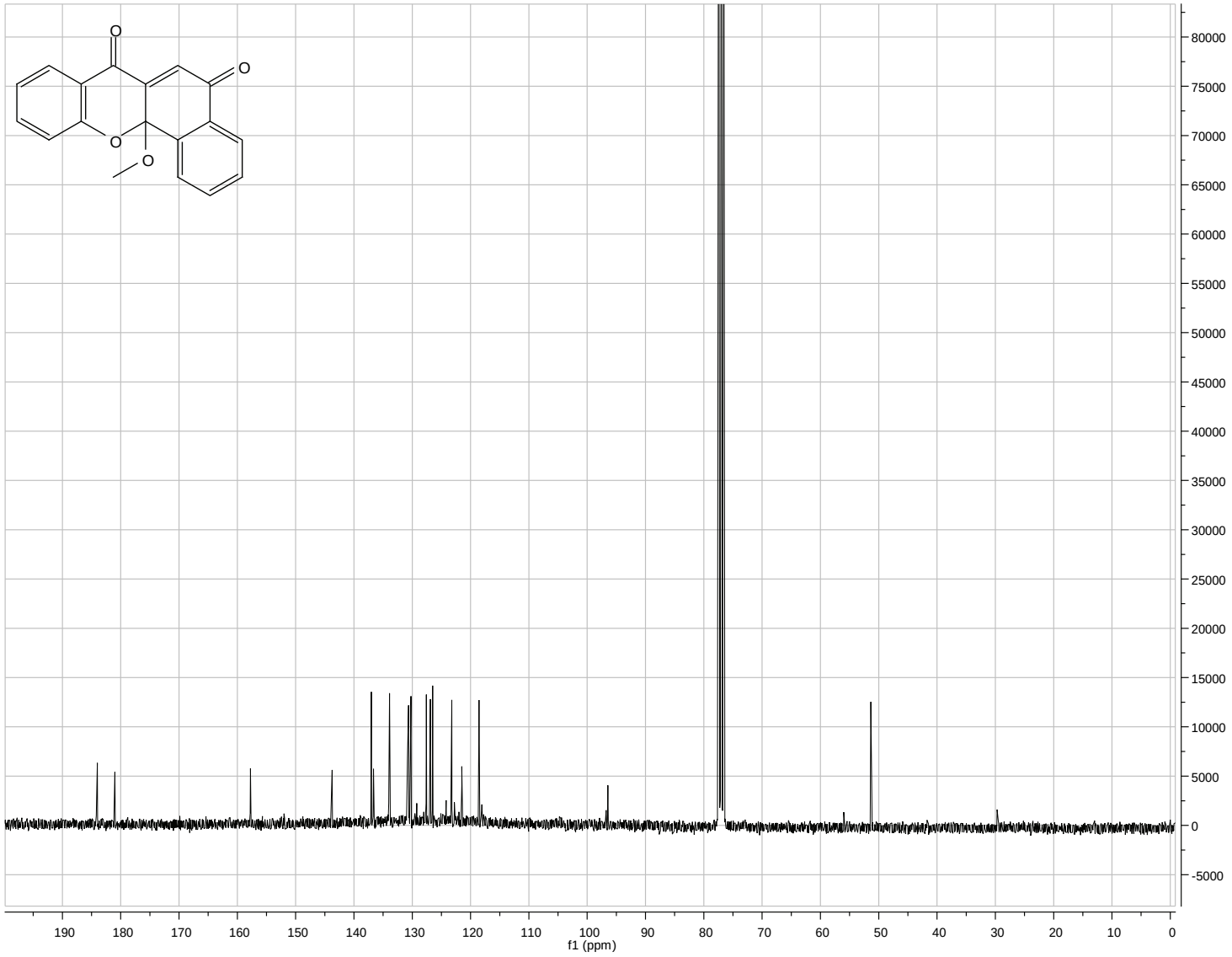
O
O
O
O
80000
75000
70000
65000
60000
55000
50000
45000
40000
35000
30000
25000
20000
15000
10000
5000
0
-5000
190
180
170
160
150
140
130
120
110
100
90
80
70
60
50
40
30
20
10
0
f1 (ppm)

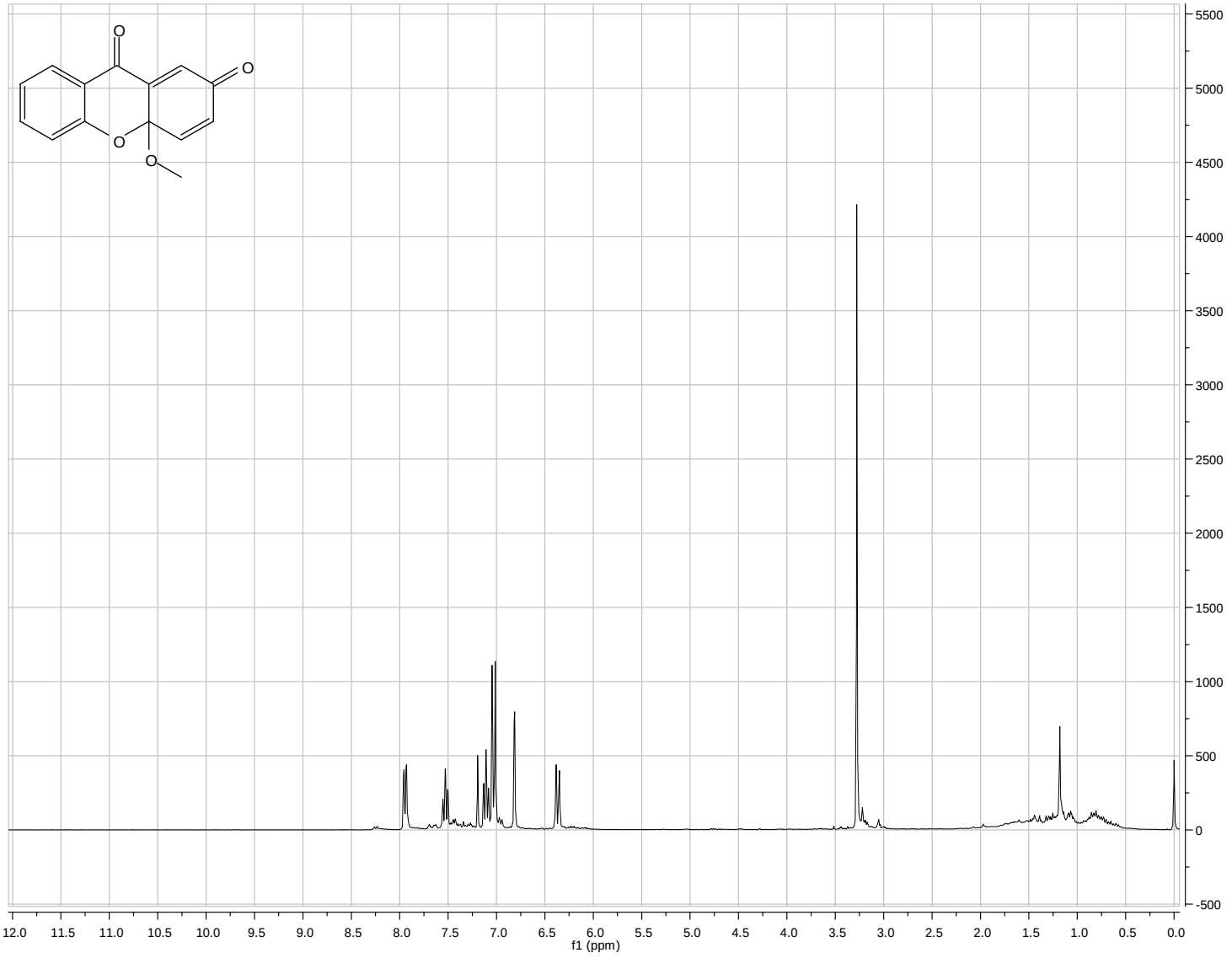
O
O
O
O
5500
5000
4500
4000
3500
3000
2500
2000
1500
1000
500
0
-500
12.0
11.5
11.0
10.5
10.0
9.5
9.0
8.5
8.0
7.5
7.0
6.5
6.0
5.5
5.0
4.5
4.0
3.5
3.0
2.5
2.0
1.5
1.0
0.5
0.0
f1 (ppm)

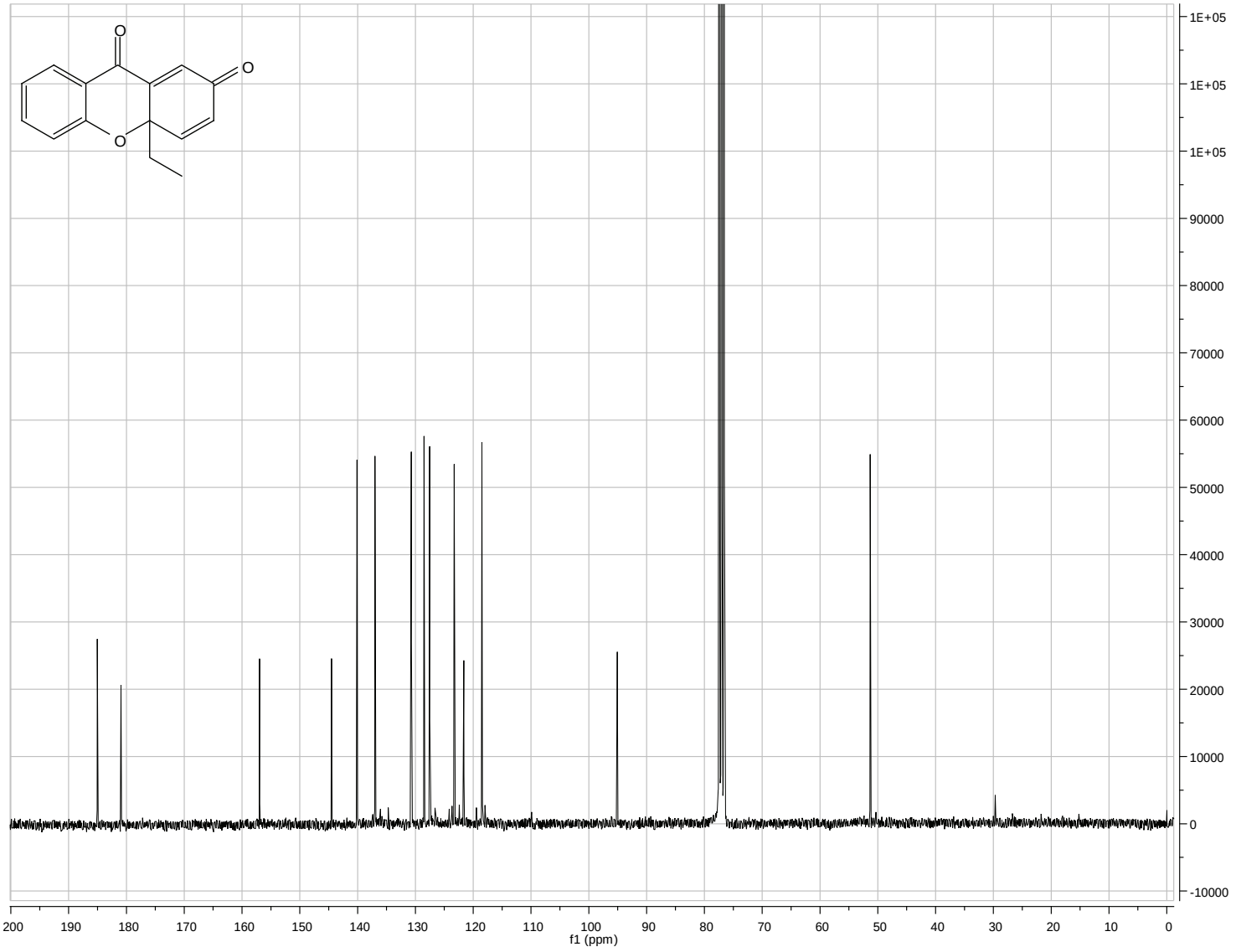
O
O
O
1E+05
1E+05
1E+05
90000
80000
70000
60000
50000
40000
30000
20000
10000
0
-10000
200
190
180
170
160
150
140
130
120
110
100
90
80
70
60
50
40
30
20
10
0
f1 (ppm)

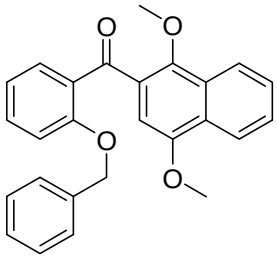

MSC0408_HR_20090320-c1 #27 RT: 1.57 AV: 1 NL: 2.13E6
T: + c EI Full ms [379.50-406.50]

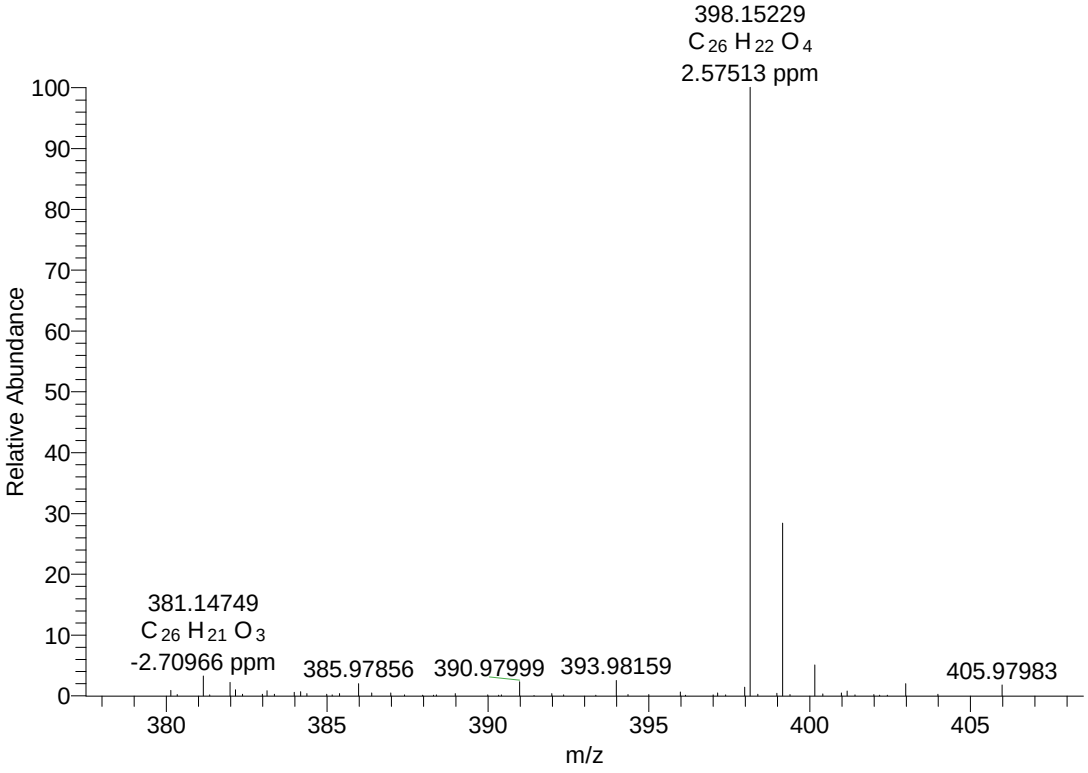

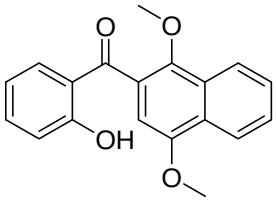

MSC0708_HR_20090320-c1 #62 RT: 4.06 AV: 1 NL: 2.11E6
T: + c EI Full ms [291.50-320.50]

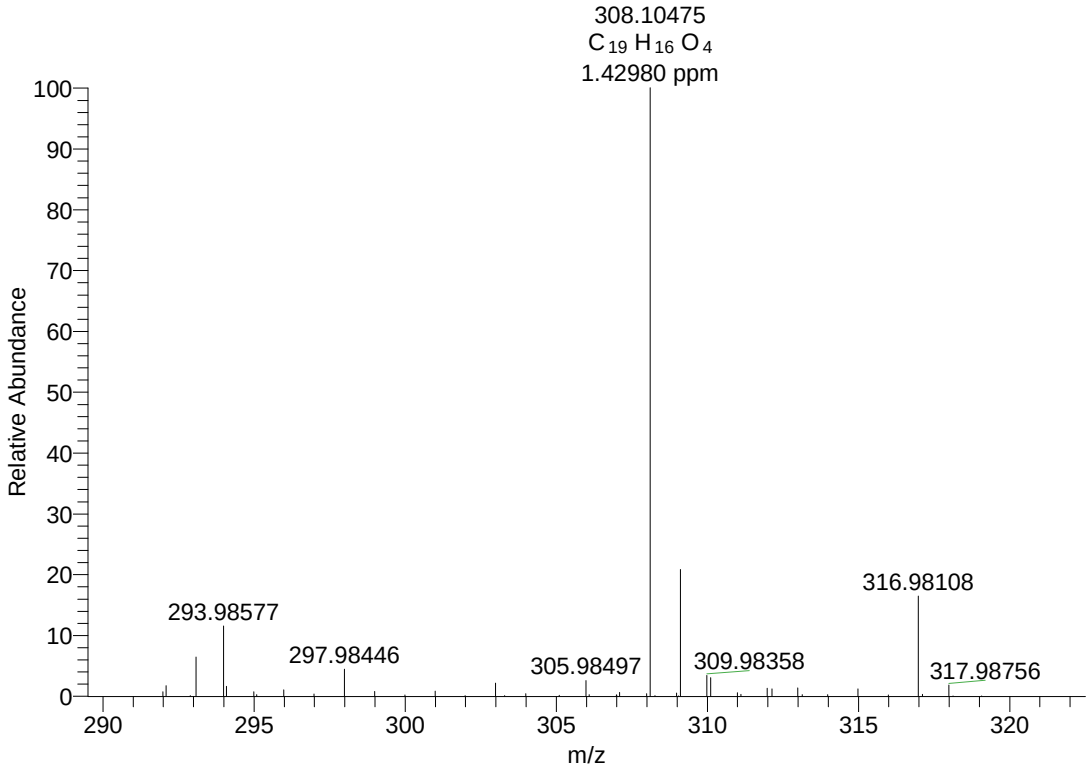

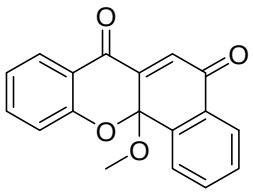

MSC0908_HR_20090320-c1 #82 RT: 5.67 AV: 1 NL: 8.93E5
T: + c EI Full ms [267.50-294.50]

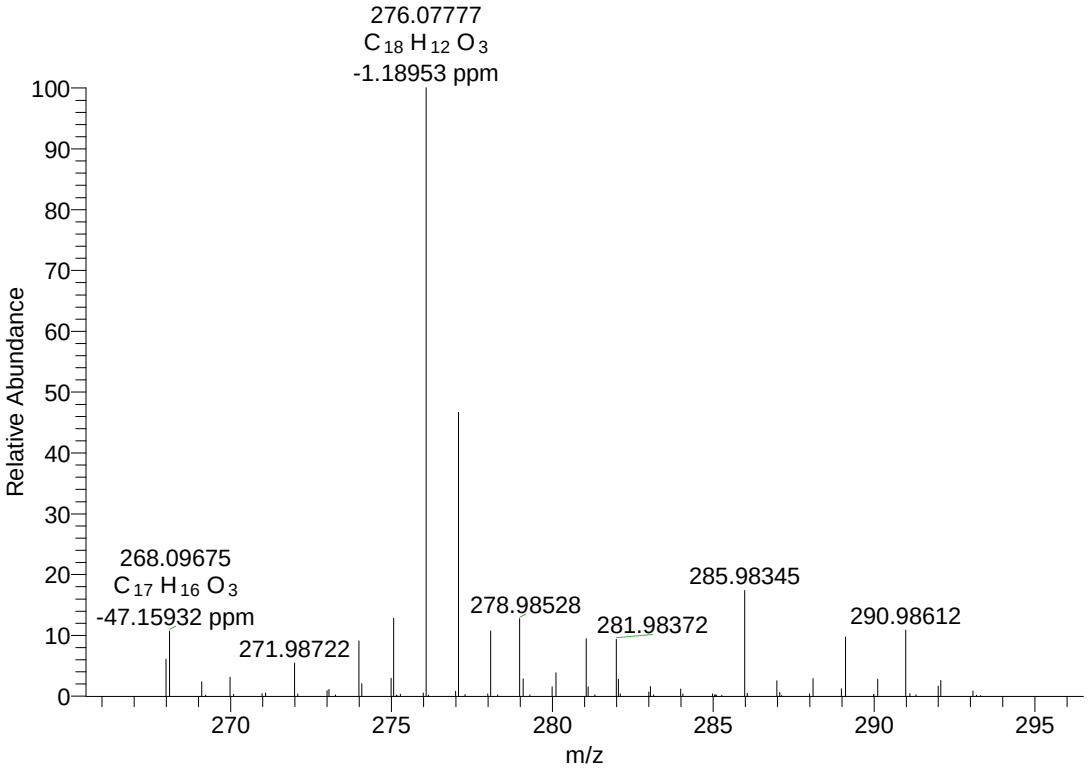

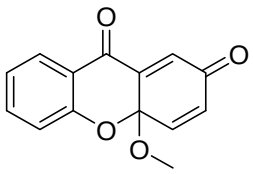

MSC13b08_HR_20090320-c1 #26 RT: 2.38 AV: 1 NL: 1.25E6
T: + c EI Full ms [229.50-256.50]

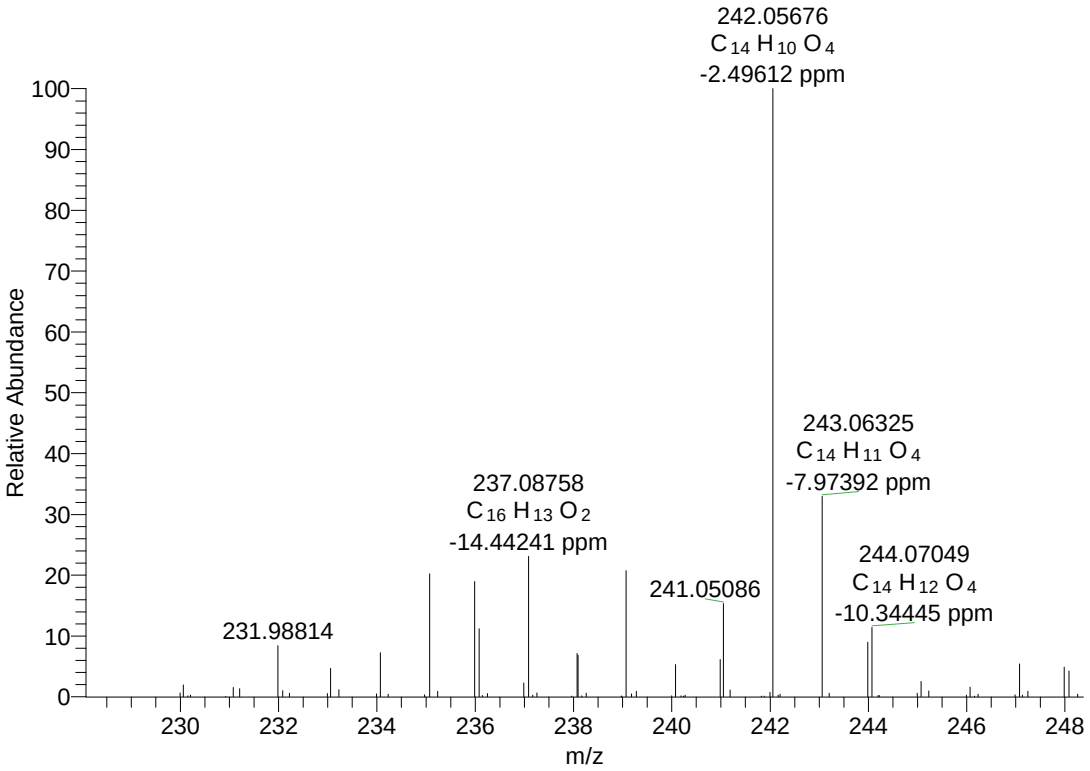

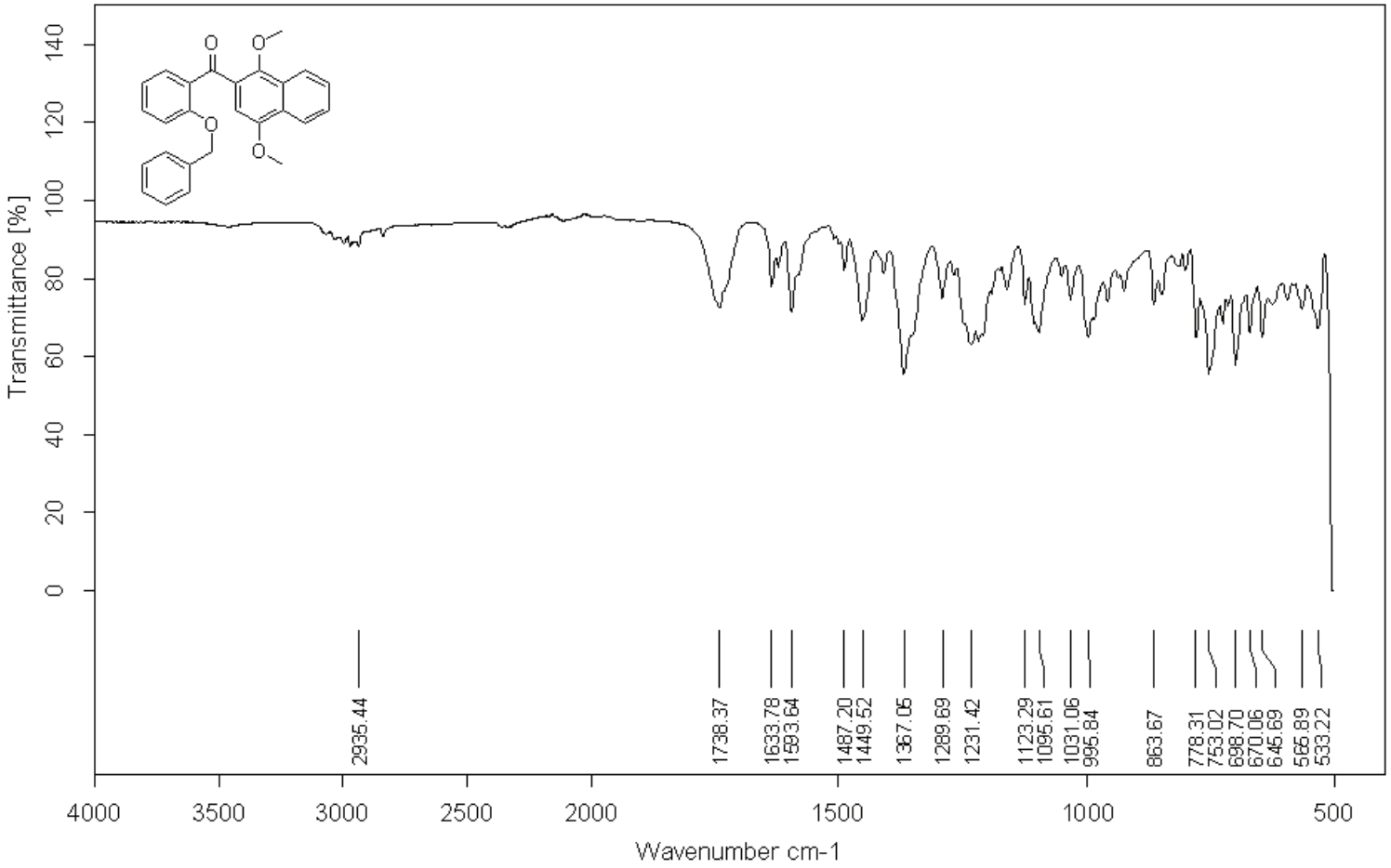
Transmittance [%]
0
20
40
60
80
100
120
140
2935.44
1738.37
1633.78
1593.64
1487.20
1449.52
1367.05
1289.69
1231.42
1123.29
1095.61
1031.06
995.84
863.67
778.31
753.02
698.70
670.06
645.69
565.89
533.22
4000
3500
3000
2500
2000
1500
1000
500
Wavenumber cm-1

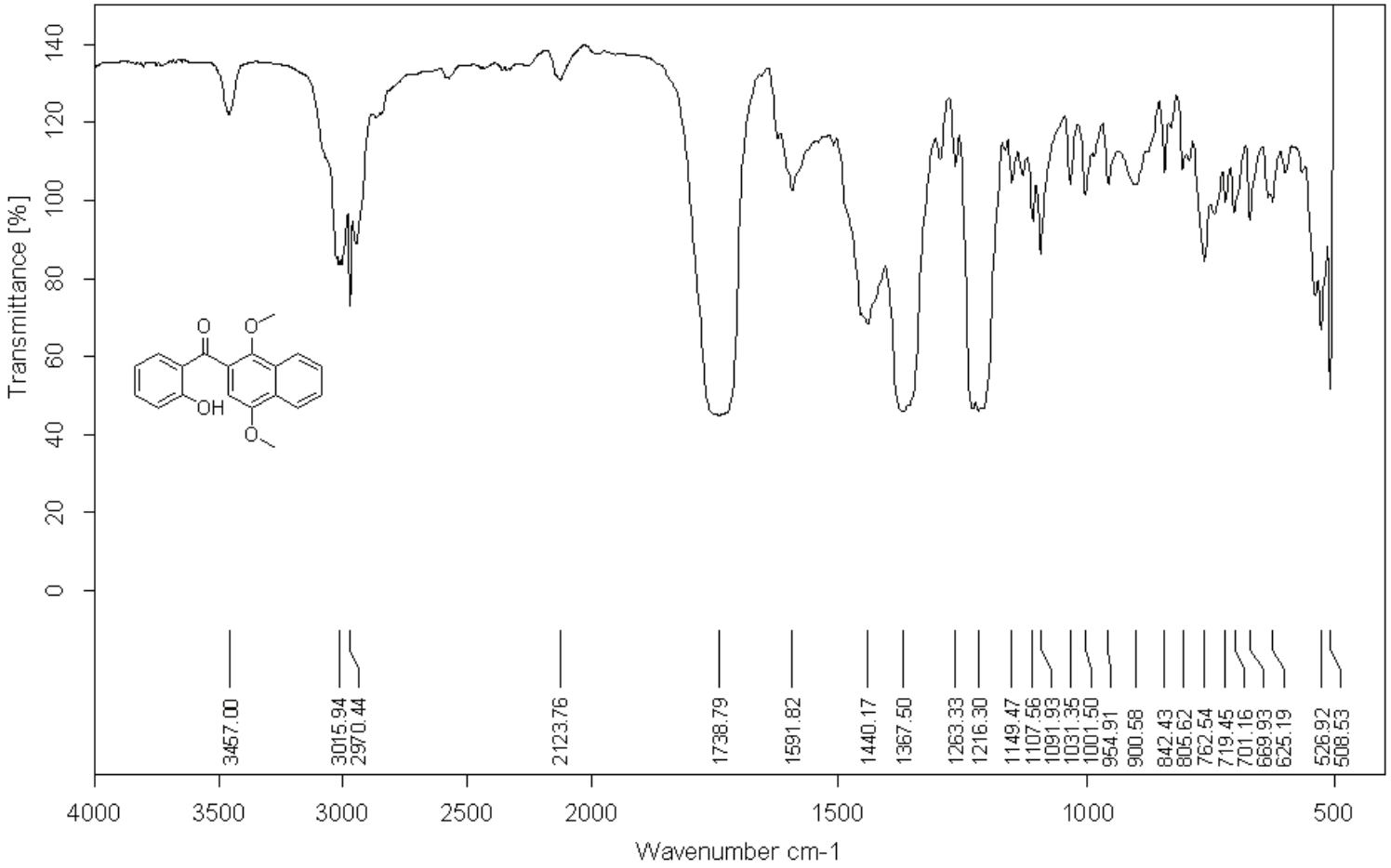
Transmittance [%]
0
20
40
60
80
100
120
140
O
O
OH
O
3457.00
3015.94
2970.44
2123.76
1738.79
1591.82
1440.17
1367.50
1263.33
1216.30
1149.47
1107.56
1091.93
1031.35
1001.50
954.91
900.58
842.43
805.62
762.54
719.45
701.16
669.93
625.19
526.92
508.53
4000
3500
3000
2500
2000
1500
1000
500
Wavenumber cm-1

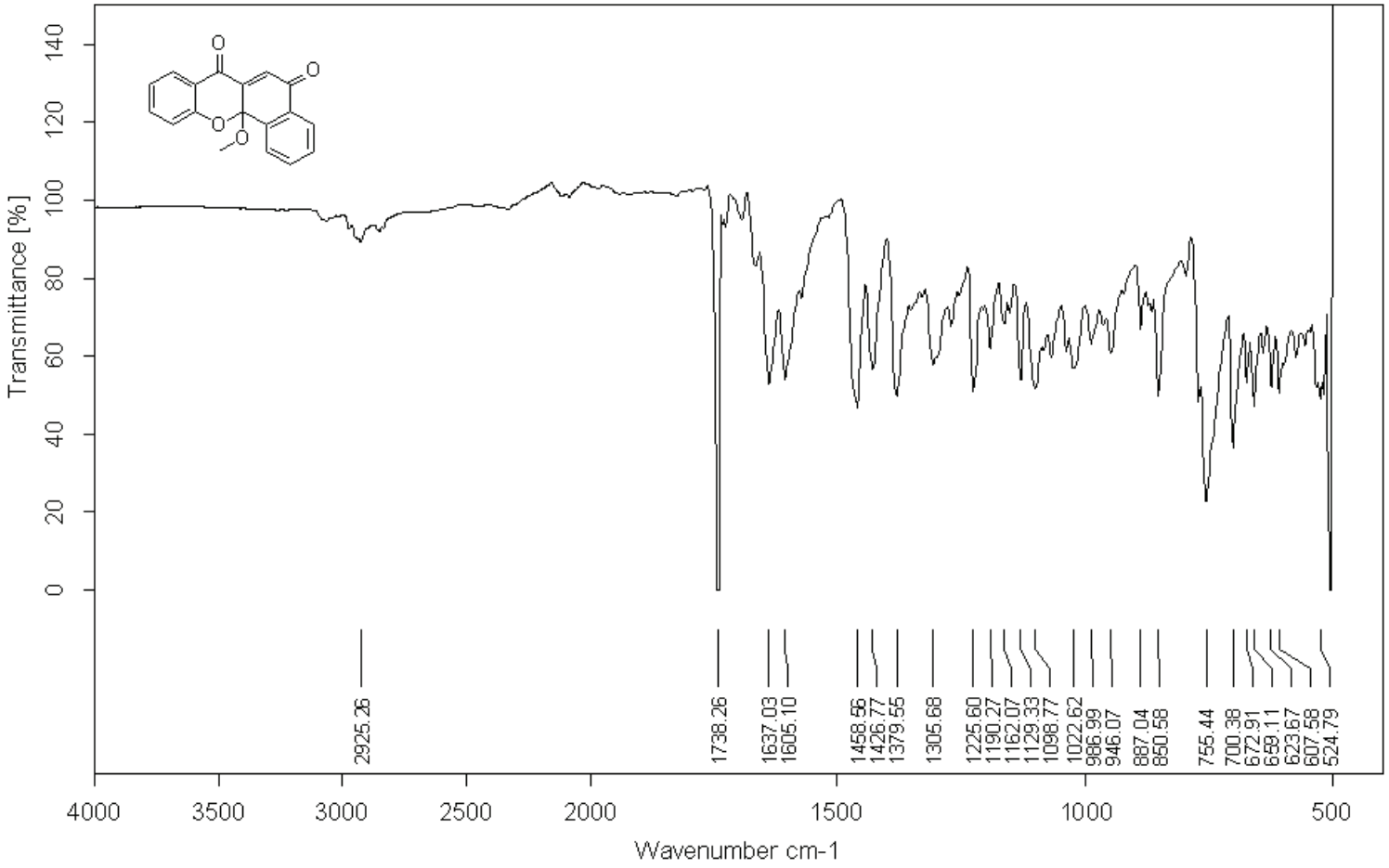
Transmittance [%]
0
20
40
60
80
100
120
140
4000
3500
3000
2500
2000
1500
1000
500
Wavenumber cm-1
2925.26
1738.26
1637.03
1605.10
1458.56
1426.77
1379.55
1305.68
1225.60
1190.27
1162.07
1129.33
1098.77
1022.62
986.99
946.07
887.04
850.58
755.44
700.38
672.91
659.11
623.67
607.58
524.79
O
O
O
O

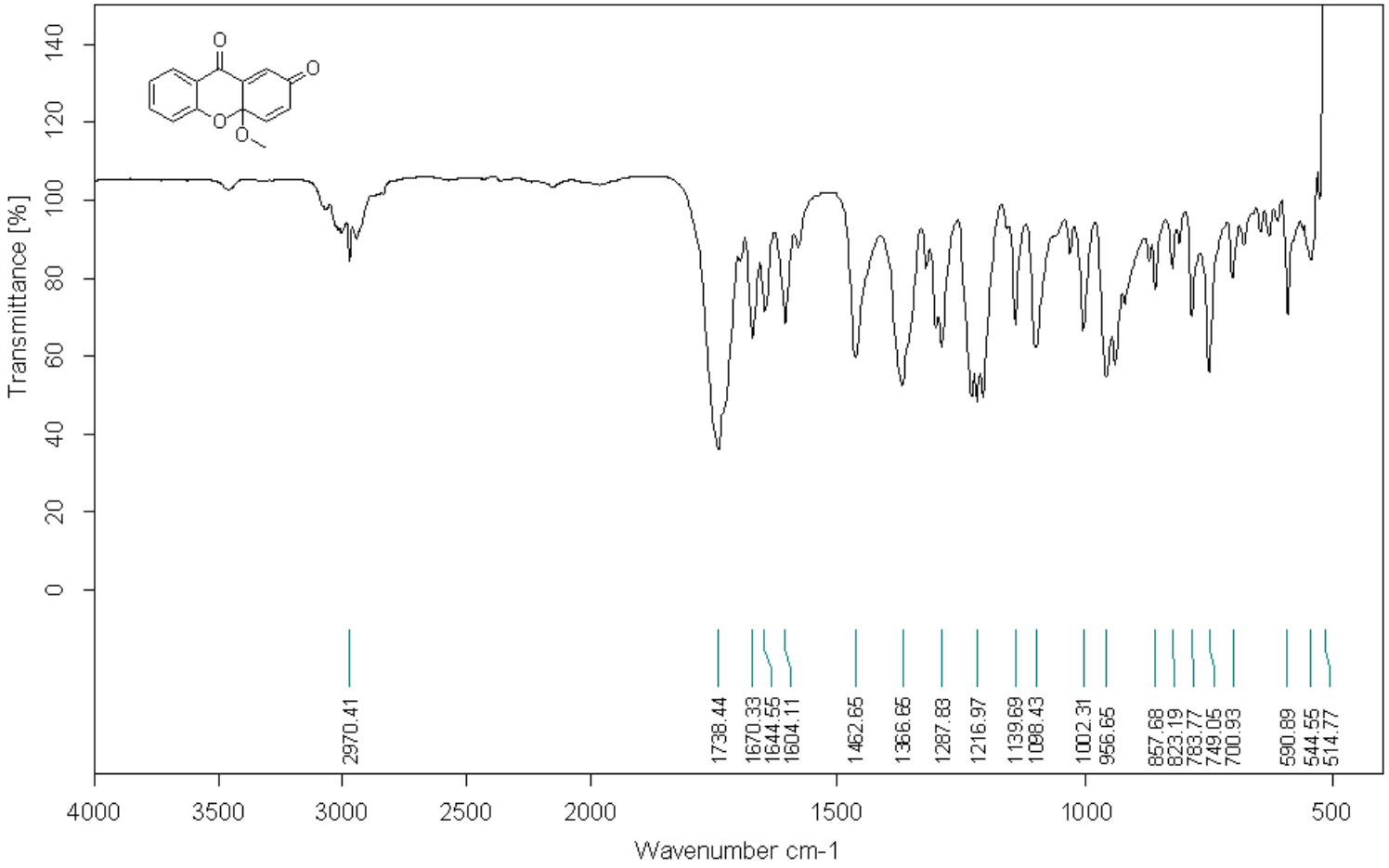
Transmittance [%]
0
20
40
60
80
100
120
140
2970.41
1738.44
1670.33
1644.55
1604.11
1462.65
1366.66
1287.88
1216.97
1139.69
1098.43
1002.31
956.65
857.68
823.19
783.77
749.05
700.93
590.89
544.55
514.77
4000
3500
3000
2500
2000
1500
1000
500
Wavenumber cm-1